Stellar Dynamos and Winds

Dr. Allan Sacha Brun

Department of Astrophysics, CEA Paris-Saclay

(sacha.brun@cea.fr)

Magnetohydrodynamics, Dynamo effect

mean field theory, Stellar Wind

Plan Part I:

- Stellar Convection
- Stellar rotation and large scale mean flows
- Dynamo main concepts and application to stellar rotating convection zone (alpha-omega vs Babcock-Leighton)
- Mean field 2-D dynamos vs 3-D convection dynamos
- Role of dynamo families on stellar activity
- Sunspot Dynamo Paradox

All what I will speak about can be found in this 2017 Living Review in Solar Physics

Springer Link

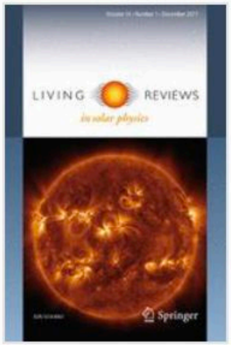

Living Reviews in Solar Physics
December 2017, 14:4 | Cite as

Magnetism, dynamo action and the solar-stellar connection

Authors | Authors and affiliations

Allan Sacha Brun, Matthew K. Browning

LIVING REVIEWS
in solar physics

Sun in UV

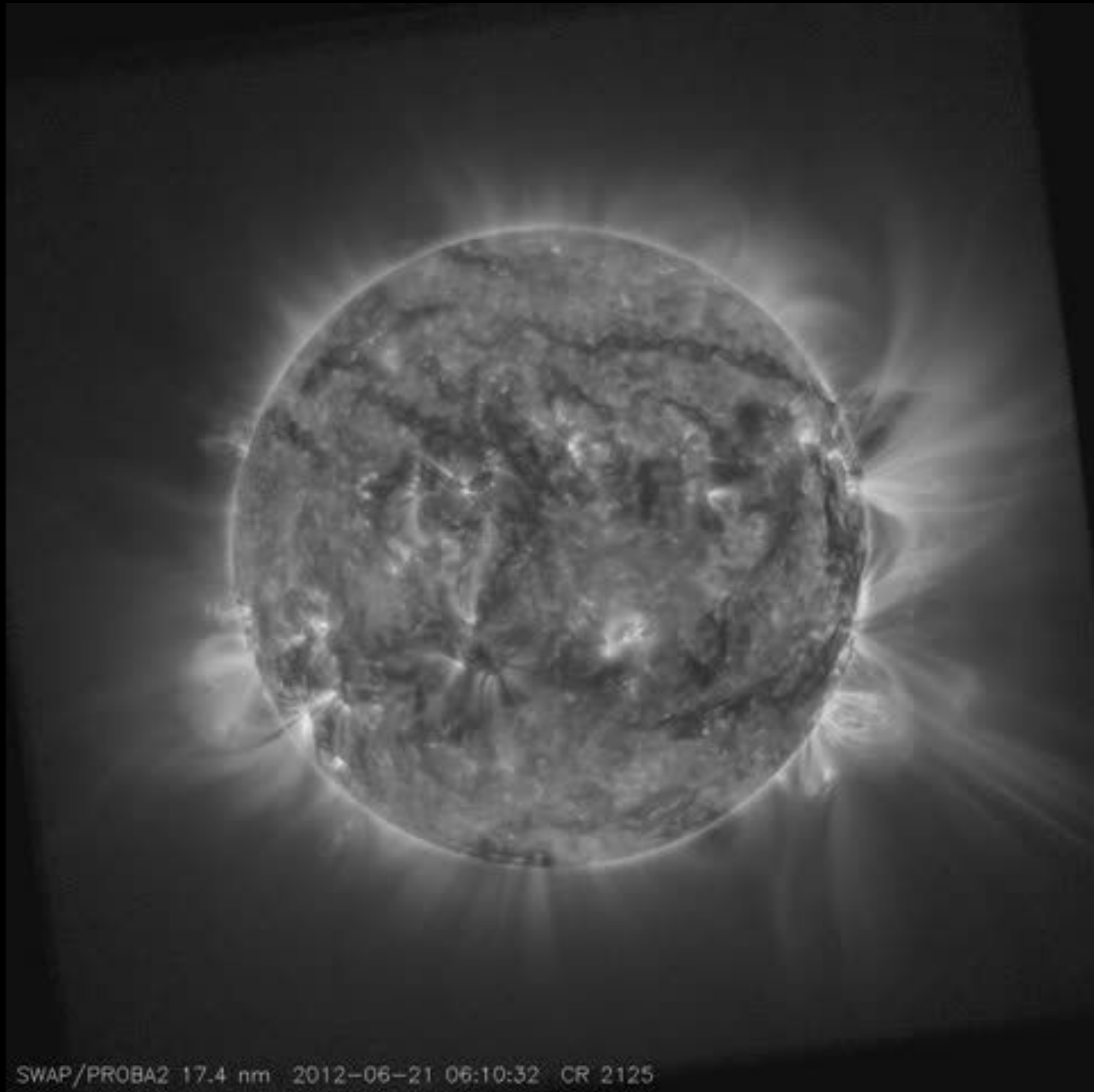

ESA Proba2

Échelles Spatio-Temporelles dans la Zone Convective Solaire

Plasma= gaz chaud (ionisé)
4eme etat de la matière

L’Ordre dans le Chaos!

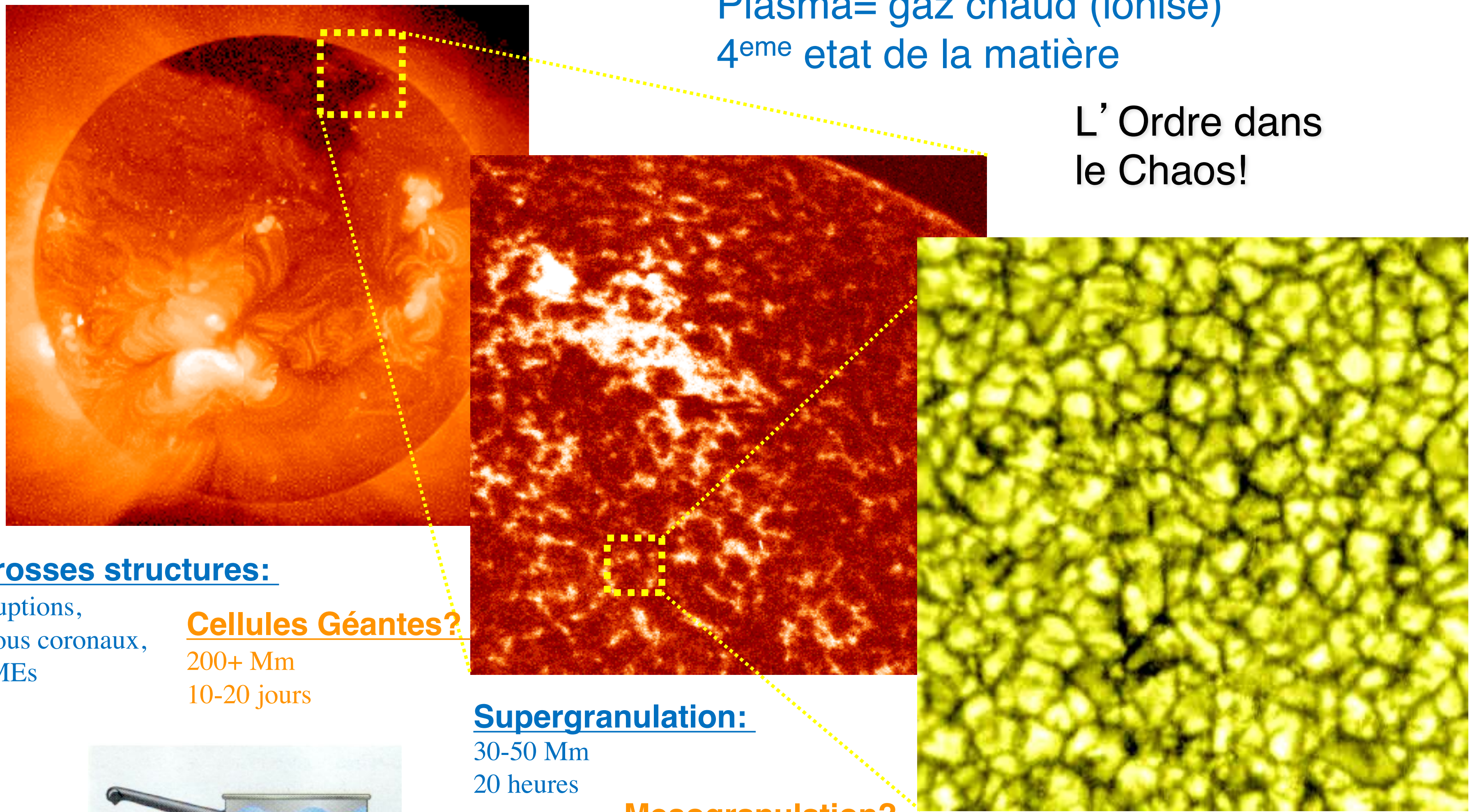

Grosses structures:
Eruptions,
Trous coronaux,
CMEs

Cellules Géantes?
200+ Mm
10-20 jours

Supergranulation:
30-50 Mm
20 heures

Mesogranulation?
7-10 Mm
2 heures

Granulation:
1-2 Mm
5 mins

Petites structures:
Lignes Intergranulaires,
Points magnétiques brillants, diffusion

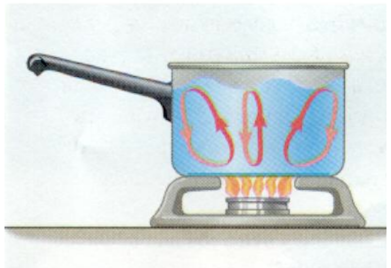

Le Diagramme d'Hertzsprung-Russell Théorique

Most Figures from: The Cosmic Perspective, Bennett et al. 2003, ed. Pearson or ESA, NASA.

Carte « michelin » des étoiles

diagramme de Hertzsprung-Russell où l'on représente le type spectral de l'étoile en fonction de sa luminosité

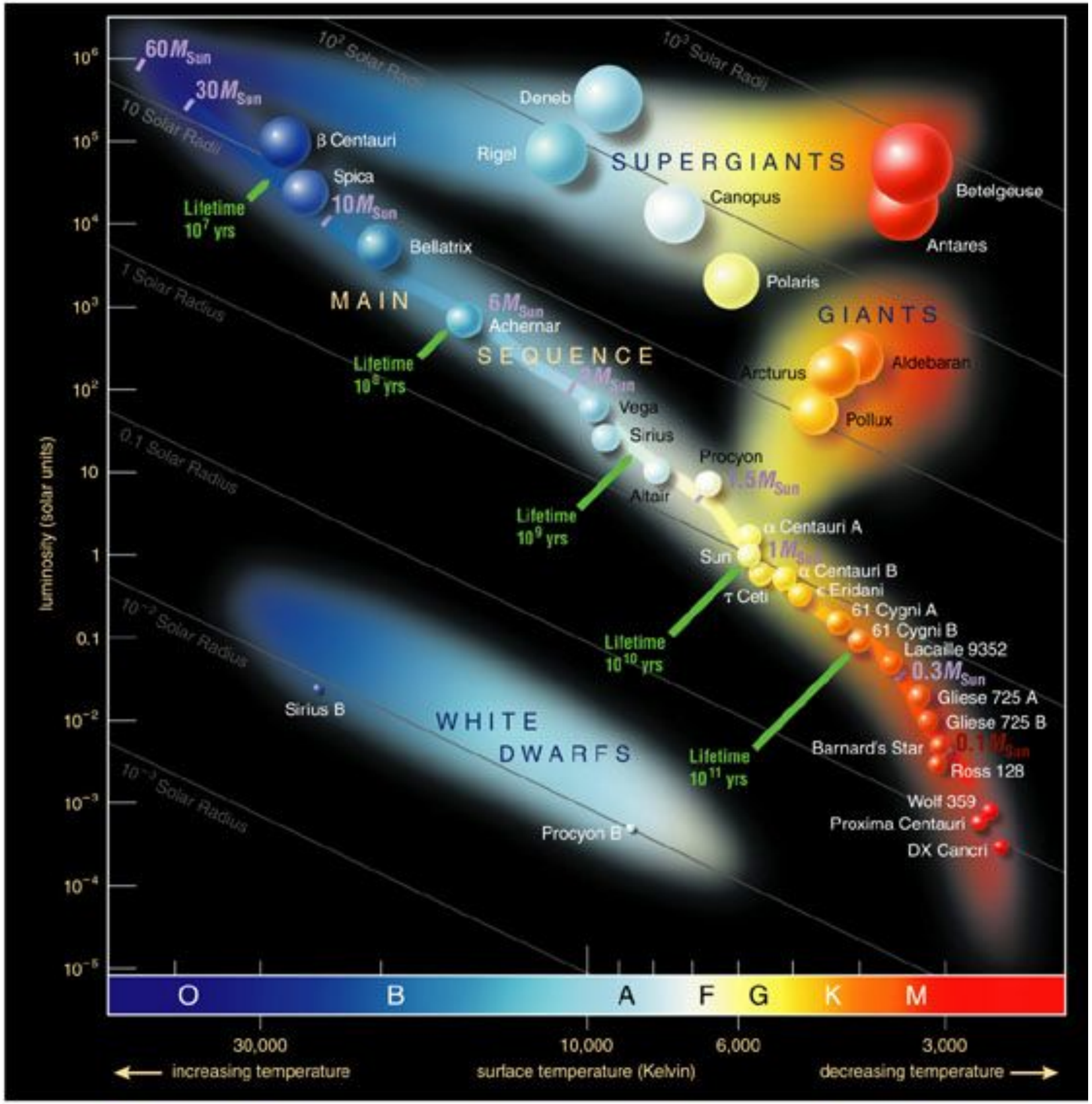

Zones Convectives dans les Etoiles

Transition between envelope and core convection: ~1.3 Msol

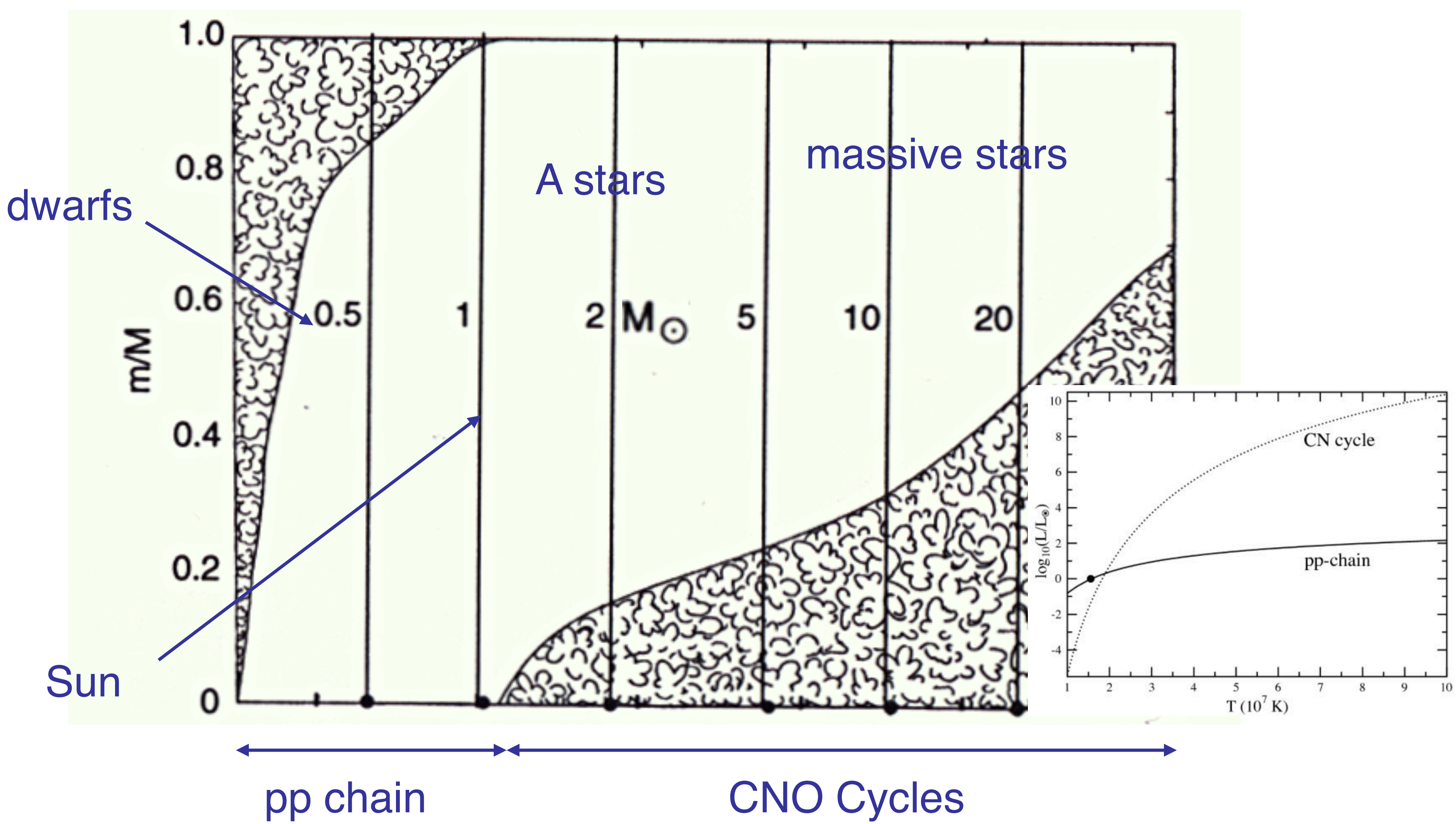

Critères de Stabilité

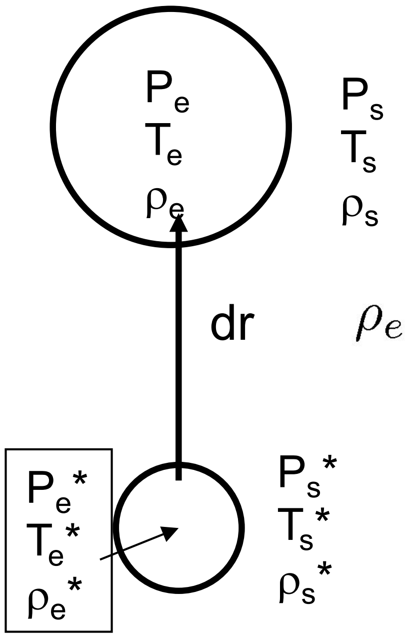

$$\rho_e = \rho_e^* + dr\left(\frac{d\rho}{dr}\right)_e \qquad \rho_s = \rho_s^* + dr\left(\frac{d\rho}{dr}\right)_s$$

$$\rho_e - \rho_s = dr\left[\left(\frac{d\rho}{dr}\right)_e - \left(\frac{d\rho}{dr}\right)_s\right] > 0 \quad \left(\frac{d\rho}{dr}\right)_e - \left(\frac{d\rho}{dr}\right)_s > 0 \ (1)$$

Equation d'etat: $\rho=\rho(P,T,\mu)$

$$\frac{d\rho}{\rho} = \alpha\frac{dP}{P} - \delta\frac{dT}{T} + \phi\frac{d\mu}{\mu}$$

Échelle de pression

$$\frac{1}{H_p} = -\frac{d\ln P}{dr}$$

$\rho_e^* = \rho_s^*$

$$\left(\frac{\alpha}{P}\frac{dP}{dr}\right)_e - \left(\frac{\delta}{T}\frac{dT}{dr}\right)_e - \left(\frac{\alpha}{P}\frac{dP}{dr}\right)_s + \left(\frac{\delta}{T}\frac{dT}{dr}\right)_s - \left(\frac{\phi}{\mu}\frac{d\mu}{dr}\right)_s > 0$$

$P_e = P_s$ et $P_e^* = P_s^*$

$d\mu$ nul pour l'élément

Multiplions par Hp:

$$\left(\frac{d\ln T}{d\ln P}\right)_s < \left(\frac{d\ln T}{d\ln P}\right)_e + \frac{\phi}{\delta}\left(\frac{d\ln \mu}{d\ln P}\right)_s$$

Stable

ou $$\nabla < \nabla_e + \frac{\phi}{\delta}\nabla_\mu$$

∇_e et ∇_{ad} sont similaires en ce sens que les deux décrivent la variation de température d'un gaz subissant une variations de pression. ∇_{rad} et ∇_μ par contre décrivent la variation spatiale de T et μ du milieu.

Critères de Stabilité de Schwartzschild et de Ledoux

Considérons une atmosphère dans laquelle l'énergie est transportée par radiation (ou conduction) seulement. Alors $\nabla = \nabla_{rad}$. Testons la stabilité de cette atmosphère et considérons que l'élément se déplace adiabatiquement: $\nabla_e = \nabla_{ad}$

L'atmosphère est stable si:

Critère de Ledoux $\nabla_{rad} < \nabla_{ad} + \frac{\phi}{\delta}\nabla_{\mu}$

Gaz parfait : $P = R \rho T/ \mu$
$\Rightarrow \alpha=\delta=\phi=1$

S'il n'a pas de variation de composition ou d'ionisation:

Critère de Schwarzschild $\nabla_{rad} < \nabla_{ad}$

Overshooting

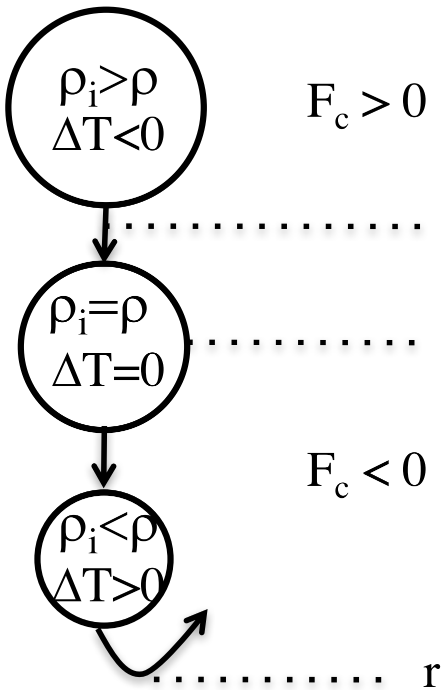

$F_c > 0$

$\nabla = \nabla_{ad}$ à $r = r_s$

$r = r_f$ $F_c = 0$ $\nabla < \nabla_{ad}$

$F_c < 0$

$r = r_{ov}$

Péclet number: $Pe= vL/\kappa$
$Pe >> 1$ (Soleil) -> change stratification
$Pe \sim 1$, extended overshoot

If a heavy sinking convective parcel penetrates into a subadiabatic layer, when the temperature fluct changes sign, parcel is neutrally buoyant but continues to sink by virtue of inertia until the Buoyancy force reverses the direction of its motion.

Zahn 1991

Critères de Stabilité de Schwartzschild et de Ledoux

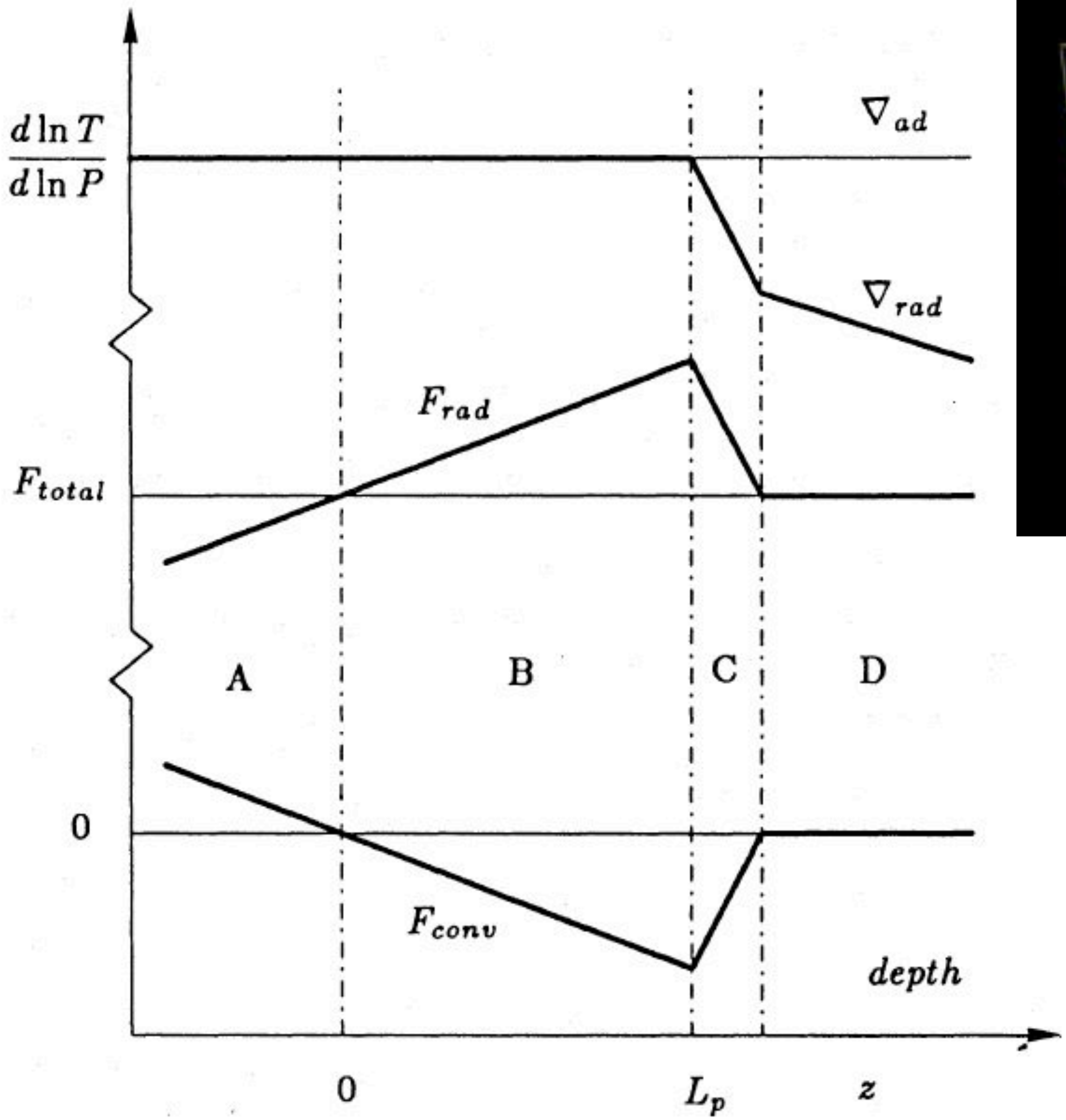

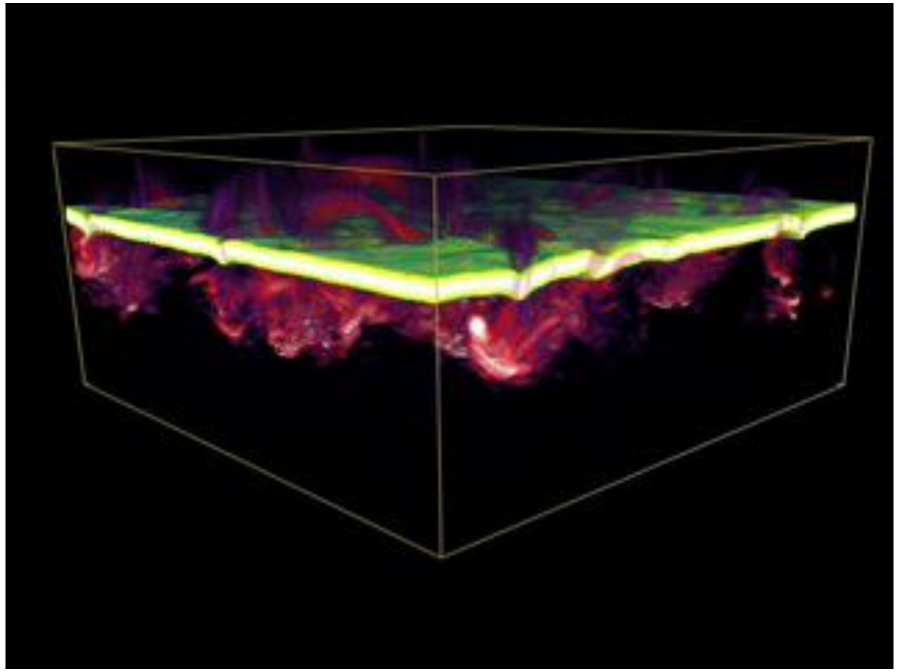

Péclet number: Pe= vL/κ
Pe >> 1 (Soleil) -> change stratification
Pe ~1 , extended overshoot

If a heavy sinking convective parcel penetrates into a subadiabatic layer, when the temperature fluct changes sign, parcel is neutrally buoyant but continues to sink by virtue of inertia until the Buoyancy force reverses the direction of its motion.

Zahn 1991

Fluid Equations

$$\frac{\partial \rho}{\partial t} = -\boldsymbol{\nabla}\cdot(\rho\mathbf{v}), \quad (1)$$

$$\rho\frac{\partial \mathbf{v}}{\partial t} = -\rho(\mathbf{v}\cdot\boldsymbol{\nabla})\mathbf{v} - \boldsymbol{\nabla}P + \rho\mathbf{g}$$
$$- \ 2\rho\boldsymbol{\Omega_o}\times\mathbf{v} - \boldsymbol{\nabla}\cdot\boldsymbol{\mathcal{D}}, \quad (2)$$

$$\rho T\frac{\partial S}{\partial t} = -\rho T(\mathbf{v}\cdot\boldsymbol{\nabla})S + \boldsymbol{\nabla}\cdot(\kappa_r\rho c_p\boldsymbol{\nabla}T)$$
$$+ \ 2\rho\nu\left[e_{ij}e_{ij} - 1/3(\boldsymbol{\nabla}\cdot\mathbf{v})^2\right] + \rho\epsilon, \quad (3)$$

Tenseur visqueux:

$$\mathcal{D}_{ij} = -2\rho\nu[e_{ij} - 1/3(\boldsymbol{\nabla}\cdot\mathbf{v})\delta_{ij}],$$

Diffusivity in the Sun

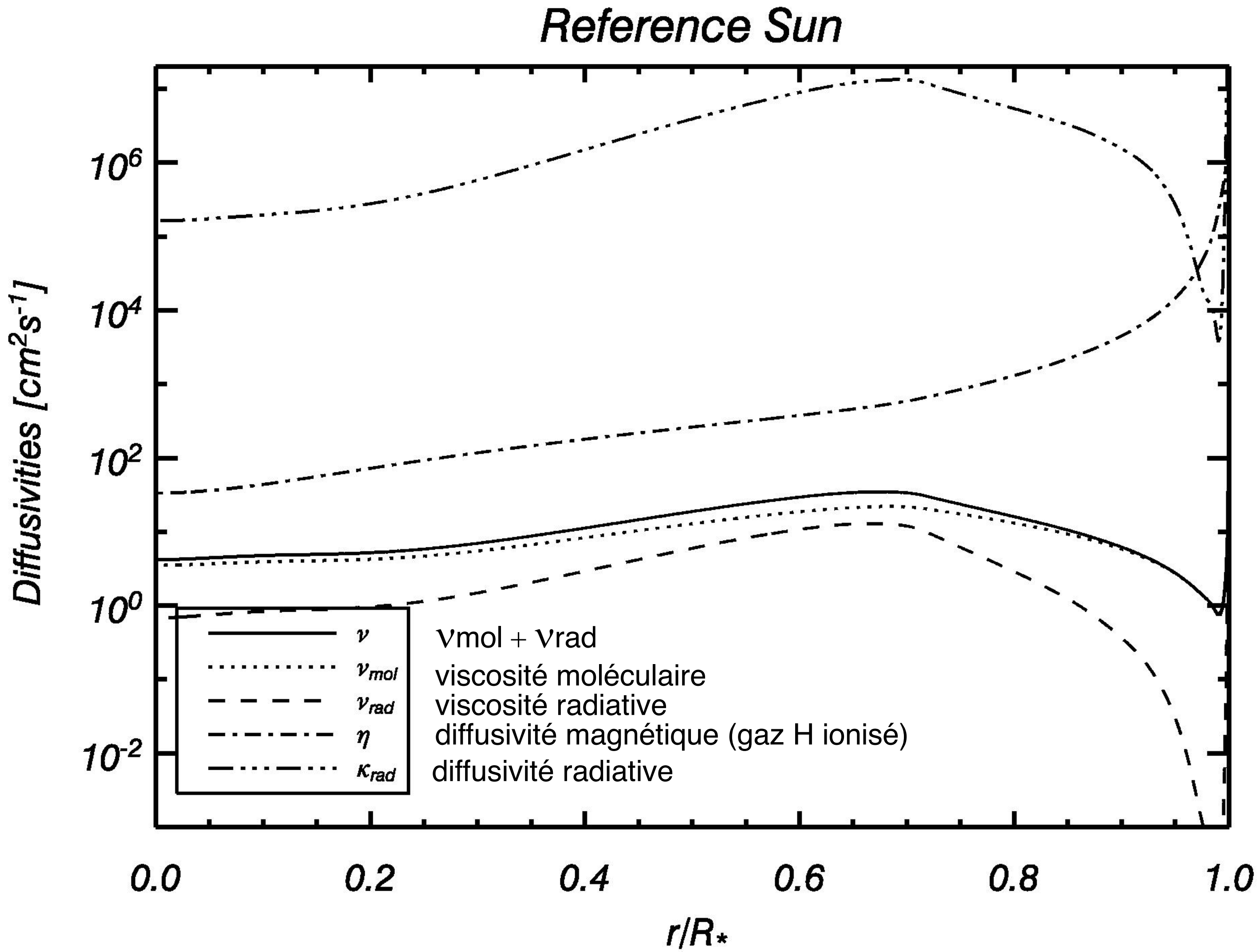

$$\nu_{rad} = \frac{4}{15}\frac{a}{c}\frac{T^4}{\rho^2\kappa_{opa}} \quad \nu_{mol} = \frac{2.2\,10^{-15}}{\ln\Lambda}\frac{T^{5/2}}{\rho} \quad \eta = 5.2\,10^{11}\ln\Lambda\, T^{-3/2}$$

$$\kappa_{rad} = \frac{\chi}{\rho c_p} = \frac{4}{3}\frac{acT^3}{\rho^2 c_p \kappa_{opa}}$$

See Zeldovich et al. 1983, for a discussion of the formula of ν, η, κ

Prandtl (Pr), magnetic Prandtl (Pm) & Roberts (Q) numbers

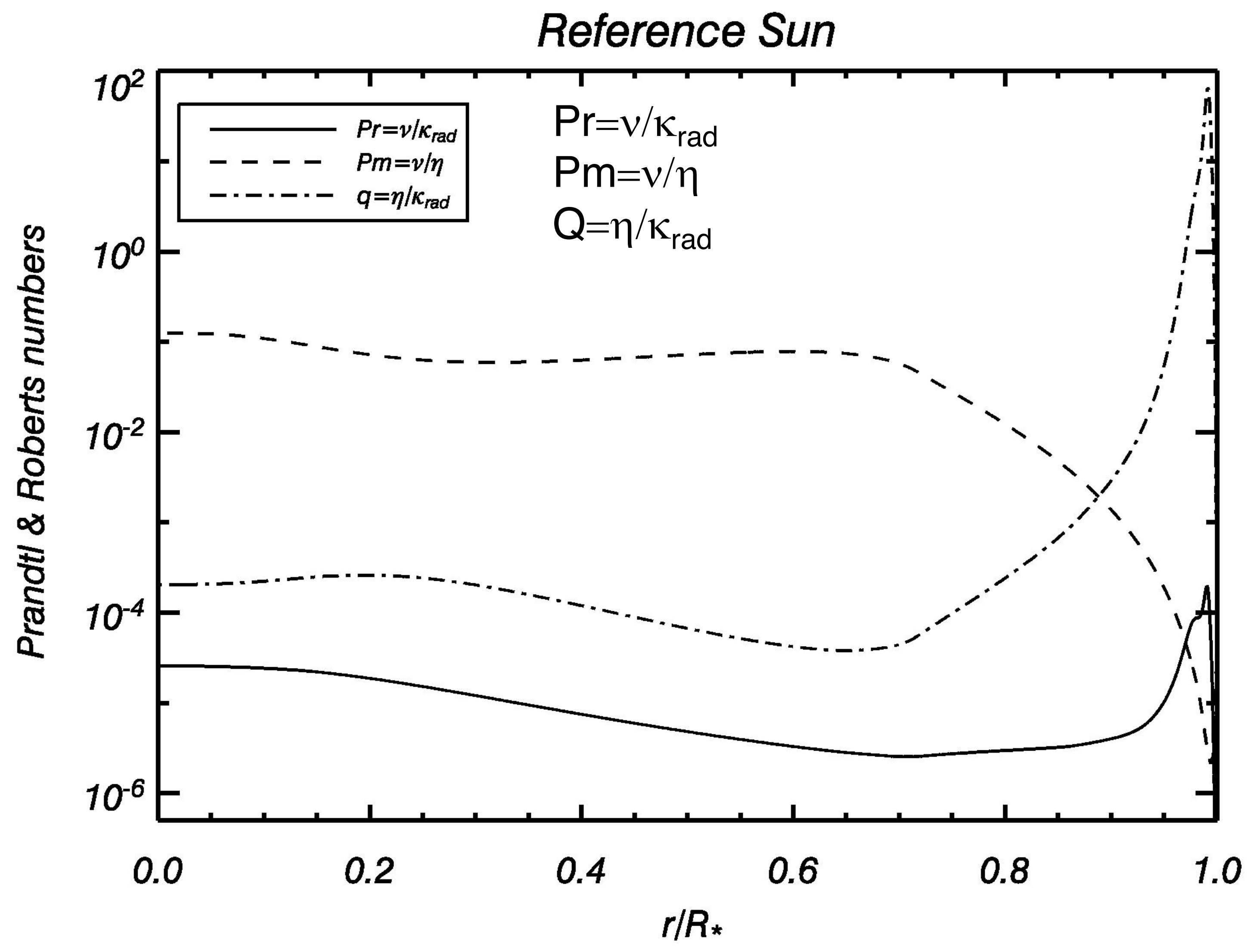

Deriving a criteria for convection with dissipation processes: Rayleigh number

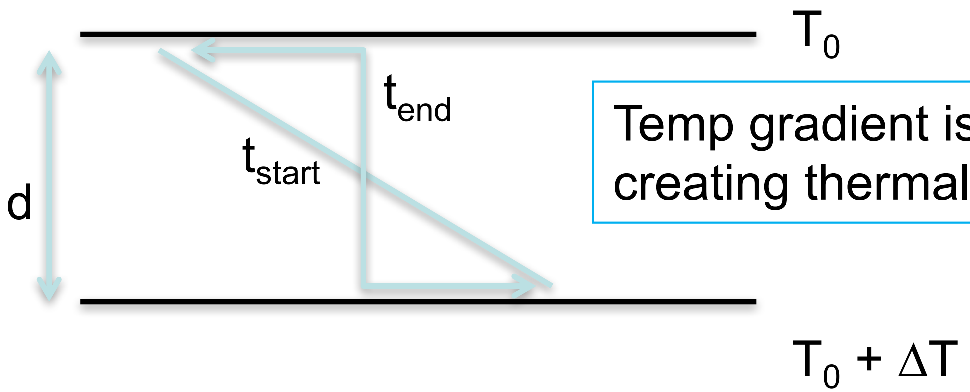

Temp gradient is being homogenized in convection layer creating thermal boundary layers

Bubble is less dense than medium and rise at vertical speed w but as to “fight” against viscous drag:
$\delta\rho\, g = \nu\, \Delta\, w \sim \nu\, w/d^2 \Rightarrow\ w = \delta\rho\, g\, d^2 / \nu$.

With an ideal gas we can relate density fluctuation to temperature variation ΔT via thermal expansion factor α , e.g. $\delta\rho = \alpha\, \Delta T$

so $w = \alpha\, \Delta T\, g\, d^2 / \nu$

While it rises and since it is hot it radiates away its heat. So in order to retain its buoyancy
Rise time < thermal time ⇔ $d/w < d^2/\kappa$

$\Rightarrow 1 < \alpha\, \Delta T\, g\, d^3 / \nu\, \kappa = Ra$ ⇔ Rayleigh number Ra must be greater than one (Ra > 1)
(in this back of the envelope derivation)

Plane Layer Convection

Plane layer conv (cf. Chandrasekhar's book in 1961)

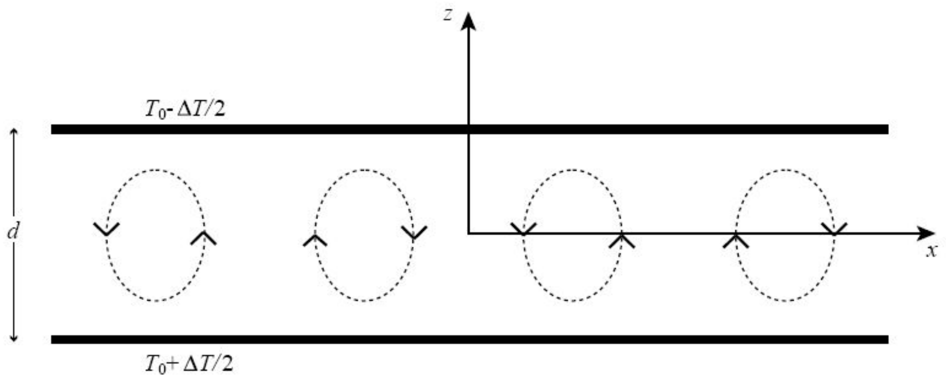

Fig. 17.1: Rayleigh-Bernard convection. A fluid is confined between two horizontal surfaces separated by a vertical distance d. When the temperature difference between the two plates ΔT is increased sufficiently, the fluid will start to convect heat vertically. The reference effective pressure P'_0 and reference temperature T_0 are the values of P' and T measured at the midplane $z = 0$.

Rayleigh Number:

$$Ra = \frac{g\alpha\Delta T d^3}{\kappa\nu}$$

Si Ra est suffisament grand alors la convection se déclenche. La différence Avec le critère de Schwatzschild vient du fait qu'ici on prend en compte l'effet des diffusivités

Conditions aux limites stress-free top & bottom: $Ra_c = 658$
stress-free top & no slip bottom: $Ra_c = 1100$
no slip top & bottom : $Ra_c = 1708$

With a vertical magnetic field pervading the system:
BC's stress free top & bottom for V, radial field BC's for B: Ra_c depends on Hartman number, i.e Ha >> 1, alors $Ra_c = \pi^2(Ha)^2$

$$Ha = \left(\frac{\sigma B_0^2 d^2}{\rho\nu}\right)$$

Convection

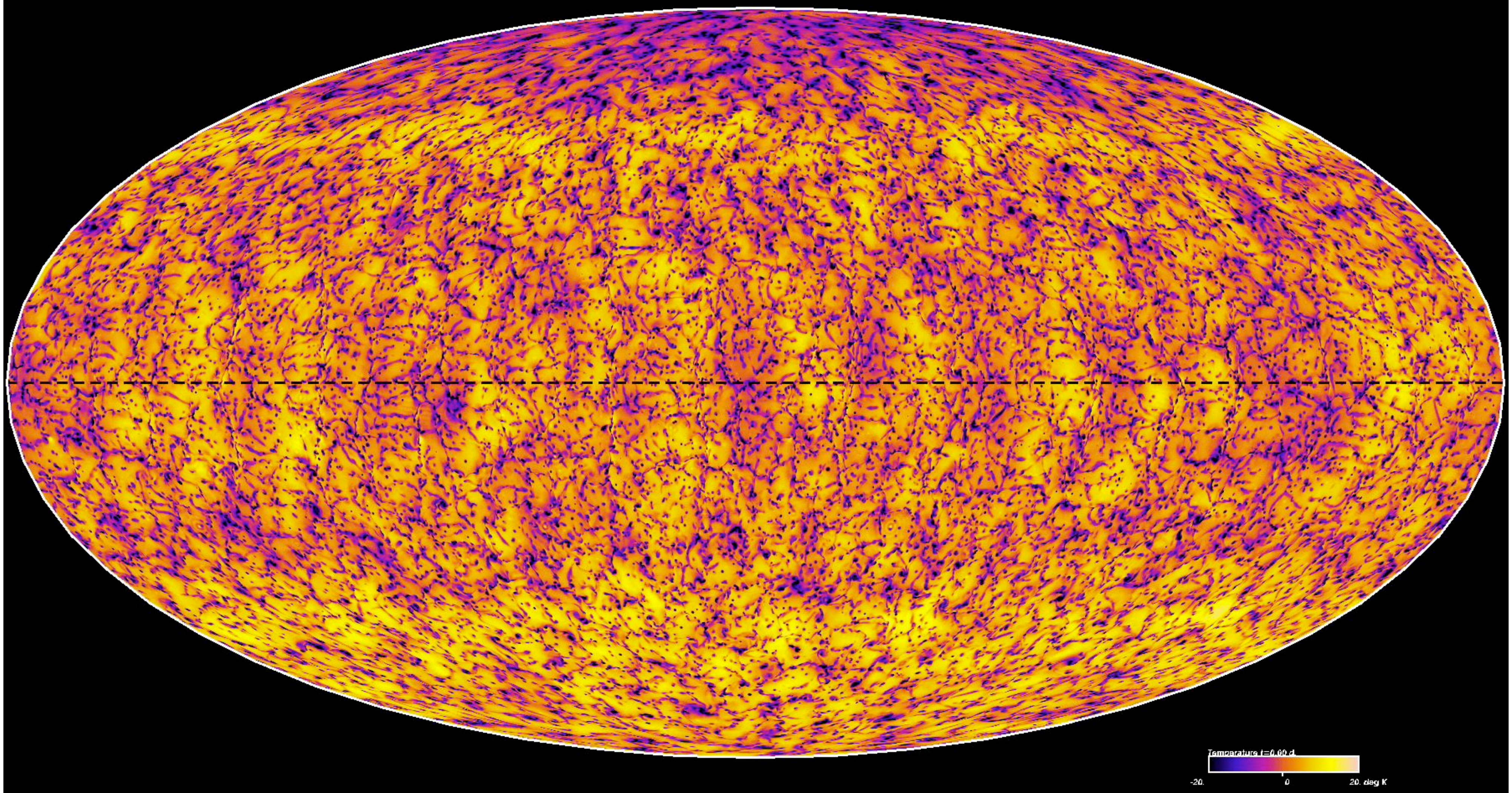

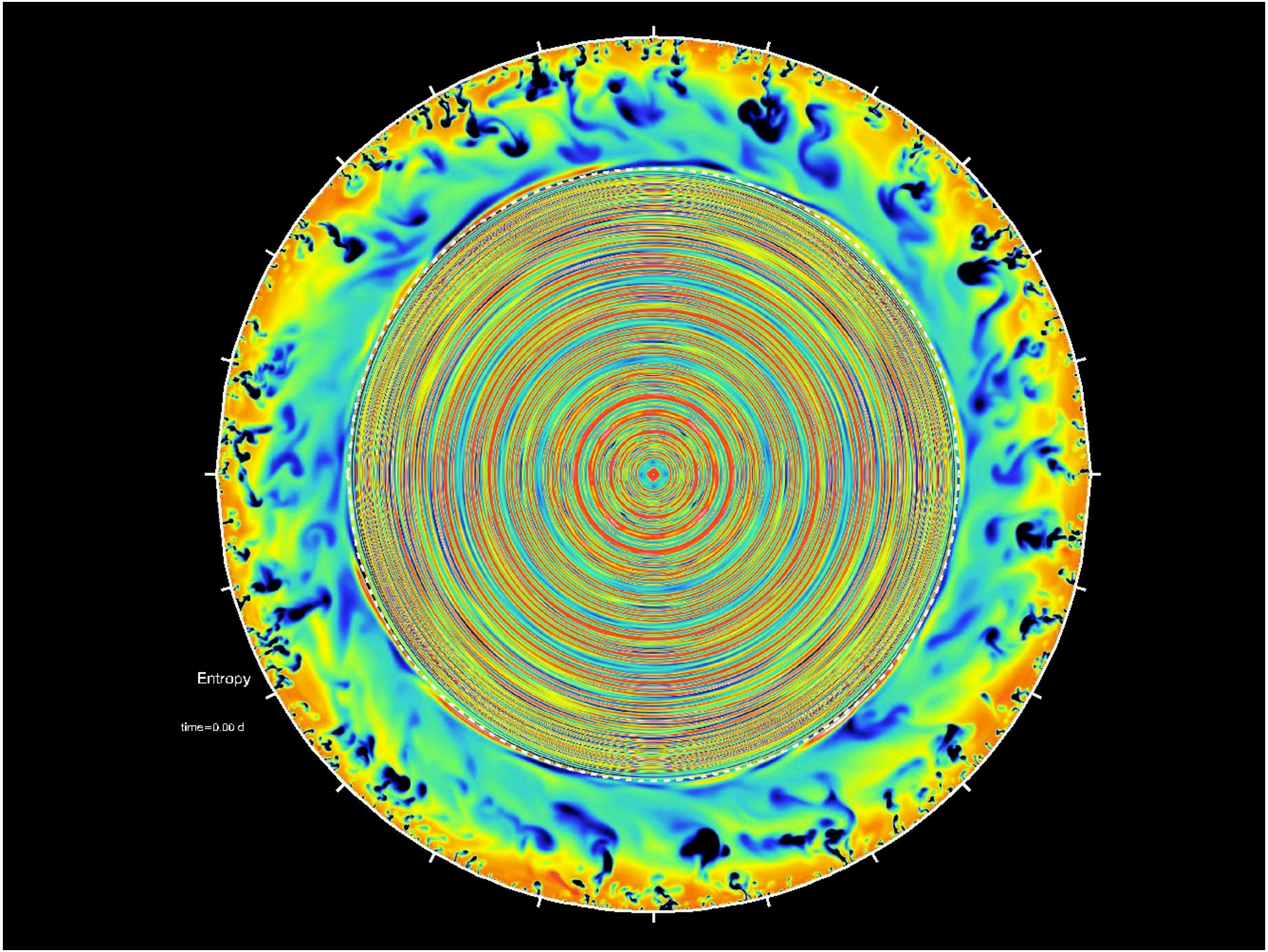
Entropy
time=0.00 d

Our G & K star Models

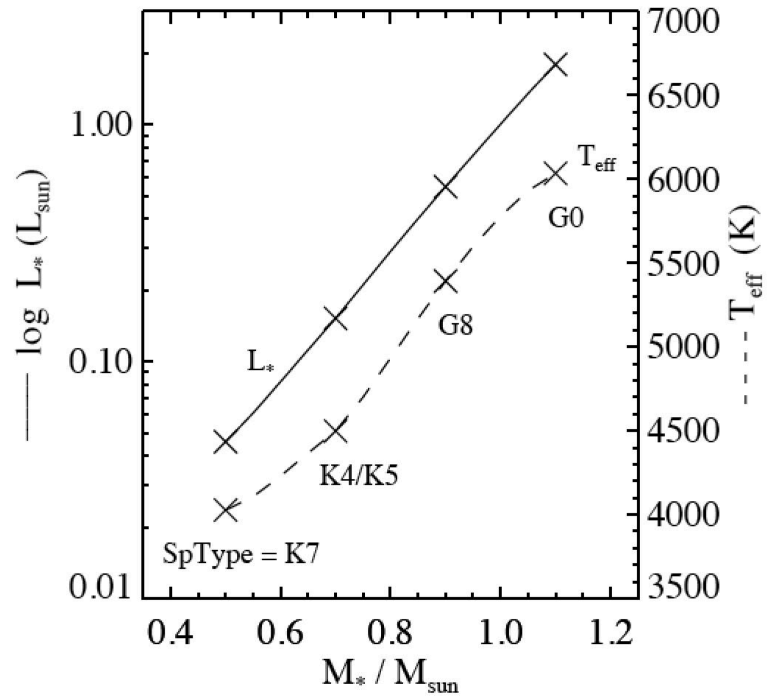

Mass ($M_\odot$)	Radius ($R_\odot$)	L_* ($L_\odot$)	$T_{\rm eff}$ (K)	SpT	$M_{\rm cz}$ ($M_\odot$, M_*)	$R_{\rm cz}$ ($R_\odot$, R_*)
0.5	0.44	0.046	4030	K7	0.18, 0.36	0.25, 0.56
0.7	0.64	0.15	4500	K4/K5	0.079, 0.11	0.42, 0.66
0.9	0.85	0.55	5390	G8	0.042, 0.046	0.59, 0.69
1.1	1.23	1.79	6030	G0	0.011, 0.0100	0.92, 0.75

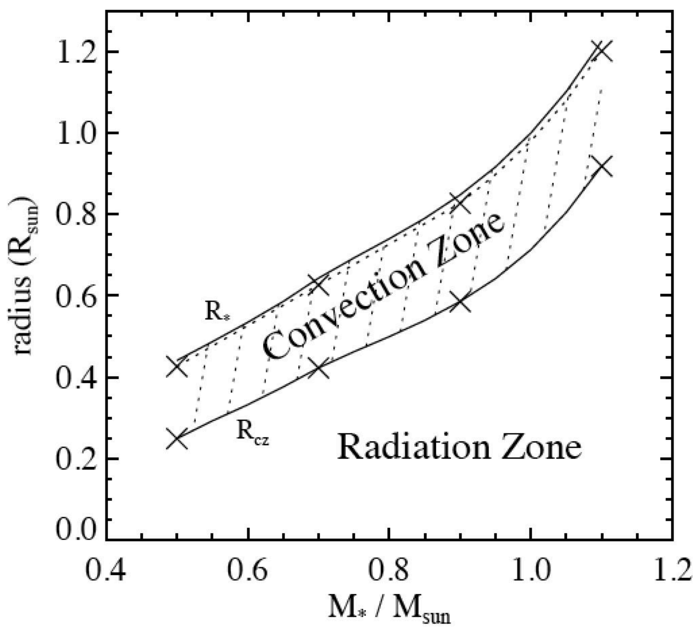

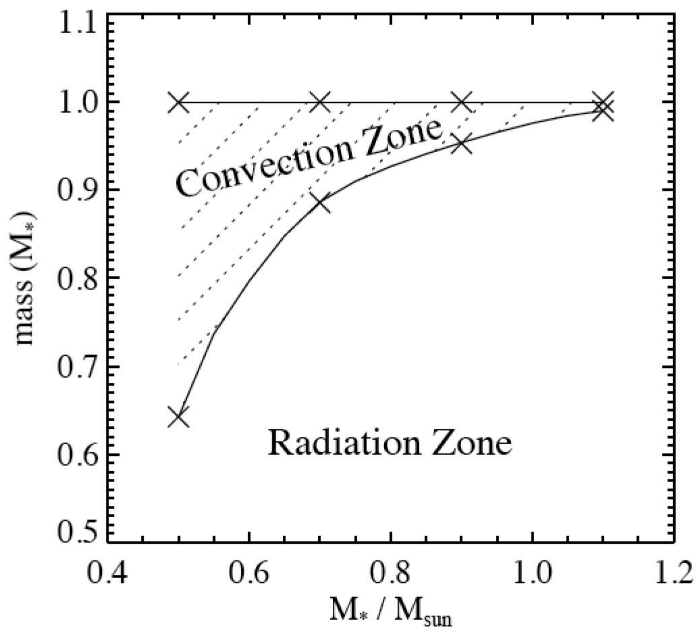

Effect of Rotation on Convection

Matt,…, Brun et al. 2011
Brun et al. 2015, 2017

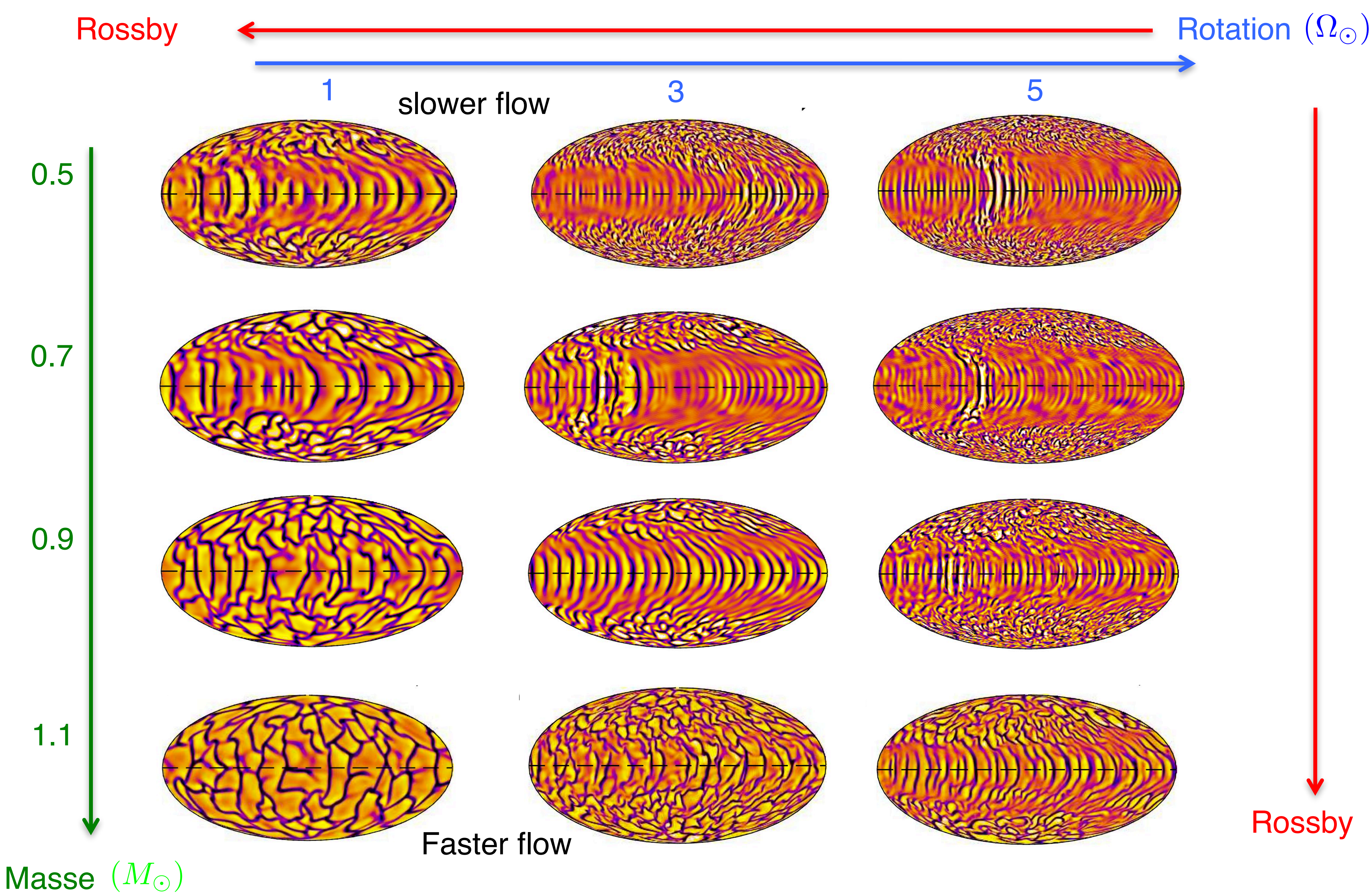

Turbulent Convection in Stars

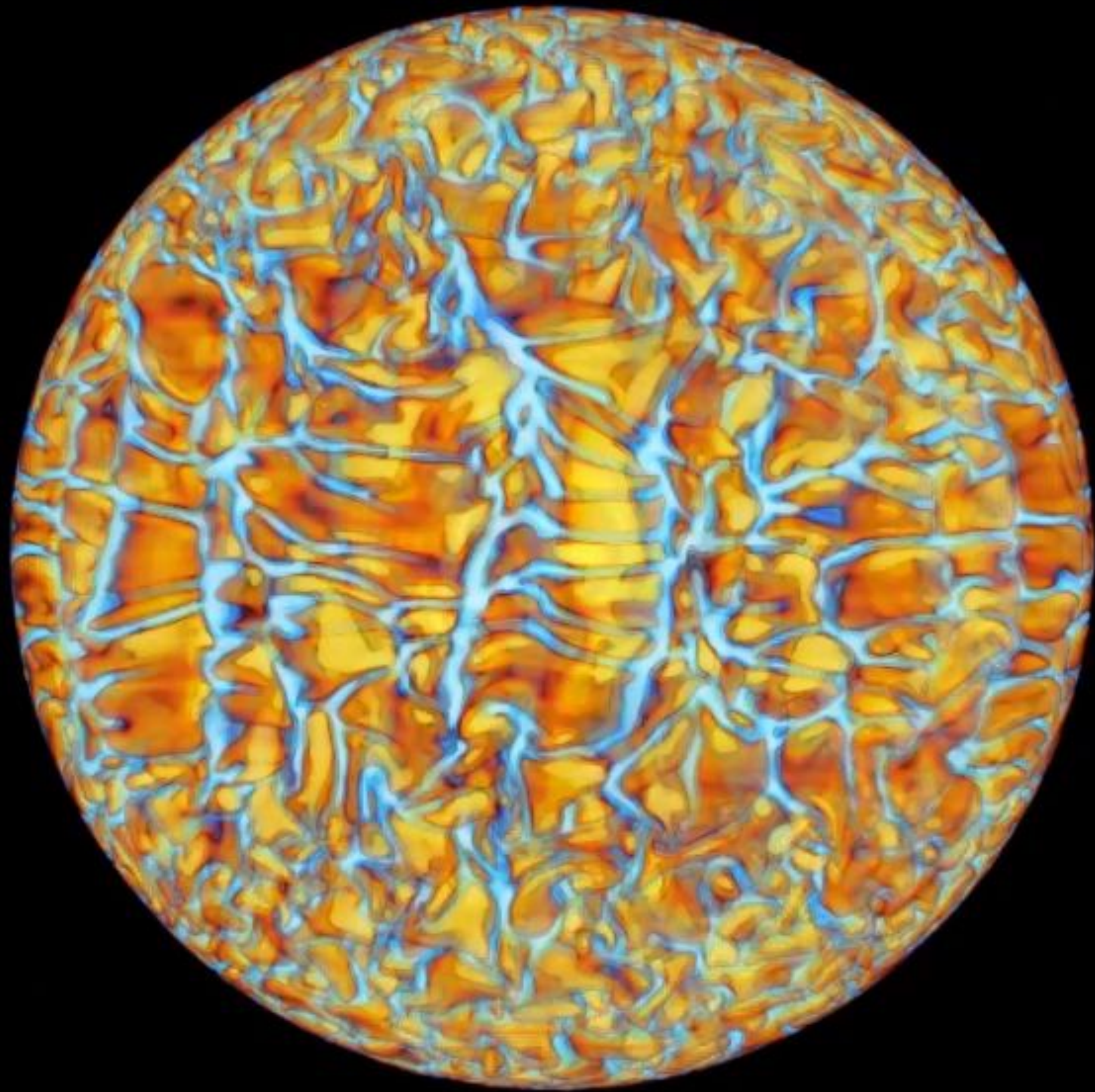

Bessolaz & Brun 2011

Solar Internal Rotation

(GONG, MDI data)

Helioseismology Results

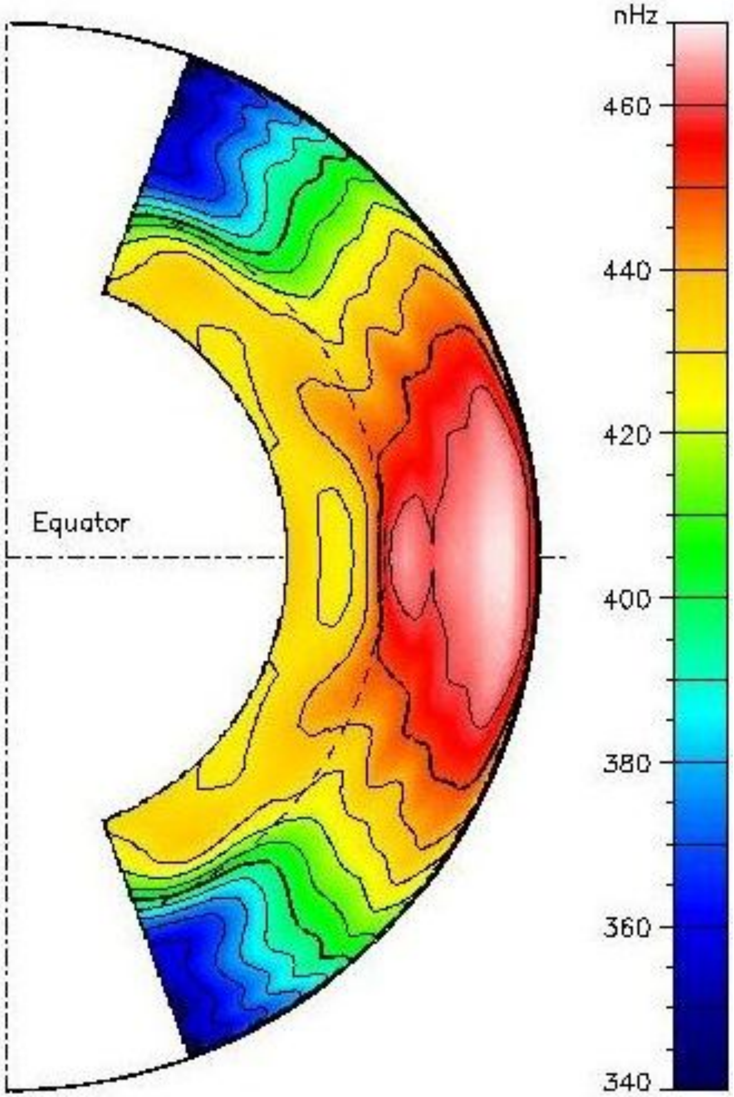

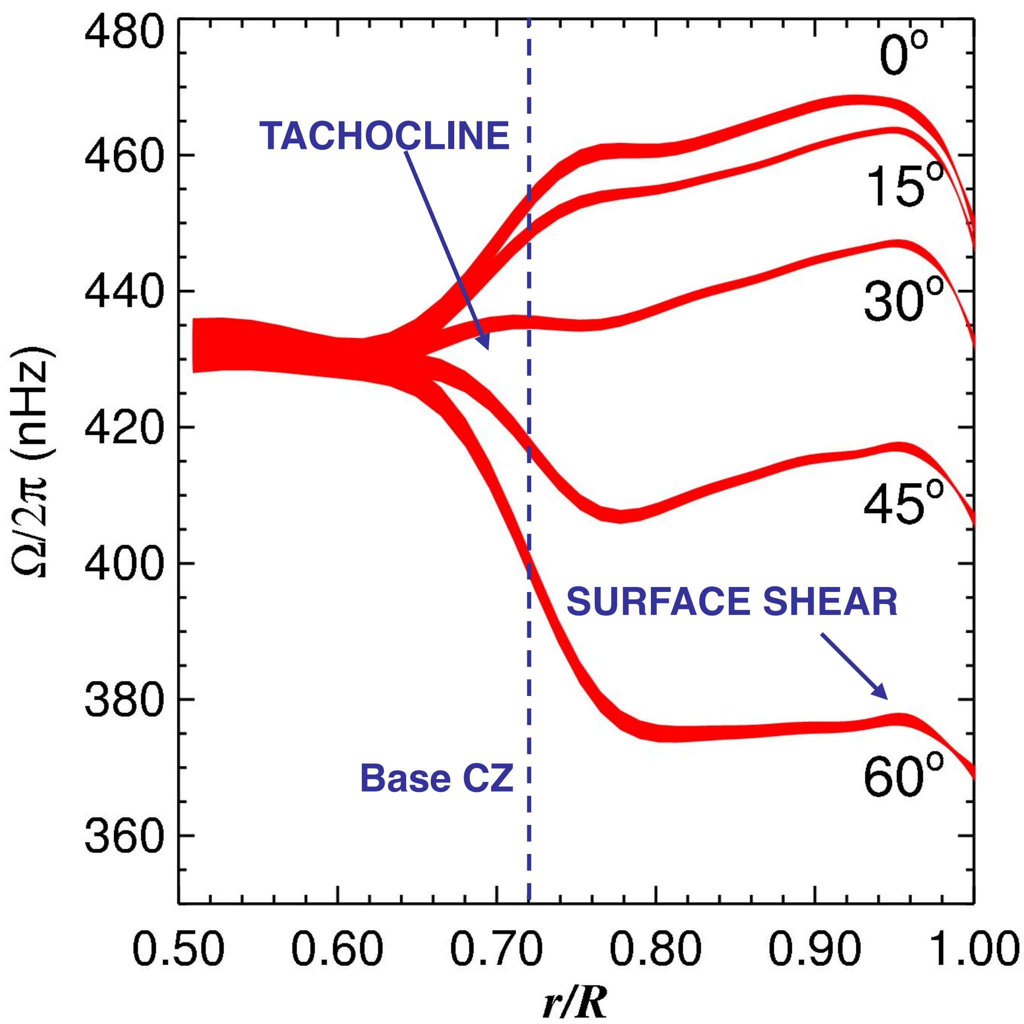

Taylor-Proudman Theorem & Thermal Wind

The curl of the momentum equation gives the equation for vorticity $\omega = \vec{\nabla} \times \vec{v}$:

$$\frac{\partial \vec{\omega}}{\partial t} + \vec{v}.\vec{\nabla}\vec{\omega} - \vec{\omega}.\vec{\nabla}\vec{v} = \nu \vec{\nabla}^2 \vec{\omega} + \frac{1}{\rho^2} \vec{\nabla}\rho \wedge \vec{\nabla} p \qquad \text{(a)}$$

Taylor-Proudman Theorem:

In a stationary state, the φ component of (a) can be simplified to:

$$2\Omega \frac{\partial \hat{v}_\varphi}{\partial z} = 0$$ **=> $v\varphi$ is cst along z**

the differential rotation is cylindrical (Taylor columns) and the flows quasi 2-D.

Thermal Wind:

The presence of cross gradient between p and ρ (baroclinic effects) can break this constraint (as well as Reynolds & viscous stresses) :

$$2\Omega \frac{\partial \hat{v}_\varphi}{\partial z} = -\frac{1}{\hat{\rho}^2} \vec{\nabla}\hat{\rho} \wedge \vec{\nabla}\hat{p}\Big|_\varphi = \frac{1}{\hat{\rho} C_p} \left[\vec{\nabla}\hat{S} \wedge -\hat{\rho}\vec{g}\right]_\varphi = \frac{g}{r C_p} \frac{\partial \hat{S}}{\partial \theta}$$

Baroclinicity

(Brun & Toomre 2002, ApJ, 570, 865)

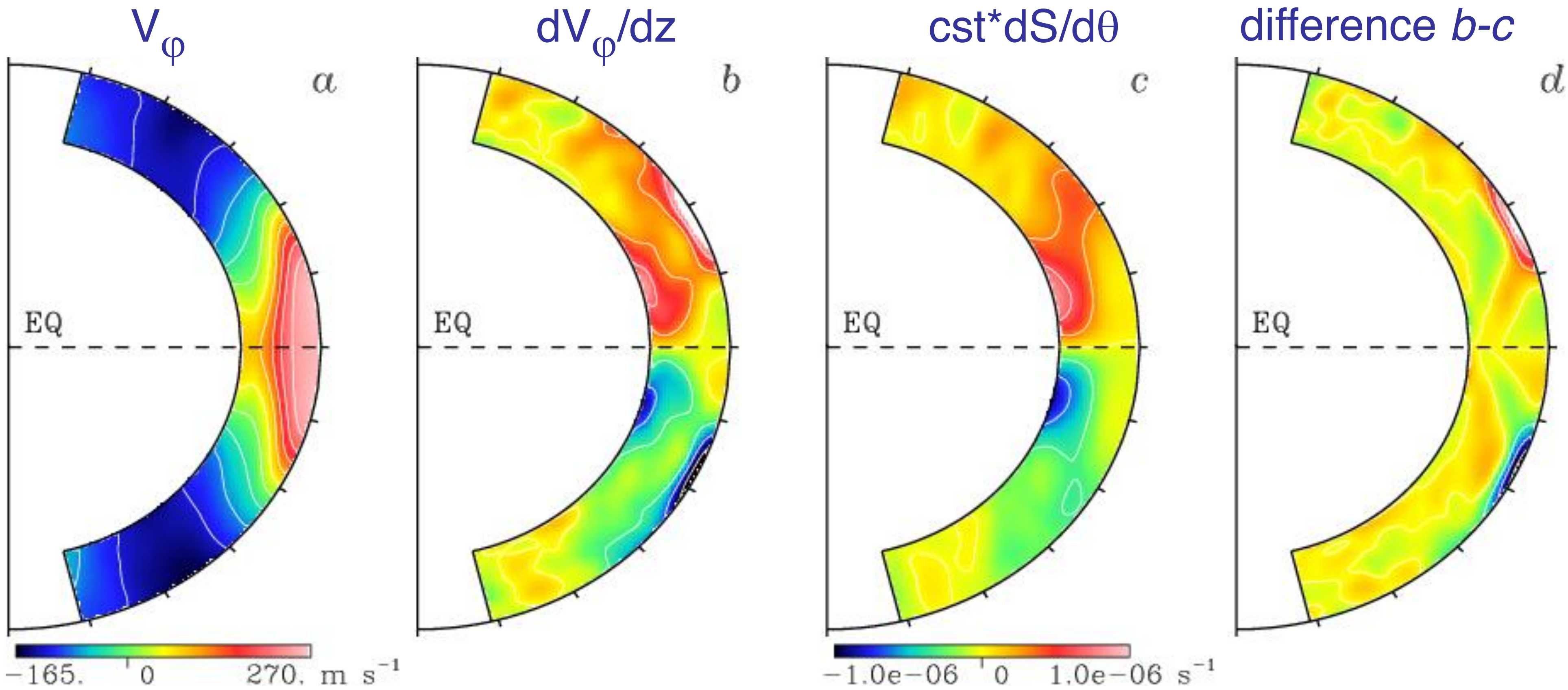

The thermal wind contributes for some but not all of the non cylindrical differential rotation achieved in our simulation.
Reynolds stresses are the dominant players confirming the dynamical origin of Ω

Baroclinicity

Entropy

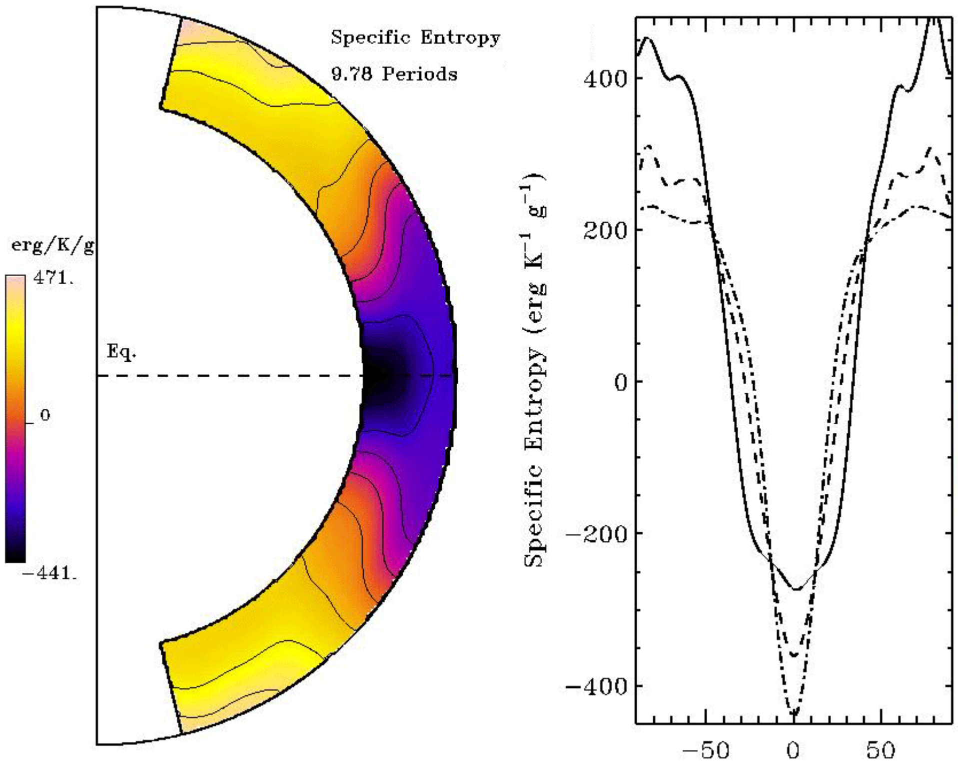

Temperature

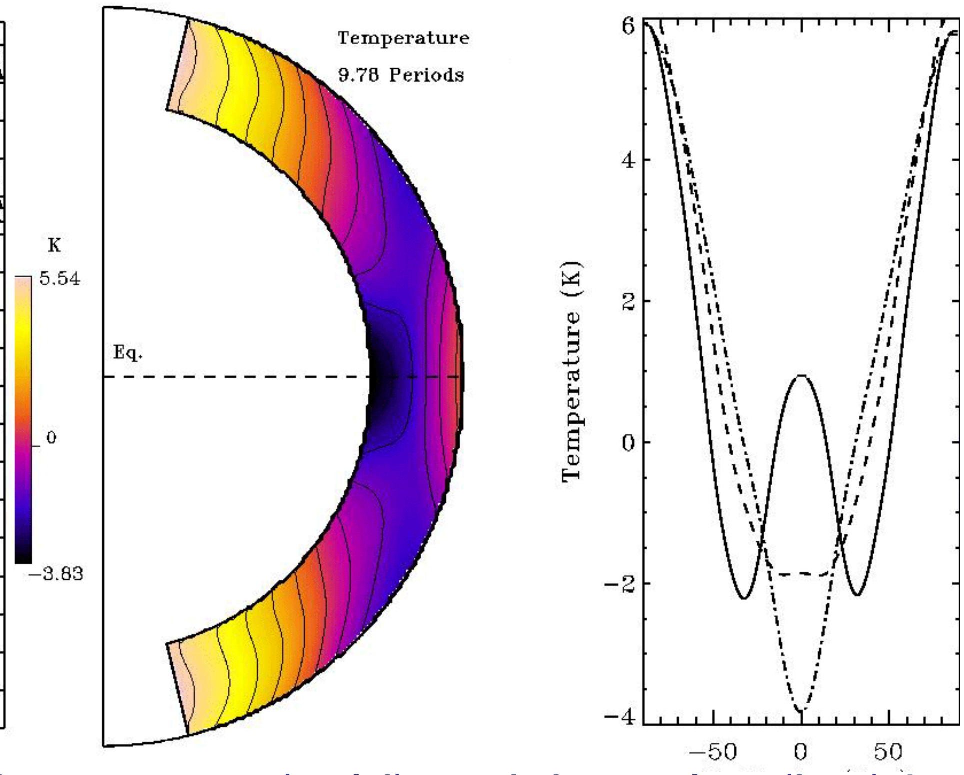

A variation of few degree K between the equator (cold) and the poles (hot) is established for a contrast of Ω of 30%

Thermal BC's Influence

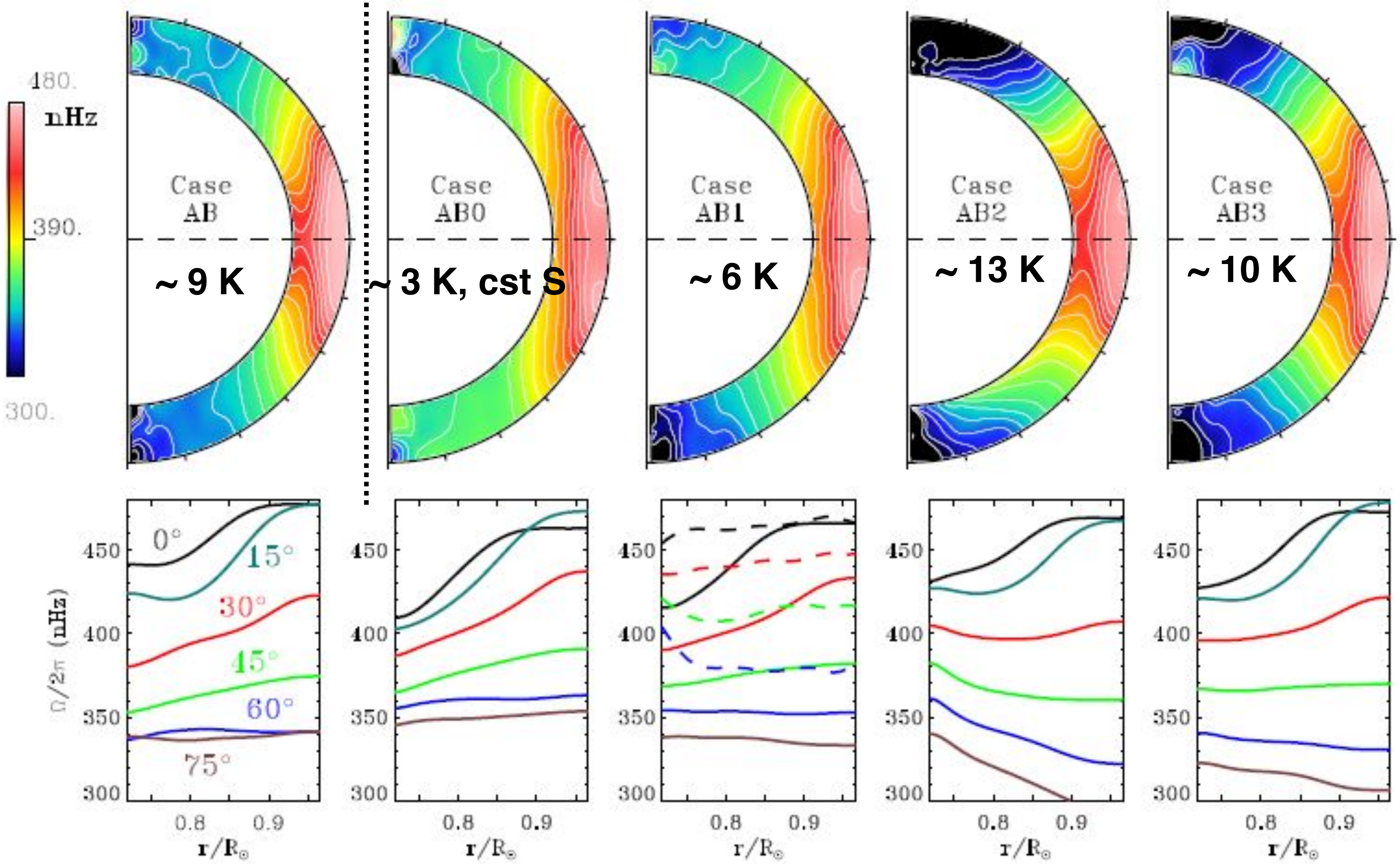

Miesch, Brun & Toomre 2006

Trends in Differential Rotation with Ω & Mass (Teff)

Weak trend with Ω

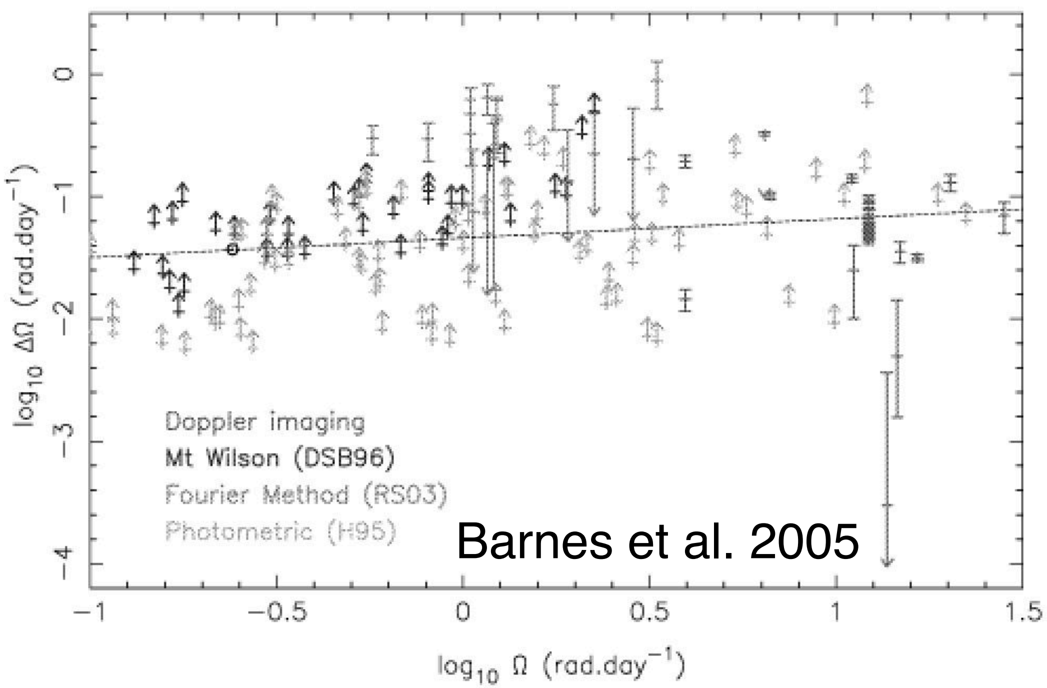

Barnes et al. 2005

$\Delta\Omega$ increases with M_*

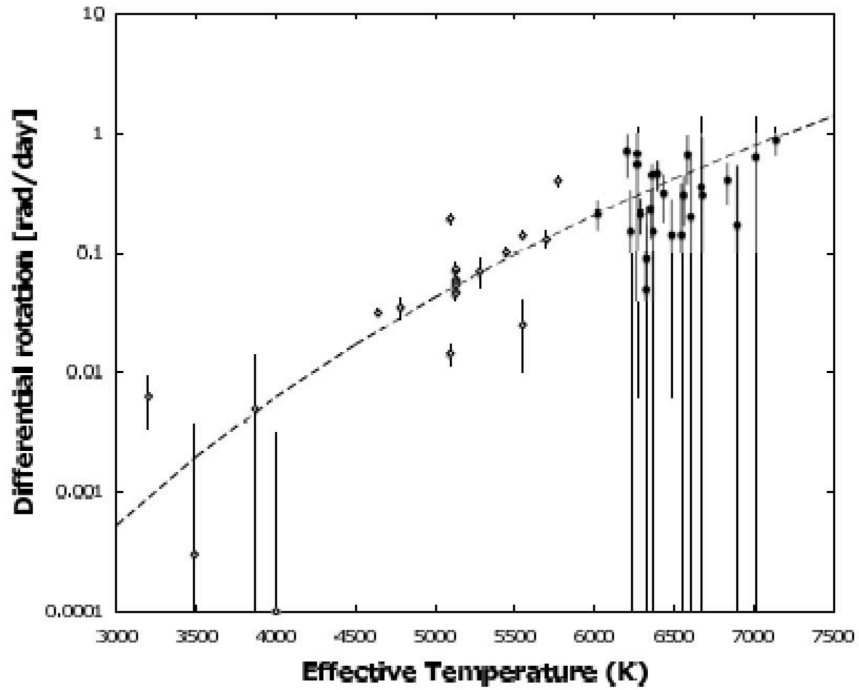

Collier-Cameron 2007

In Donahue et al. 1996: $\Delta\Omega$ propto $\Omega^{0.7}$

Confirming these observational scaling is key

Differential Rotation In G & K stars

Matt et al. 2011
Brun et al. 2015, 2017

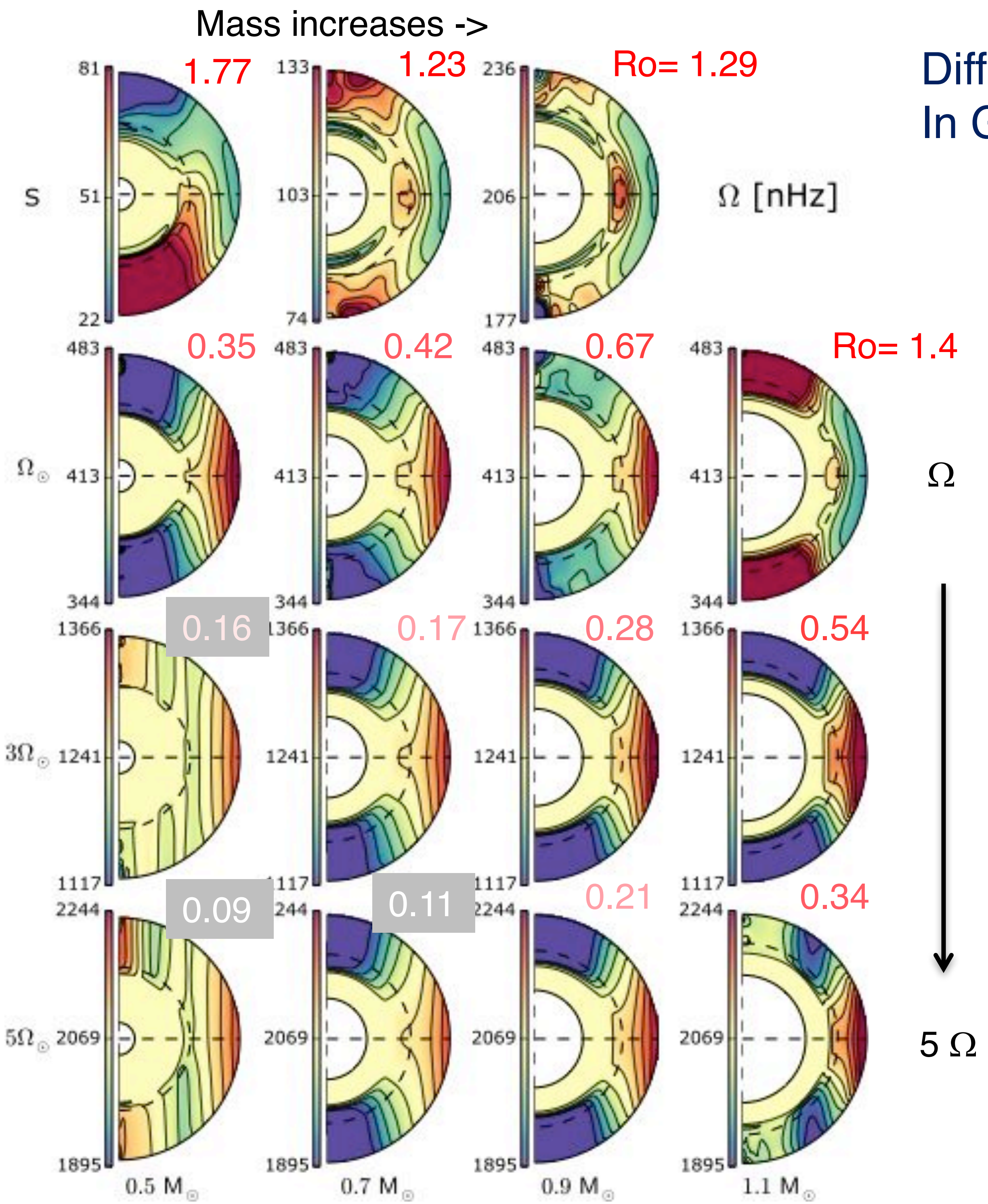

Rossby nb
$Ro = \omega / 2\Omega_*$

Rotation
Increases

Rossby Number vs Stellar Mass and Rotation

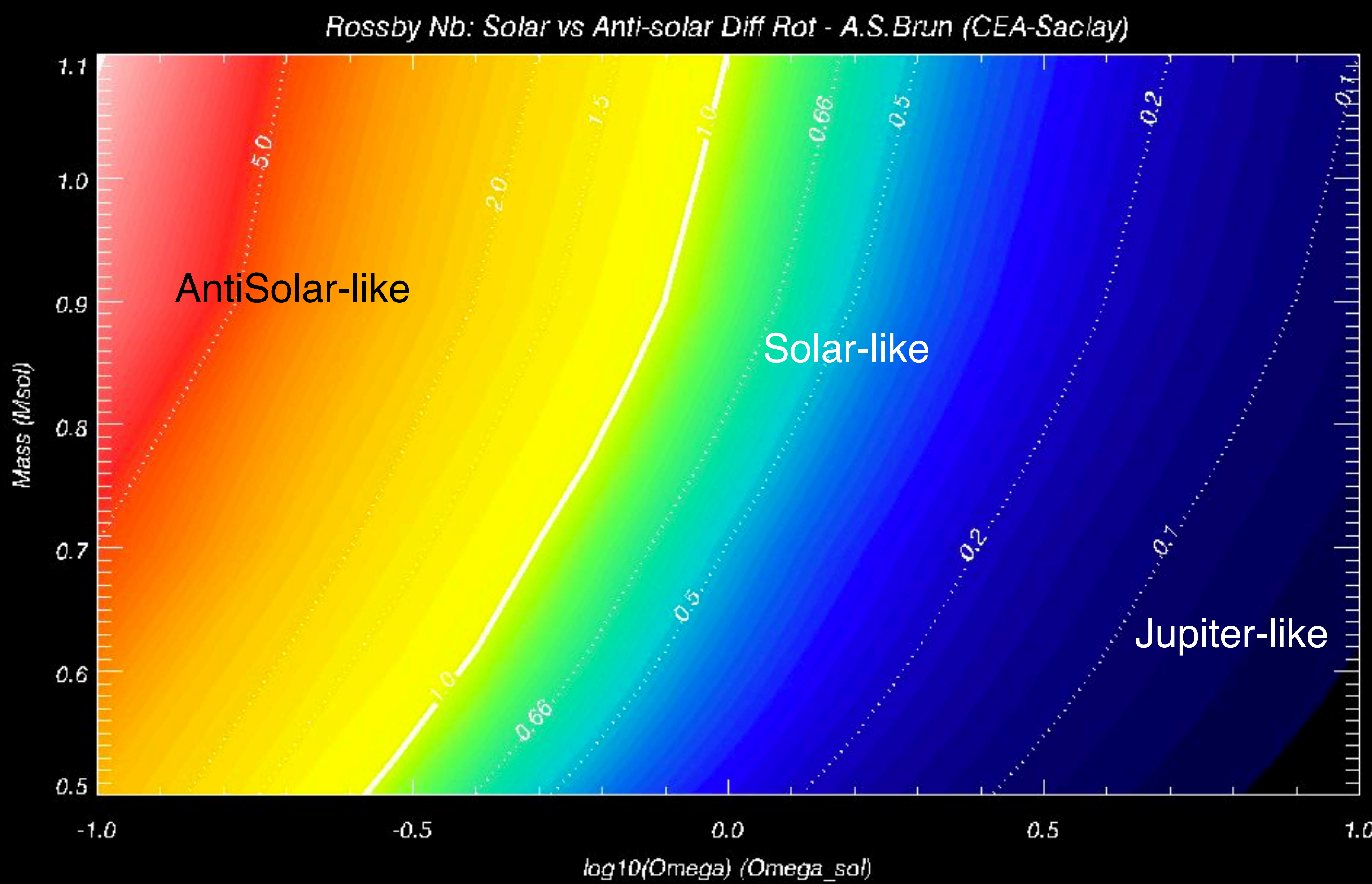

Brun et al. 2015, 2017

Scaling Law for $\Delta\Omega$

Matt et al. 2011, 2013

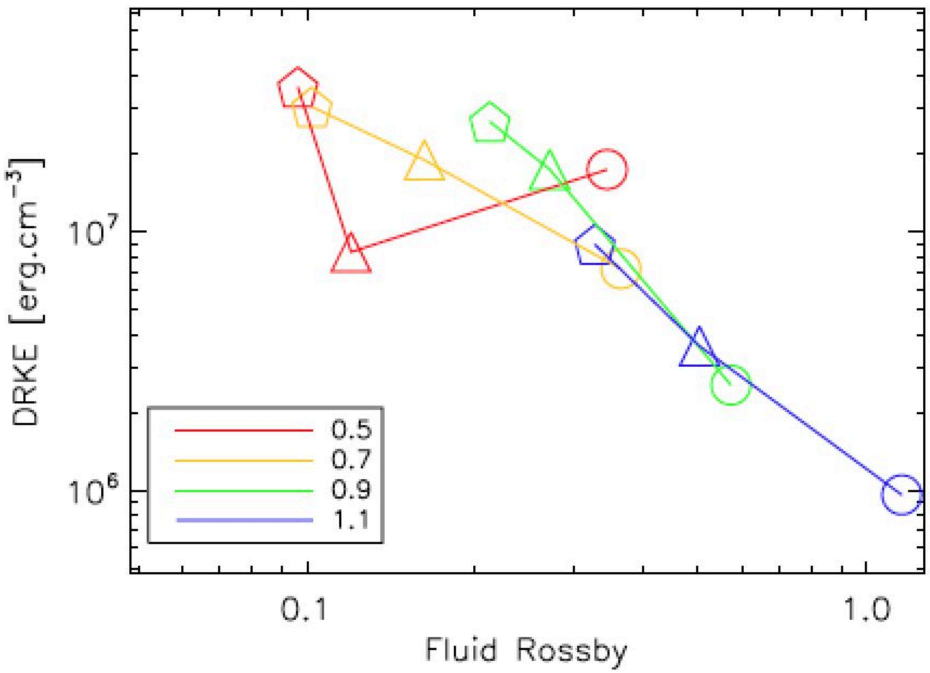

1.2, 1.3 M

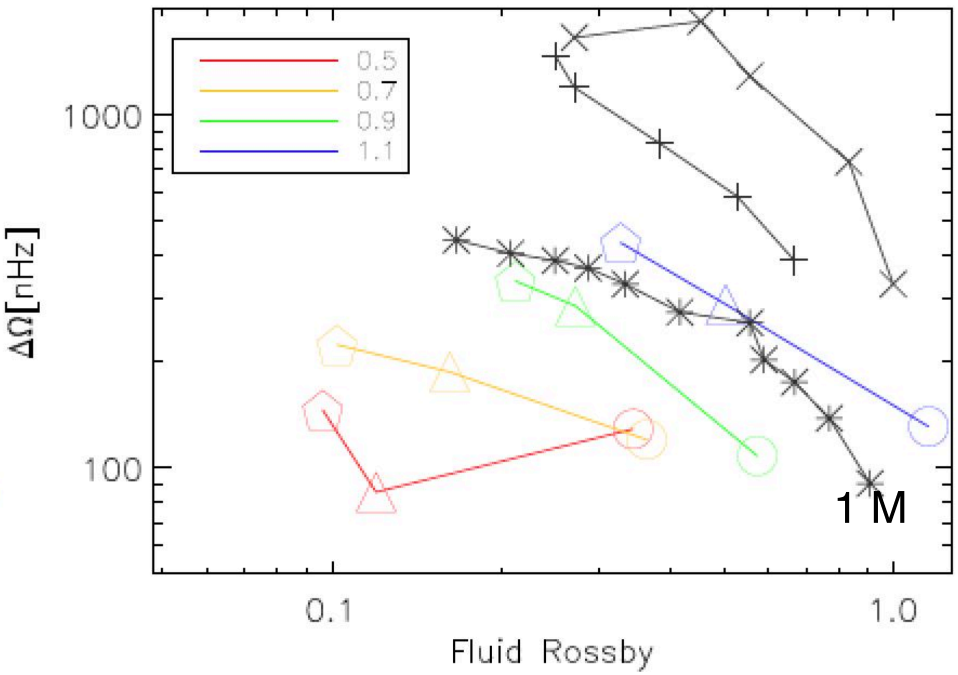

Brown et al. 2008
Augustson et al. 2012

$$\Delta\Omega = 156.0\ \mathrm{nHz}\left(\frac{M}{M_\odot}\right)^{1.0}\left(\frac{\Omega_0}{\Omega_\odot}\right)^{0.47}$$
$$= 150.3\ \mathrm{nHz}\left(\frac{M}{M_\odot}\right)^{1.85} R_{of}^{-0.52}$$

Smaller $\Delta\Omega$ with smaller Mass

Solar Cycle and Rotation

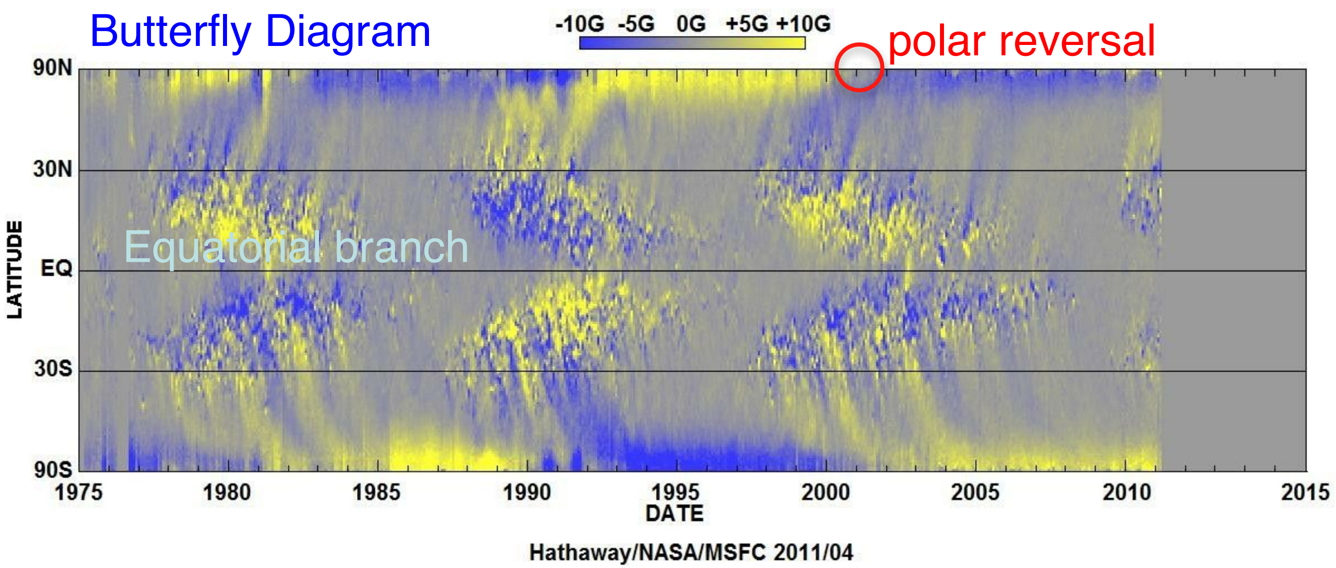

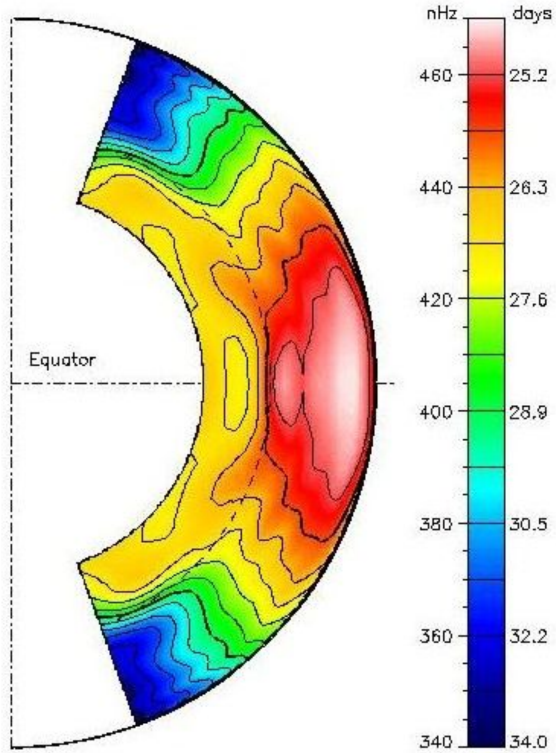

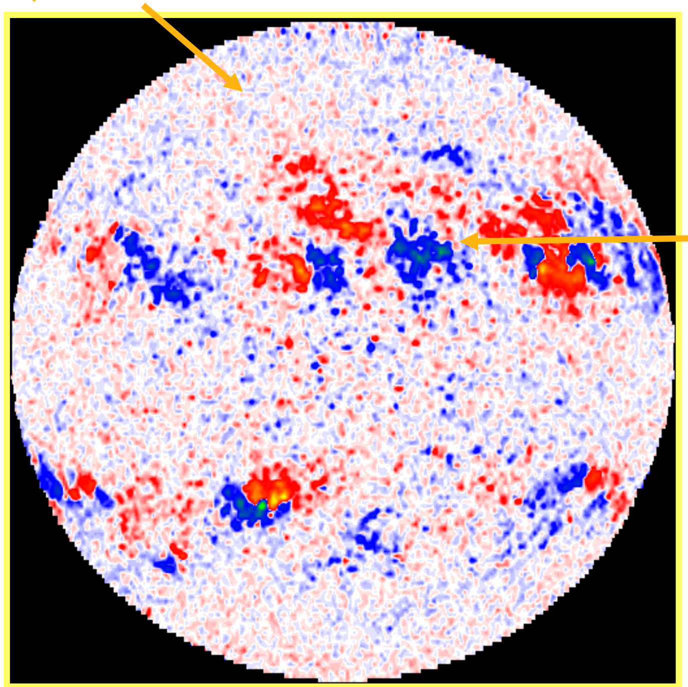

Small vs Large Scale Dynamos

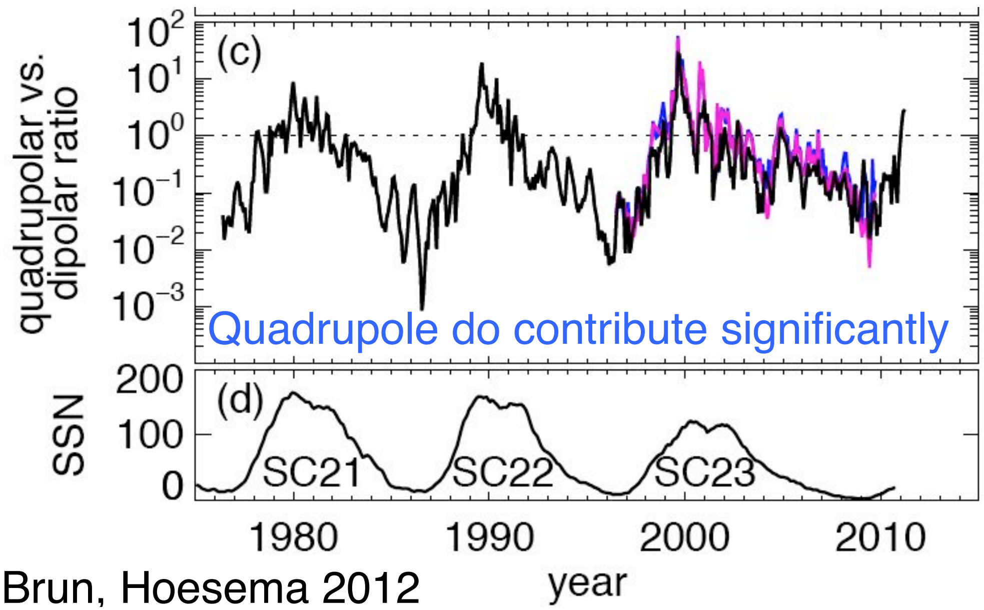

Derosa, Brun, Hoesema 2012

Magnetic Fields in Various Objects

Most Figures from: The Cosmic Perspective, Bennett et al. 2003, ed. Pearson or ESA, NASA.

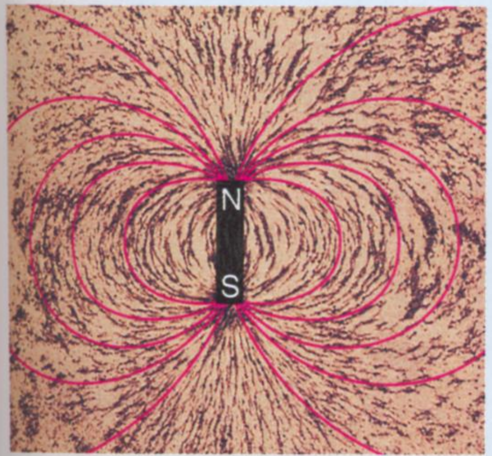

a This photo shows how a bar magnet influences iron filings (small black specks) around it. The *magnetic field lines* (red) represent this influence graphically.

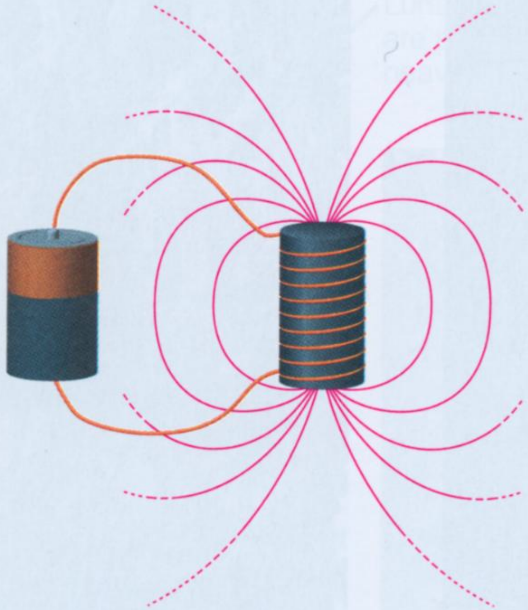

b A similar magnetic field is created by an electromagnet, which is essentially a coiled wire attached to a battery. The field is created by the battery-forced motion of charged particles (electrons) along the wire.

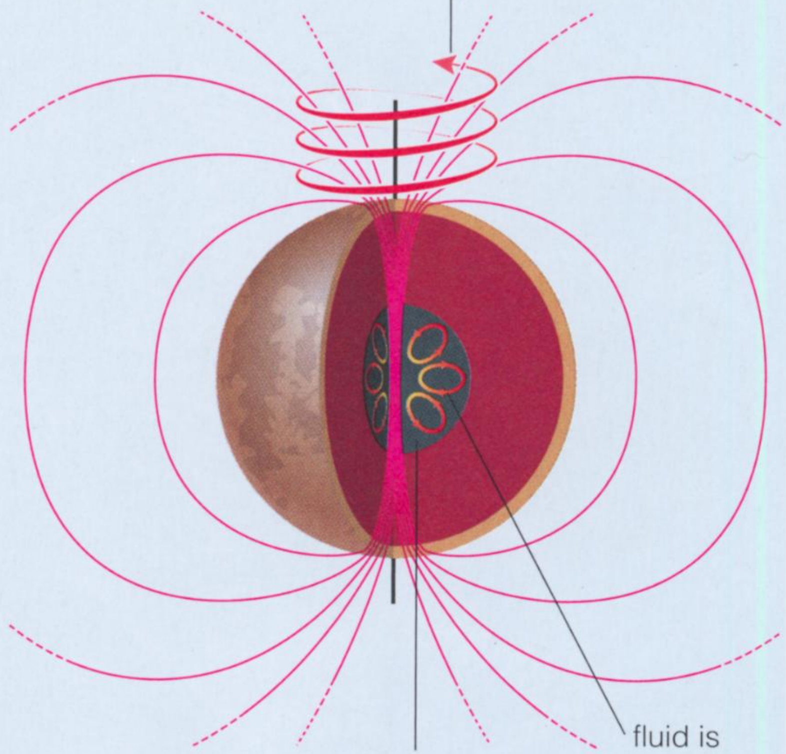

c A planet's magnetic field also arises from the motion of charged particles. The charged particles in a terrestrial planet are in a molten metallic core, and their motion arises from the planet's rotation and interior convection.

Champ magnétique B, décroit en un temps Ohmique: $\tau_\eta = \frac{R^2}{\eta}$

Ce temps est long sauf en laboratoire et dans les petits corps célestes comme les satellites naturels (lunes) ou planètes, donc la présence de B dans les planètes et la variabilité de B dans certains corps (étoiles, galaxies) => effet dynamo

Maxwell's Equation (cgs)

$$\nabla \cdot \mathbf{E} = 4\pi\rho, \quad (4)$$

$$\nabla \times \mathbf{E} = -\frac{1}{c}\frac{\partial \mathbf{B}}{\partial t}, \quad (5)$$

$$\nabla \cdot \mathbf{B} = 0, \quad (6)$$

$$\nabla \times \mathbf{B} = \frac{4\pi}{c}\mathbf{J} + \frac{1}{c}\frac{\partial \mathbf{E}}{\partial t} \quad (7)$$

Remarque: 3 types de matériaux magnétiques ($\boldsymbol{B}=\mu\boldsymbol{H}$, $\boldsymbol{B}$ champ magnétique):
Diamagnétisme (perméabilité magnétique $\mu<1$): la plus part des matériaux sont diamagnétiques (l'eau par ex) (répulsion limitant le champ extérieur imposé) (couches électronique pleines)
Paramagnétique ($\mu>1$): attraction faible (couches électroniques non pleines) (aluminium par ex)
Ferromagnétique ($\mu>>1$): attraction forte, existence de domaines magnétiques par orientation favorable des spins électroniques, magnétisation résiduelle (hysteresis) (le fer par ex).

Induction Equation

A partir des équations de Maxwell (5) et (7), en négligeant le courant de déplacement (valable si v << c):

$$\frac{\partial \mathbf{B}}{\partial t} = -c\boldsymbol{\nabla} \times \mathbf{E} \text{ et } \mathbf{J} = \frac{c}{4\pi}(\boldsymbol{\nabla} \times \mathbf{B}),$$

et de loi d'Ohm, pour un fluide conducteur en mouvement à la vitesse $\mathbf{v}$:

$$\mathbf{J} = \sigma\left(\mathbf{E} + \frac{\mathbf{v} \times \mathbf{B}}{c}\right)$$

on peut déduire l'équation d'induction:

Induction Equation

$$\frac{\partial \mathbf{B}}{\partial t} = -c\boldsymbol{\nabla}\times\mathbf{E} = -\boldsymbol{\nabla}\times\left(\frac{c\mathbf{J}}{\sigma} - \mathbf{v}\times\mathbf{B}\right)$$

$$= -\boldsymbol{\nabla}\times\left(\frac{c^2}{4\pi\sigma}\boldsymbol{\nabla}\times\mathbf{B} - \mathbf{v}\times\mathbf{B}\right)$$

$$\boxed{\frac{\partial \mathbf{B}}{\partial t} = \boldsymbol{\nabla}\times(\mathbf{v}\times\mathbf{B}) - \boldsymbol{\nabla}\times(\eta\boldsymbol{\nabla}\times\mathbf{B})} \quad (8)$$

avec $\eta = c^2/4\pi\sigma$ la diffusivité magnétique,

$$\frac{\partial \mathbf{B}}{\partial t} = \boldsymbol{\nabla}\times(\mathbf{v}\times\mathbf{B}) + \eta\Delta\mathbf{B}, \text{ si } \eta = cst.$$

MHD Equations

Continuity, Navier-Stokes, Internal Energy (+ Lorentz force + Ohmic diffusion):

$$\begin{aligned} \frac{\partial \rho}{\partial t} &= -\boldsymbol{\nabla}\cdot(\rho\mathbf{v}), && (1)\\ \rho\frac{\partial \mathbf{v}}{\partial t} &= -\rho(\mathbf{v}\cdot\boldsymbol{\nabla})\mathbf{v} - \boldsymbol{\nabla}P + \rho\mathbf{g} - 2\rho\boldsymbol{\Omega}_{\mathbf{o}}\times\mathbf{v} \\ &- \boldsymbol{\nabla}\cdot\boldsymbol{\mathcal{D}} + \boxed{\frac{1}{4\pi}(\boldsymbol{\nabla}\times\mathbf{B})\times\mathbf{B}}, && (2)\\ \rho T\frac{\partial S}{\partial t} &= -\rho T(\mathbf{v}\cdot\boldsymbol{\nabla})S + \boldsymbol{\nabla}\cdot(\kappa_r\rho c_p\boldsymbol{\nabla}T) + \boxed{\frac{4\pi\eta}{c^2}\mathbf{J}^2} \\ &+ 2\rho\nu\left[e_{ij}e_{ij} - 1/3(\boldsymbol{\nabla}\cdot\mathbf{v})^2\right] + \rho\epsilon, && (3) \end{aligned}$$

plus induction:

$$\frac{\partial \mathbf{B}}{\partial t} = \boldsymbol{\nabla}\times(\mathbf{v}\times\mathbf{B}) - \boldsymbol{\nabla}\times(\eta\boldsymbol{\nabla}\times\mathbf{B}) \qquad (8)$$

The Dynamo Effect what is it exactly?

The main source of magnetic filed in the Universe is the due to dynamo action:

<u>A definition</u>: this is the property that a conducting fluid possesses to generate a magnetic field B via its motions (self-induction) and to sustain it against Ohmic dissipation

This is intrinsically a tri dimensional effect, there is for exemple an anti-dynamo Theorem (Cowling's theorem) forbidding purely axisymmetric dynamos

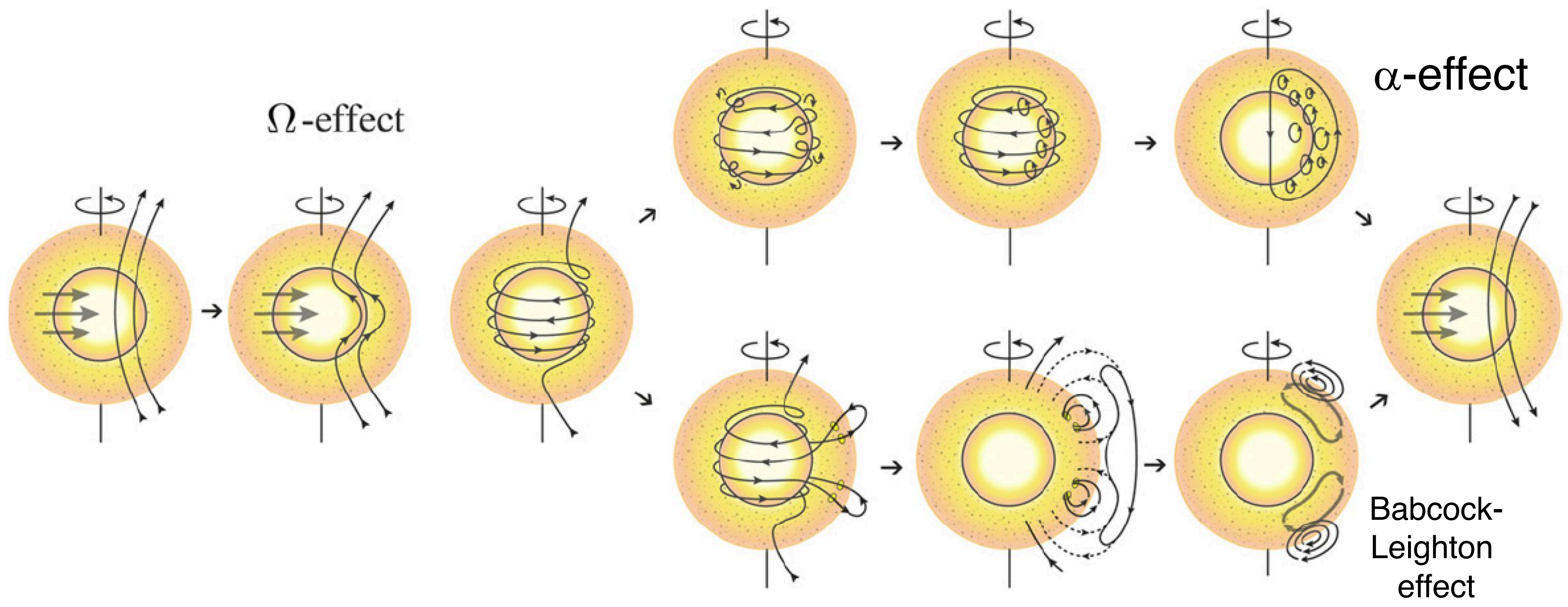

Few Remarques on Induction Equation

$$\frac{\partial \mathbf{B}}{\partial t} = \nabla \times (\mathbf{v} \times \mathbf{B}) + \eta \Delta \mathbf{B}$$

If the fluid is at rest, induction equation becomes: $$\frac{\partial \mathbf{B}}{\partial t} = \eta \Delta \mathbf{B}$$

This is a diffusion equation, the magnetic field **B** decays in a uniform sphere of radius R in a Ohmic time scale:

$$\tau_\eta = \frac{R^2}{\pi^2 \eta}$$

In laboratory, τ_η is small (10 s for a 1m copper sphere), but in cosmic conductors it can be huge (> 10^{10} yr)

By opposition if the fluid is in motion (and its resistivity negligible), the equation becomes:

$$\frac{\partial \mathbf{B}}{\partial t} = \nabla \times (\mathbf{v} \times \mathbf{B})$$

This mean that magnetic field lines are « frozen » in the fluid

(cf. E. Pariat's talk)

Few Remarques on Induction Equation

The magnetic Reynolds $Rm = vL/\eta$ allow us to know in which state the system under study is, it is usually small in laboratory experiments ($Rm \sim 1$ et < 50) & very large in cosmic bodies. You can expect (fast) dynamo action to occur if Rm is sufficiently large.

This means that in laboratory experiments electic currents and mainly determined by the conductivity σ, whereas in a cosmic body σ n'a as little influence on the amplitude of currents and $\mathbf{B}$. In these objects conductivity is used to determined the electric fielf $\mathbf{E}$ (weak) needed to have these currents (Cowling 1957).

Remarque: First term of induction equation can be slipt in 3 parts,

$$\nabla \times (\mathbf{v} \times \mathbf{B}) = (\mathbf{B} \cdot \nabla)\mathbf{v} - (\mathbf{v} \cdot \nabla)\mathbf{B} + \mathbf{B}\nabla \cdot \mathbf{v}$$

one term (1st) about distortion and shearing of $\mathbf{B}$, one term advection transport, and last term linked to compressibility of the fluid (null if Div v =0).

2-D vs 3-D Models: Pro's and Con's

- Solve for axisymmetric induction equation => add alpha effect
- alpha effect, toroidal -> poloidal
- or surface source term (Babcock-Leigthon), toroidal -> poloidal
- Assume Dfferential rotation profile => Omegaeffect (pol->tor)
- Kinematic regime (no feed back on flow)
- prescribe meridional circulation or turbulent pumping

Pros: Fast so large parameter space study.
Fine tuning of effects possible

Cons: Kinematic, no convection, prescribe ingredients that are not self-consitant with one another

- Solve full MHD equations
- Dynamical regime, feed back on the flow
- Models with or without convection including all transport processes
- Nonlinear Dynamo action
- Some models impose tachocline others don't

Pros: Dynamical, all effects are self-consistent, 3-D modulation

Cons: slow so small parameter space study, still in the "building block" approach, no full models yet, but getting there…..
Comparison to magnetic observations less easy

=> Need both approaches

Kinematic Mean Field Theory

Starting point is the magnetic induction equation of MHD:

$$\frac{\partial \mathbf{B}}{\partial t} = \nabla \times (\mathbf{u} \times \mathbf{B}) + \eta \nabla^2 \mathbf{B},$$

where **B** is the magnetic field, **u** is the fluid velocity and η is the magnetic diffusivity (assumed constant for simplicity).

Assume scale separation between large- and small-scale field and flow:

$$\mathbf{B} = \mathbf{B}_0 + \mathbf{b}, \quad \mathbf{U} = \mathbf{U}_0 + \mathbf{u},$$

where **B** and **U** vary on some large length scale L, and **u** and **b** vary on a much smaller scale l.

$$\langle \mathbf{B} \rangle = \mathbf{B}_0, \quad \langle \mathbf{U} \rangle = \mathbf{U}_0,$$

where averages are taken over some intermediate scale $l \ll a \ll L$.

For simplicity, ignore large-scale flow, for the moment.

Induction equation for mean field:

$$\frac{\partial \mathbf{B}_0}{\partial t} = \nabla \times \mathbf{E} + \eta \nabla^2 \mathbf{B}_0,$$

where mean emf is $\mathcal{E} = \langle \mathbf{u} \times \mathbf{b} \rangle.$

This equation is exact, but is only useful if we can relate $\mathcal{E}$ to $\mathbf{B}_0$.

Consider the induction equation for the fluctuating field:

$$\frac{\partial \mathbf{b}}{\partial t} = \nabla \times (\mathbf{u} \times \mathbf{B}_0) + \nabla \times \mathbf{G} + \eta \nabla^2 \mathbf{b},$$

Where $\mathbf{G} = \mathbf{u} \times \mathbf{b} - \langle \mathbf{u} \times \mathbf{b} \rangle.$ "pain in the neck term"

If, G is small, then (mean emf), can be expanded around $<B>_\phi$ as:

$$< \mathcal{E}_i >_\phi = < (u \times b)_i >_\phi = \alpha_{ij} < B_j >_\phi + \beta_{ijk} \frac{\partial < B_j >_\phi}{\partial x_k} + \ldots$$

BASIC PROPERTIES OF THE MEAN FIELD EQUATIONS

Add back in the mean flow U_0 and the mean field equation becomes

$$\frac{\partial \mathbf{B}_0}{\partial t} = \nabla \times (\alpha \mathbf{B}_0 + \mathbf{U}_0 \times \mathbf{B}_0) + (\eta + \beta)\nabla^2 \mathbf{B}_0.$$

ici α et β considérés isotropes

Now consider simplest case where $\alpha = \alpha_0 \cos\theta$ and $U_0 = U_0 \sin\theta\, e_\phi$

In contrast to the induction equation, this can be solved for axisymmetric mean fields of the form $\mathbf{B}_0 = B_{0t}\mathbf{e}_\varphi + \nabla \times (A_{0P}\mathbf{e}_\varphi)$

The Ω effect

Conversion of poloidal to toroidal field by differential rotation.

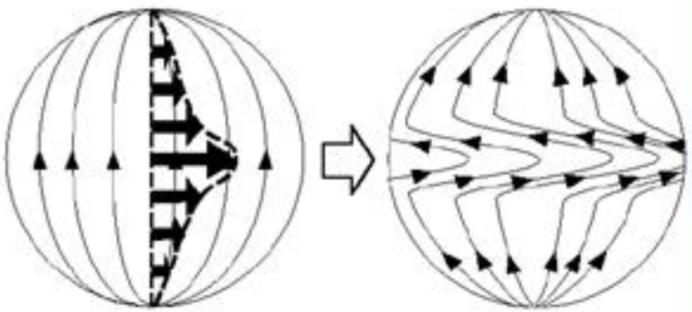

The α effect

Regeneration of poloidal field from toroidal by cyclonic events in rotating convection.

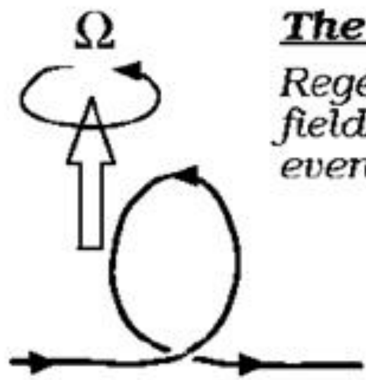

Transport & generation of toroidal field Btor

Jouve & Brun 2007, 2009, 2013, 2017

Omega effect (Ω): winding up of magnetic field lines

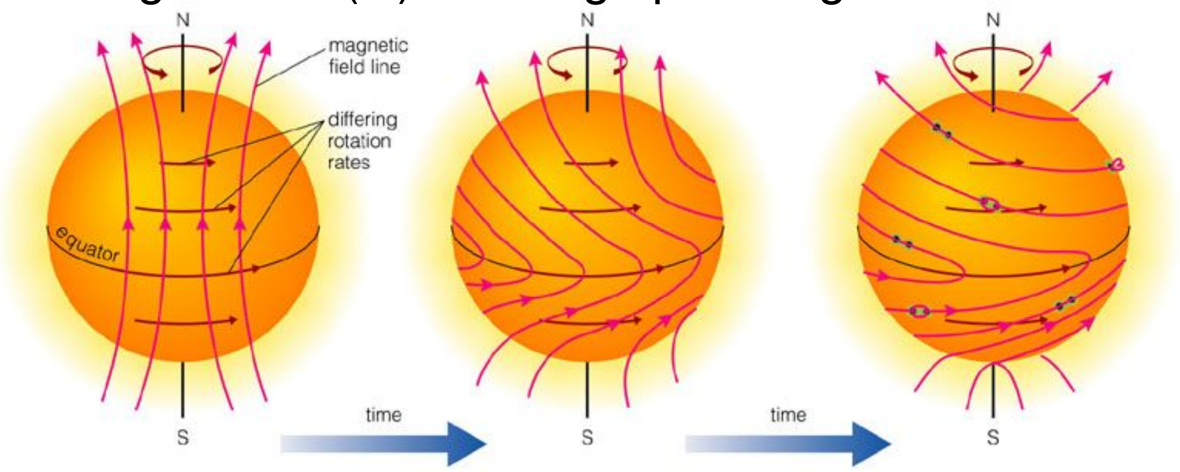

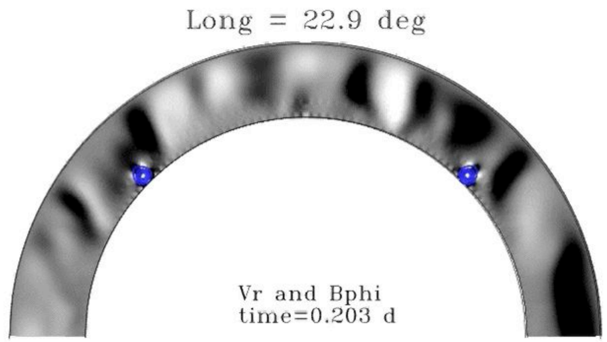

Simulations CEA
projet STARS2

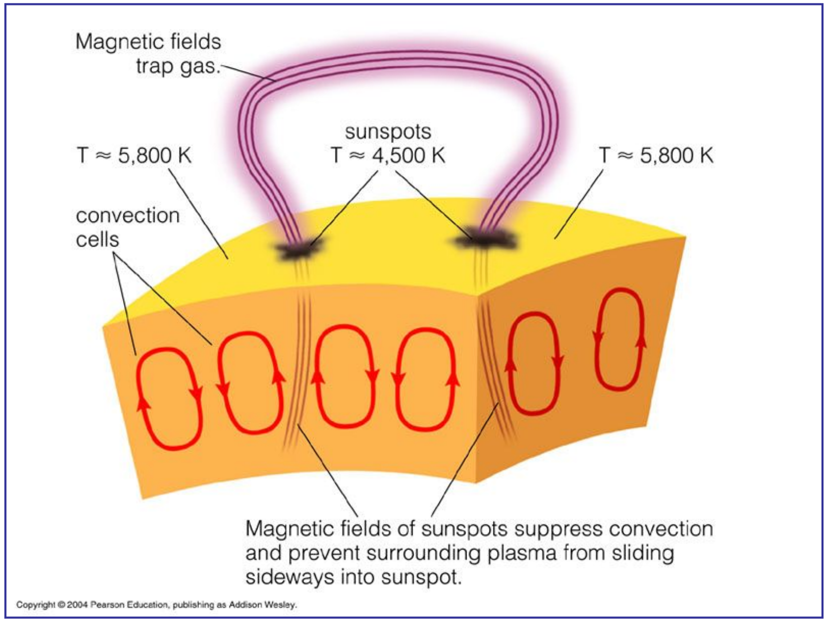

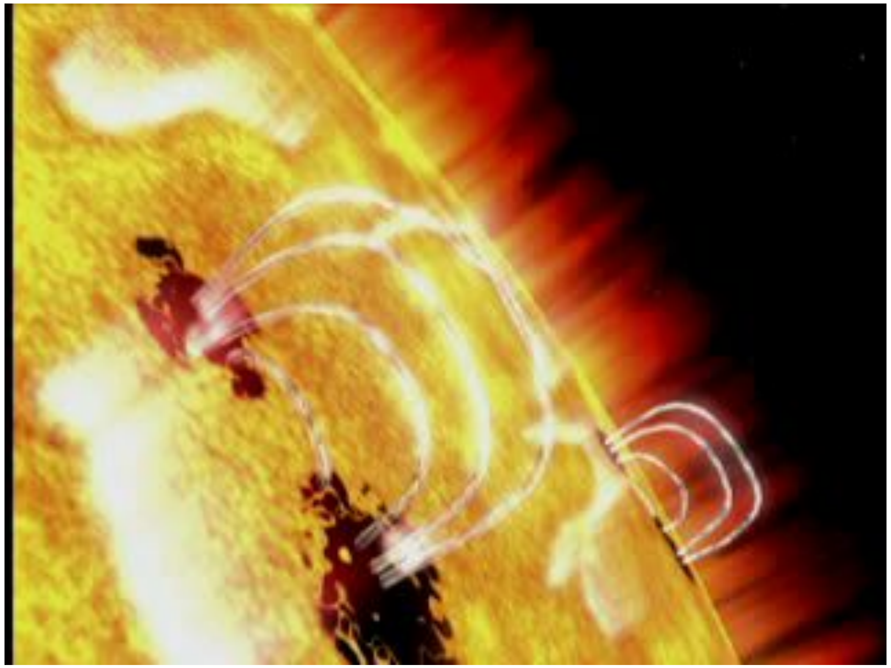

3-D Magnetic Convection & Dynamo

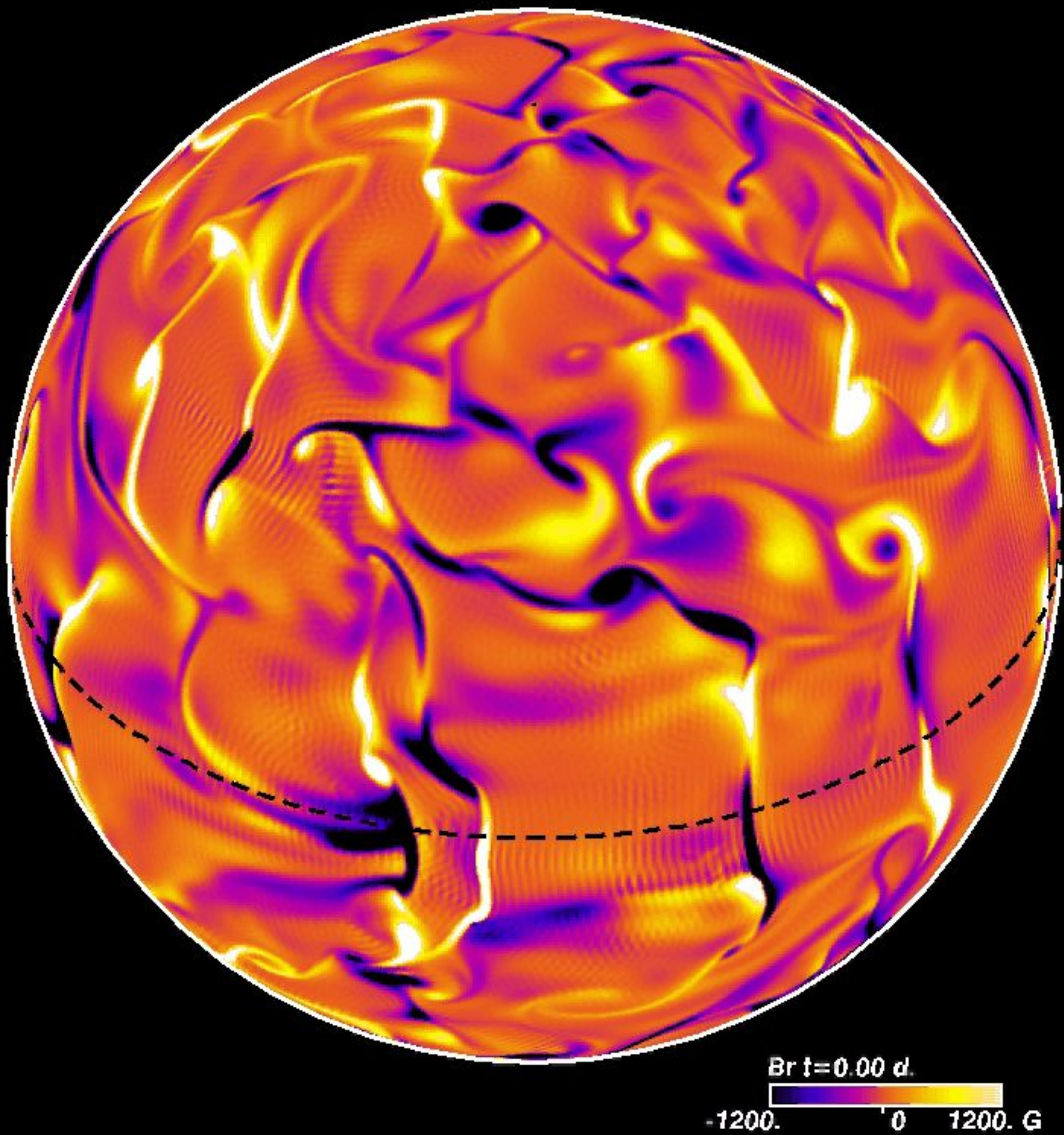

Radial component of B

stretching and shearing of B (folding too)

Brun et al. 2004, 2015

Dynamo Effect – Magnetic Energy

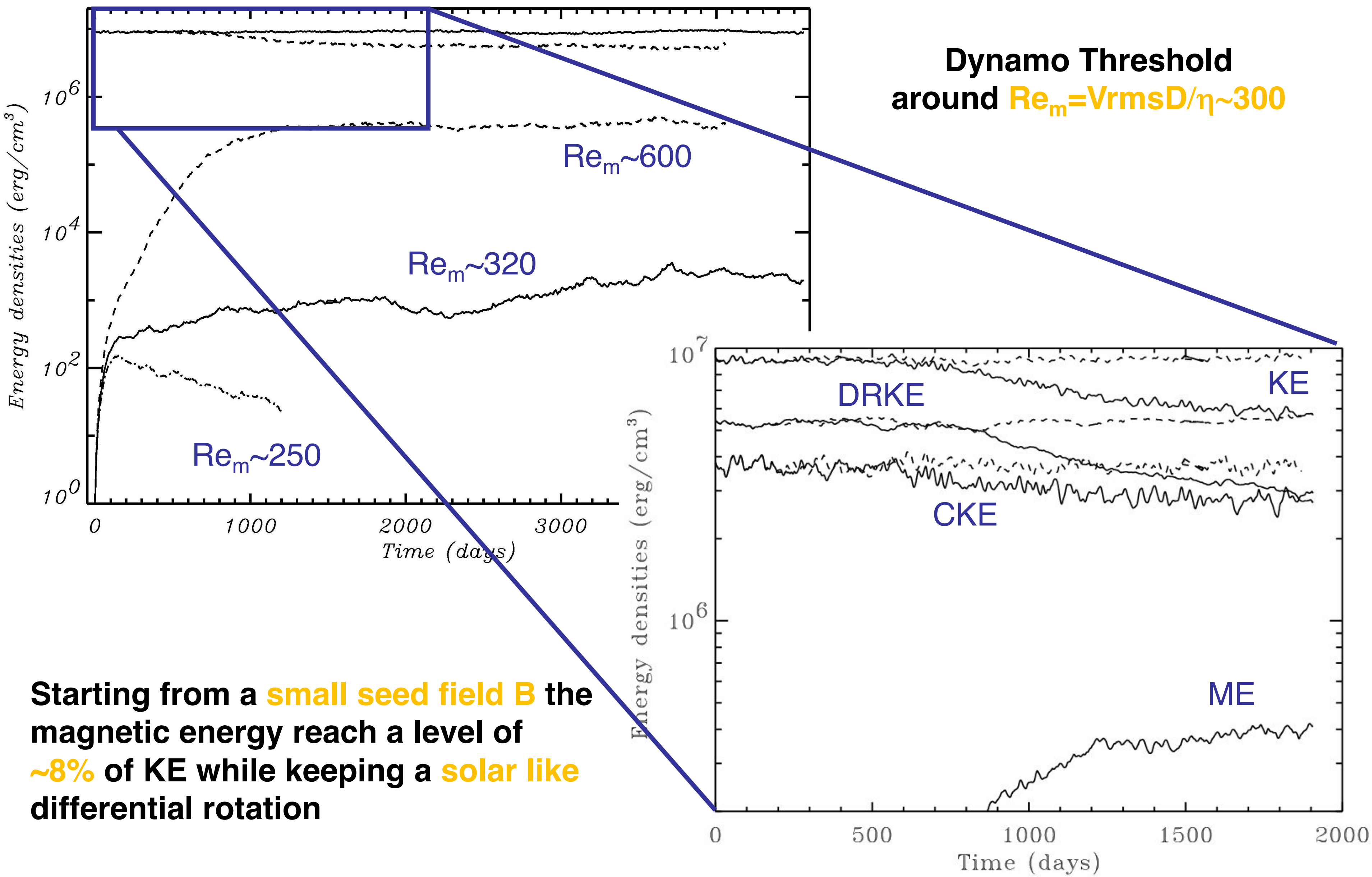

Dynamo Threshold around Re_m=VrmsD/η~300

Starting from a small seed field B the magnetic energy reach a level of ~8% of KE while keeping a solar like differential rotation

Lorentz force feedback on Differential Rotation

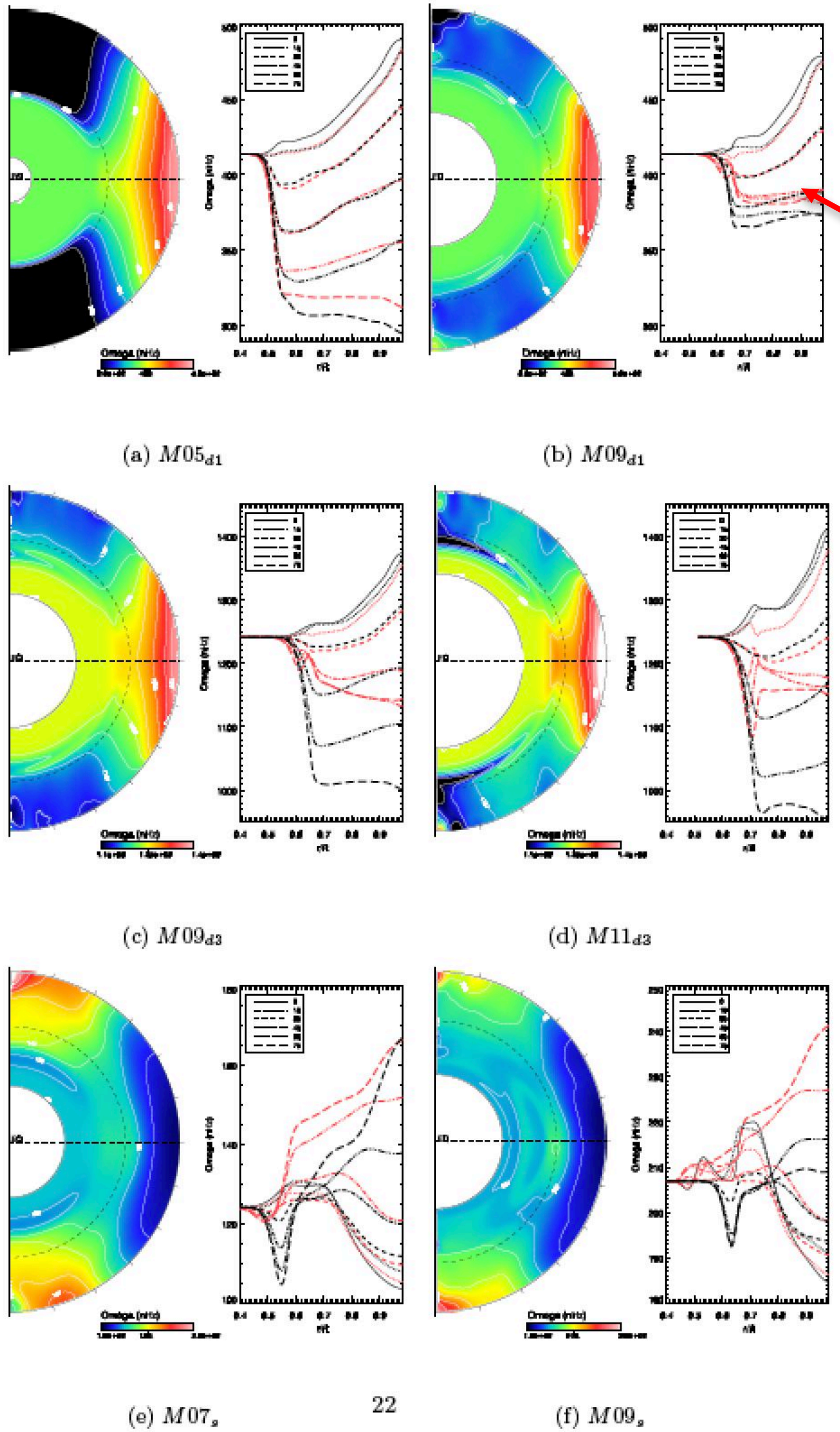

MHD solution in red
vs HD solution in black

Clear reduction of the differential rotation contrast in MHD cases (for Ro < 1)

Varela, Strugarek, Brun 2016, AdSpR
see also Karak et al. 2015, Guerrero et al. 2016

Angular Momentum Balance in Presence of B

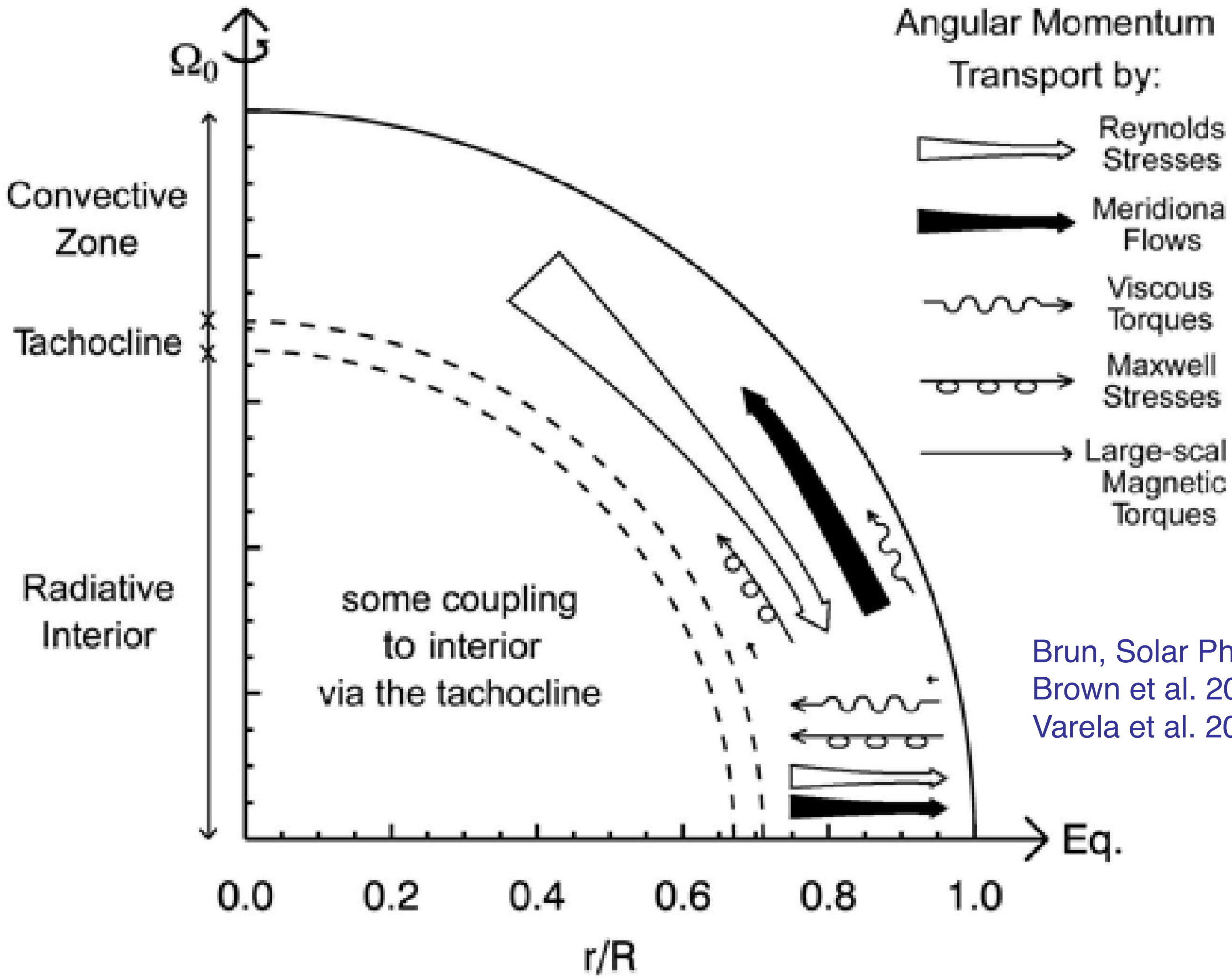

Brun, Solar Physics, 2004
Brown et al. 2010, 2011
Varela et al. 2016

The transport of angular momentum by the Reynolds stresses remains at the origin of the equatorial acceleration. The Maxwell stresses seeks to speed up the poles.

Solar Type Stars (late F, G and early K-type)

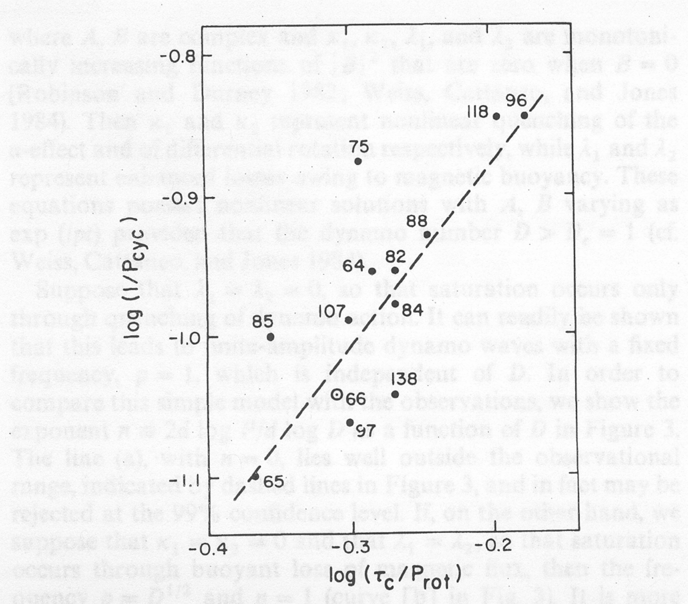

FIG. 2.—Log $(1/P_{cyc})$ vs. log (τ_c/P_{rot}) for the stars of Table 1. The dashed line is a linear least squares fit to the data.

Noyes et al. 1984

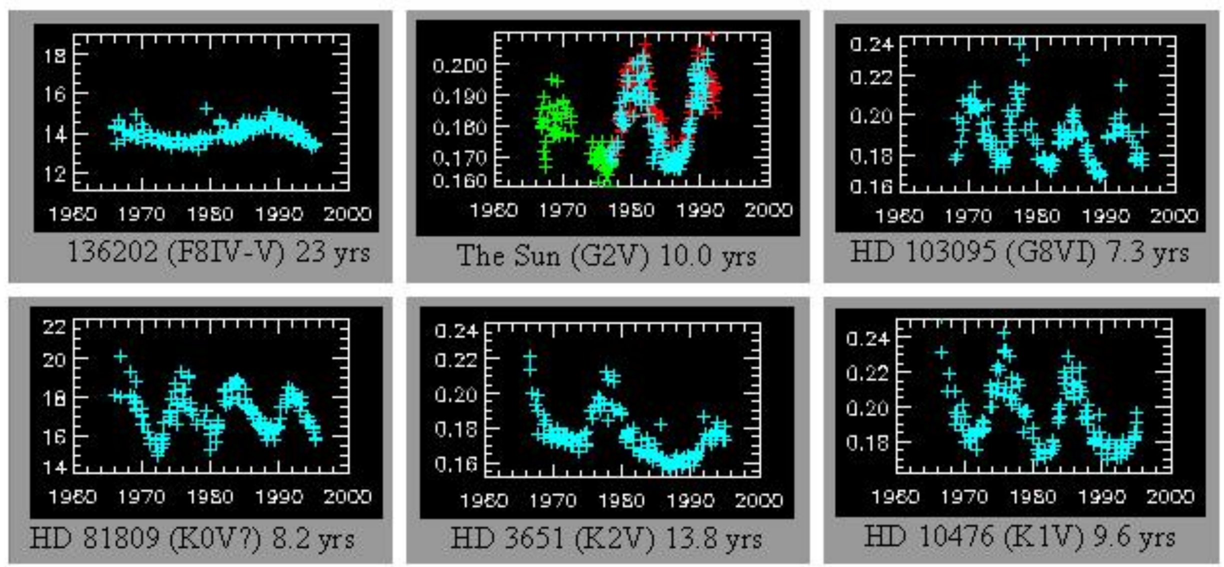

Call H & K lines , $<R'_{HK}>$

In stars activity depends on rotation & convective overturning time via Rossby nb $Ro=P_{rot}/\tau$

$<R'_{HK}> = Ro^{-1}$, $P_{cyc}=P_{rot}^{1.25+/-0.5}$??

Wilson 1978
Baliunas et al. 1995

<u>Over 111 stars in HK project (F2-M2):</u>
31 flat or linear signal
29 irregular variables
51 + Sun possess magnetic cycle

=> Much more coming in Asteroseismology Era (=> PLATO)

More recently the Pcyc vs Prot relationship has been questionned!

Strugarek et al. 2017, Egeland et al. 2017, Reinhold & Gizon 2017

Few Points We Must Address

- Source of variability (chaos, intermittency,…)
- Can we reproduce the trend $P_{cyc} \sim P_{rot}^{n}$ (n ~1+/-0.2)
- Can we reproduce the increase of the toroidal vs poloidal component
- Which « solar model» is best to explain stellar data?

BL mean field models

$$P_{cyc} = v_0^{-0.91} s_0^{-0.013} \eta^{-0.075} \Omega_0^{-0.014}$$

Strong dependancy on meridional flow amplitude

Kinematic 2-D model of the solar dynamo

- Distributed dynamo: fails
- Interface dynamo:

  1) alpha-omega $\alpha\omega$

  2) Babcock-Leigthon (flux transport)

  3) mixed of both! (best model so far)

α–Ω vs Babcock-Leighton dynamo mechanisms

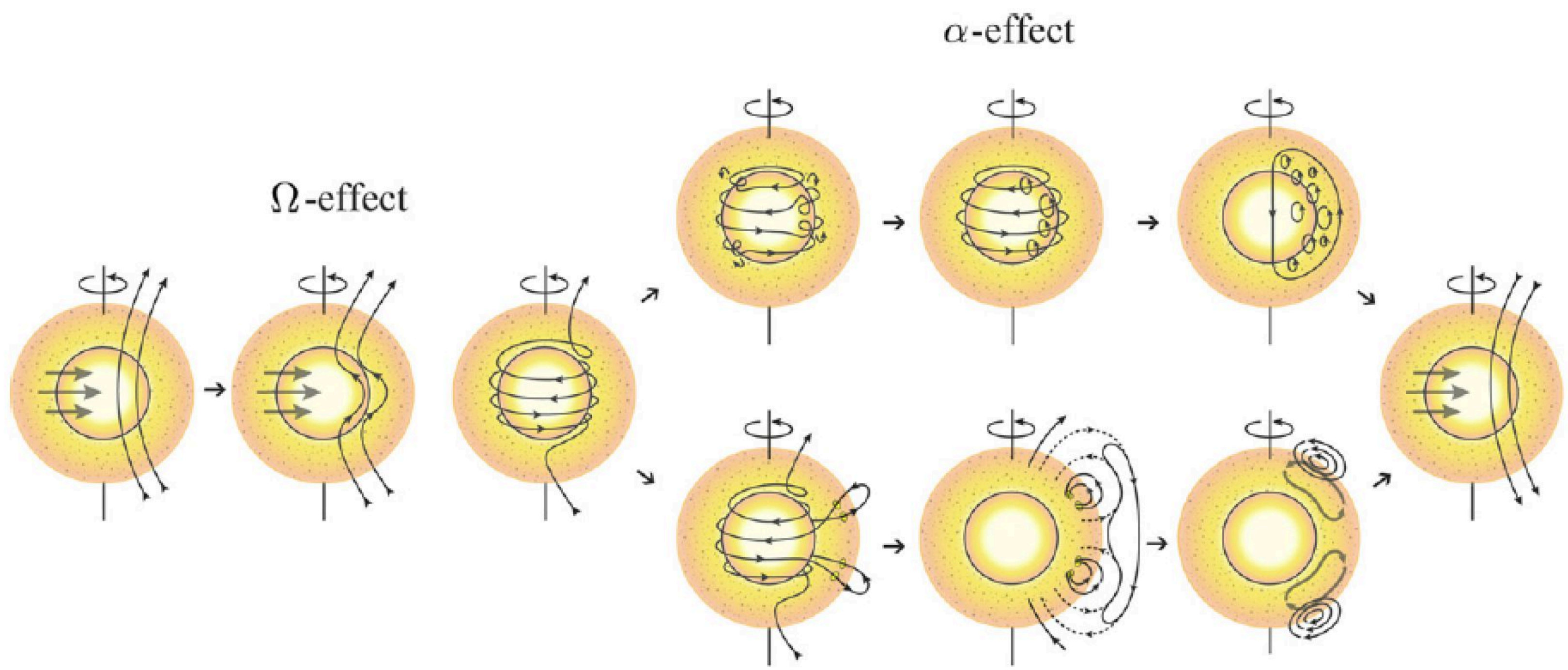

Courtesy: S. Sanchez (ApJ

Figure 1. Sketch of the main processes at work in our solar dynamo model. The Ω-effect (left) depicts the transformation of a primary poloidal field into a toroidal field by means of the differential rotation. The poloidal field regeneration is next accomplished either by the α-effect (top) and/or by the Babcock-Leighton mechanism (bottom). In the α-effect case, the toroidal field at the base of the convection zone is subject to cyclonic turbulence. Secondary small-scale poloidal fields are thereby created, and produce on average a new, large-scale, poloidal field. In the Babcock-Leighton mechanism, the primary process for poloidal field regeneration is the formation of sunspots at the solar surface from the rise of buoyant toroidal magnetic flux tubes from the base of the convection zone. The magnetic fields of those sunspots nearest to the equator in each hemisphere diffuse and reconnect, while the field due to those sunspots closer to the poles has a polarity opposite to the current one, which initiates a polarity reversal. The newly formed polar magnetic flux is transported by the meridional flow to the deeper layers of the convection zone, thereby creating a new large-scale poloidal field.

2D Mean Field models: Babcock-Leighton

1 single cell per hemisphere

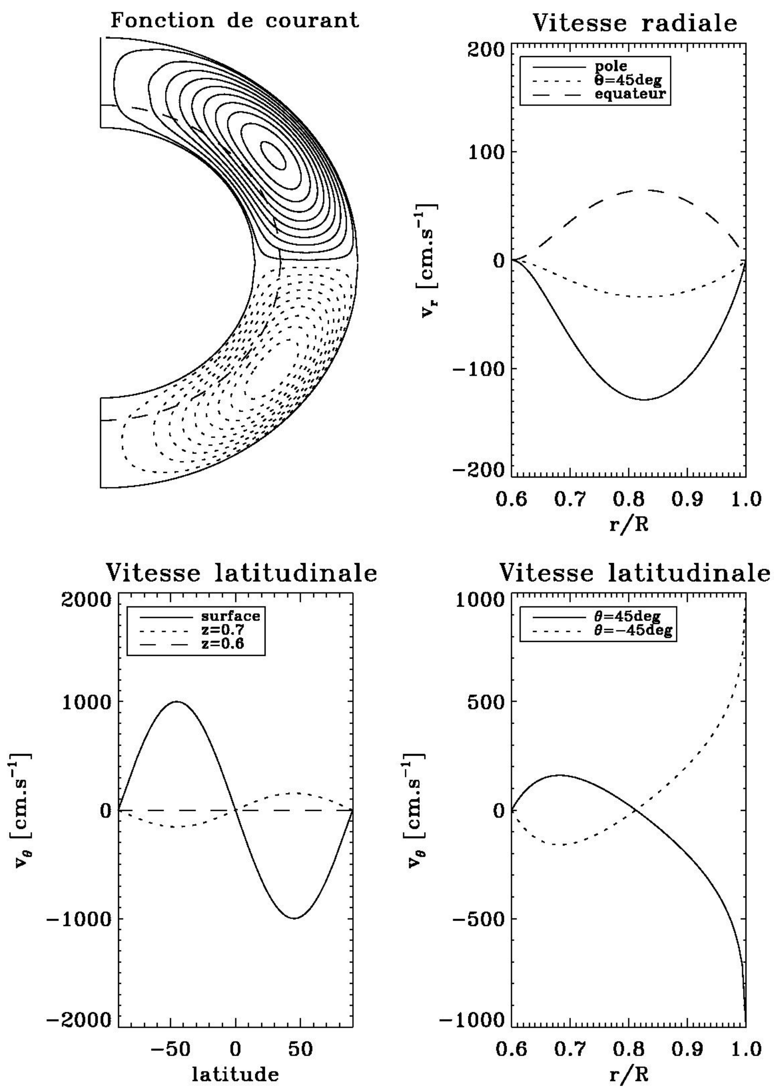

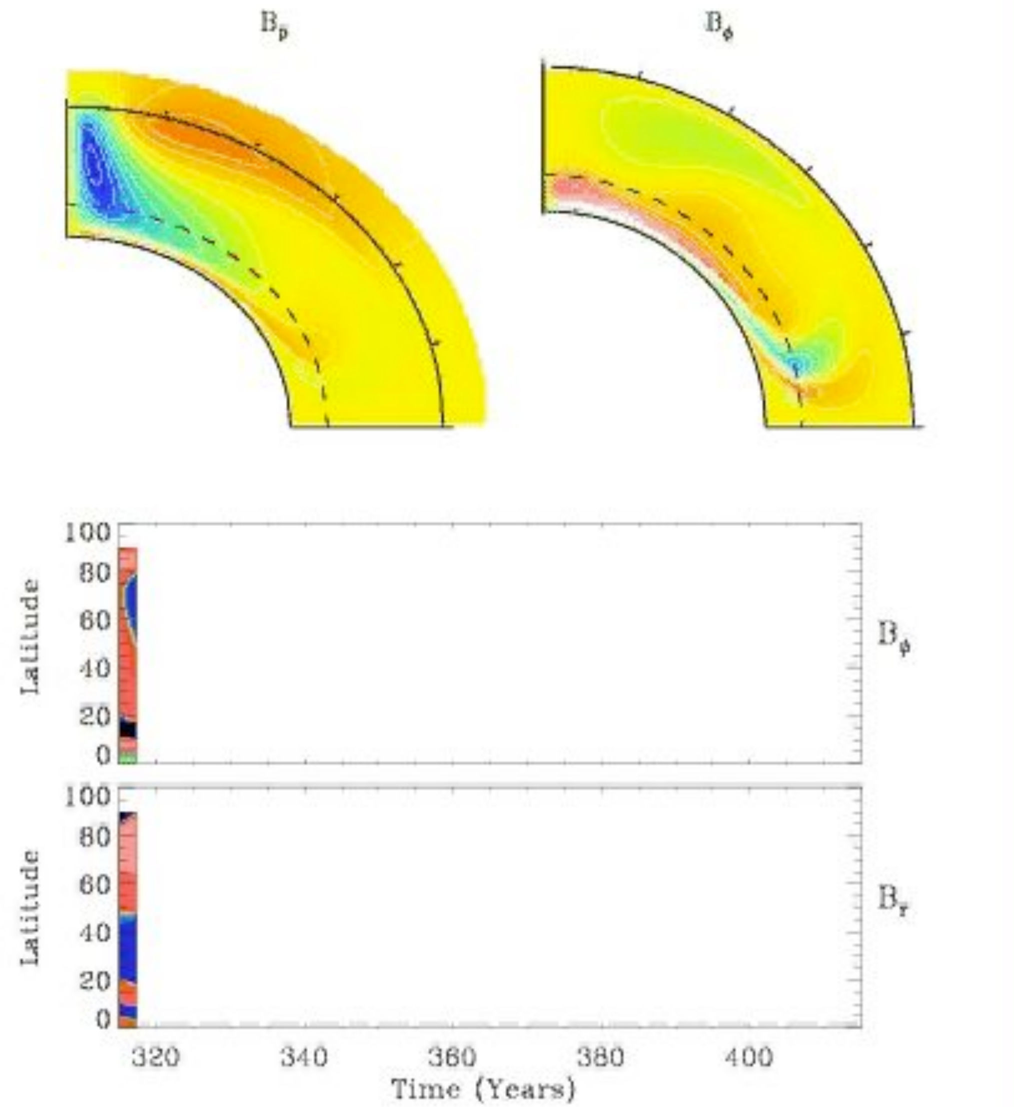

Jouve & Brun, 2007 A&A

Meridional Circulation

More & more evidence for multi cellular MC

Zhao et al. 2013

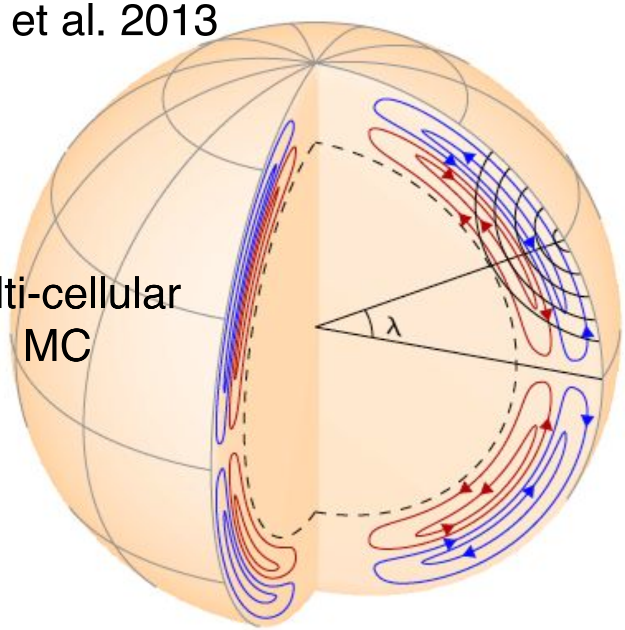

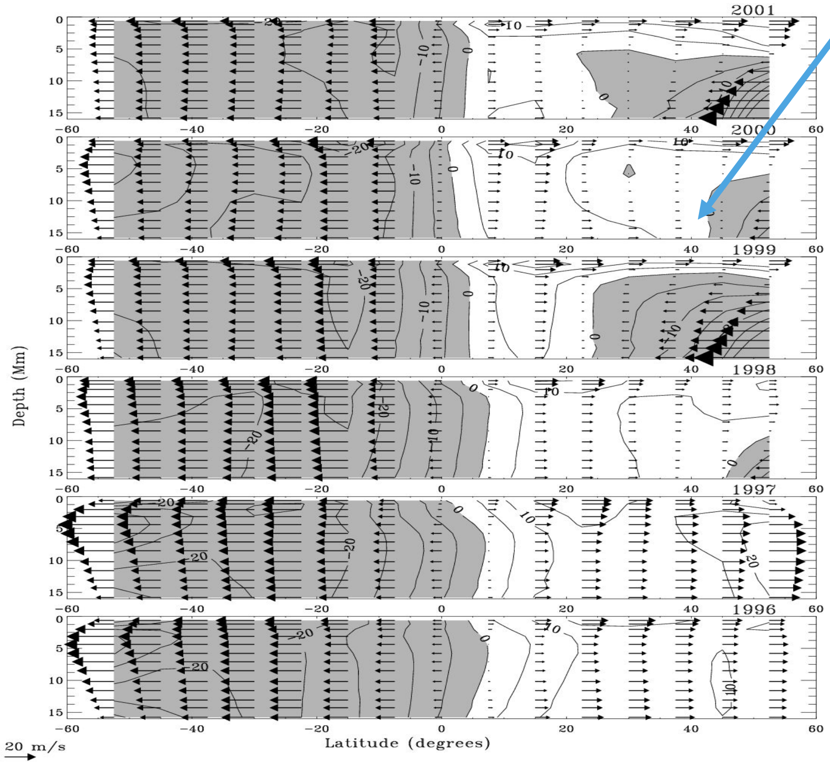

(Haber et al. 2002)

Influence of B (active region) on MC

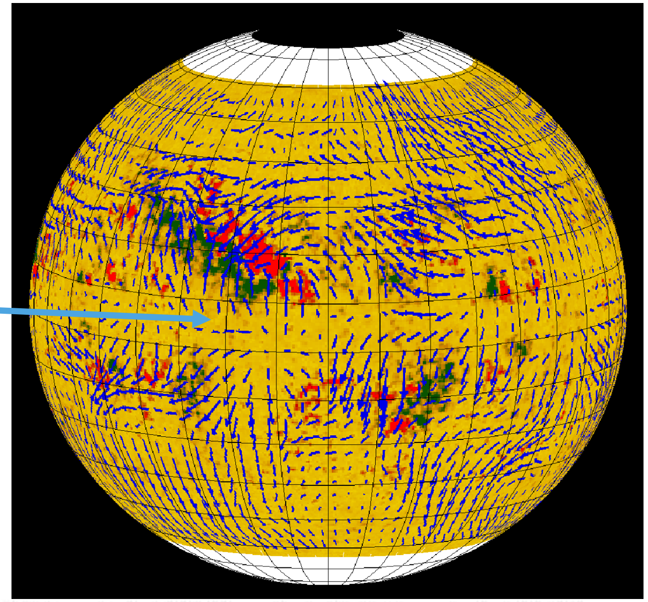

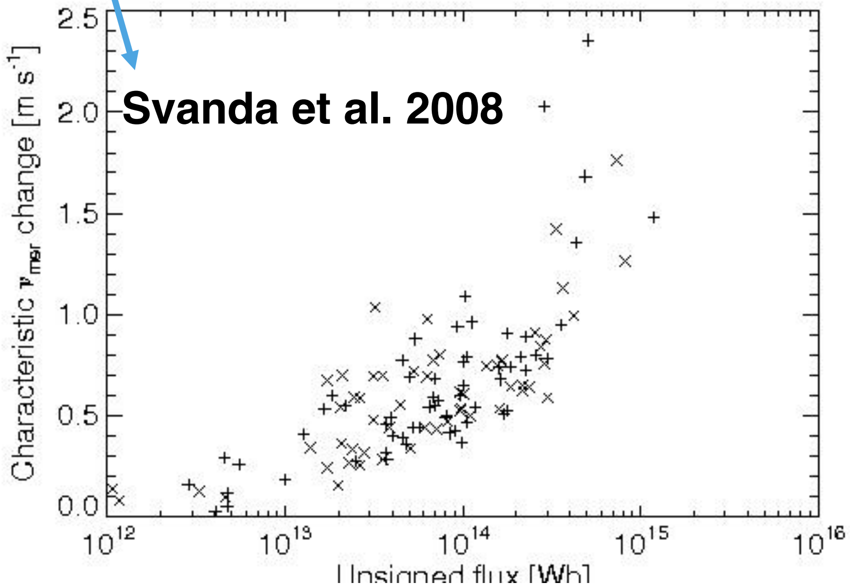

See also Hathaway et al. 1996, Gizon 2004, Zhao & Kosovichev 2004, etc…

2D Mean Field models: Babcock-Leighton

2 cells in latitude, 2 in radius per hemisphere

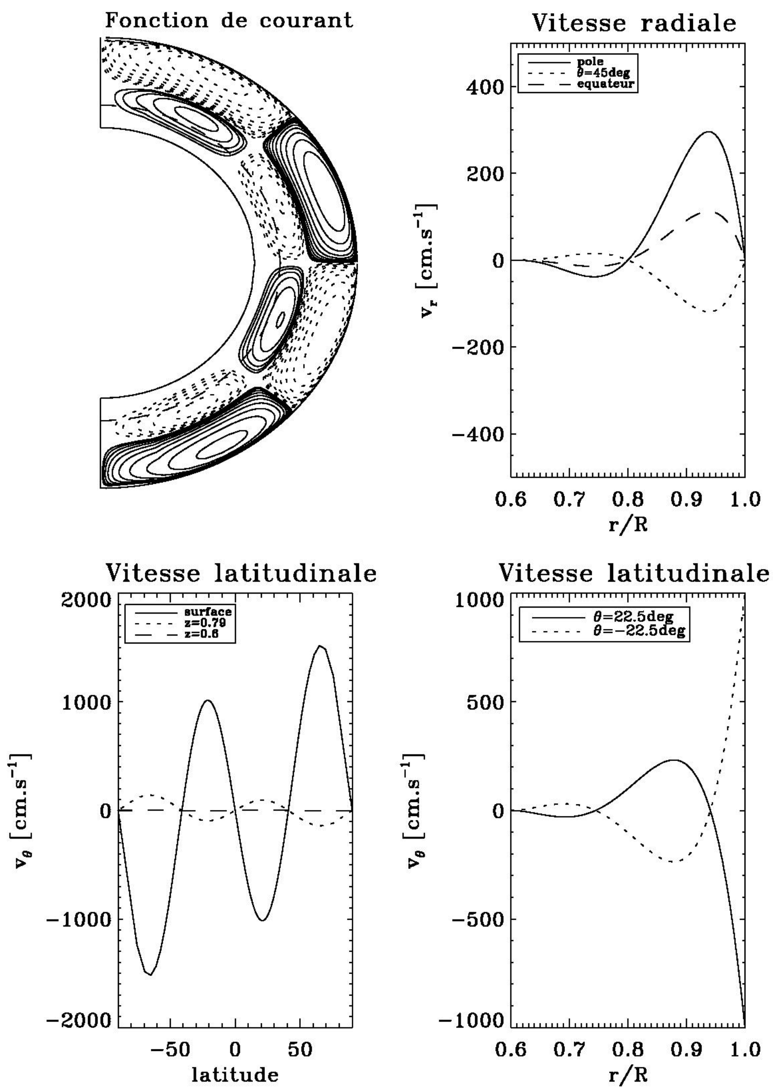

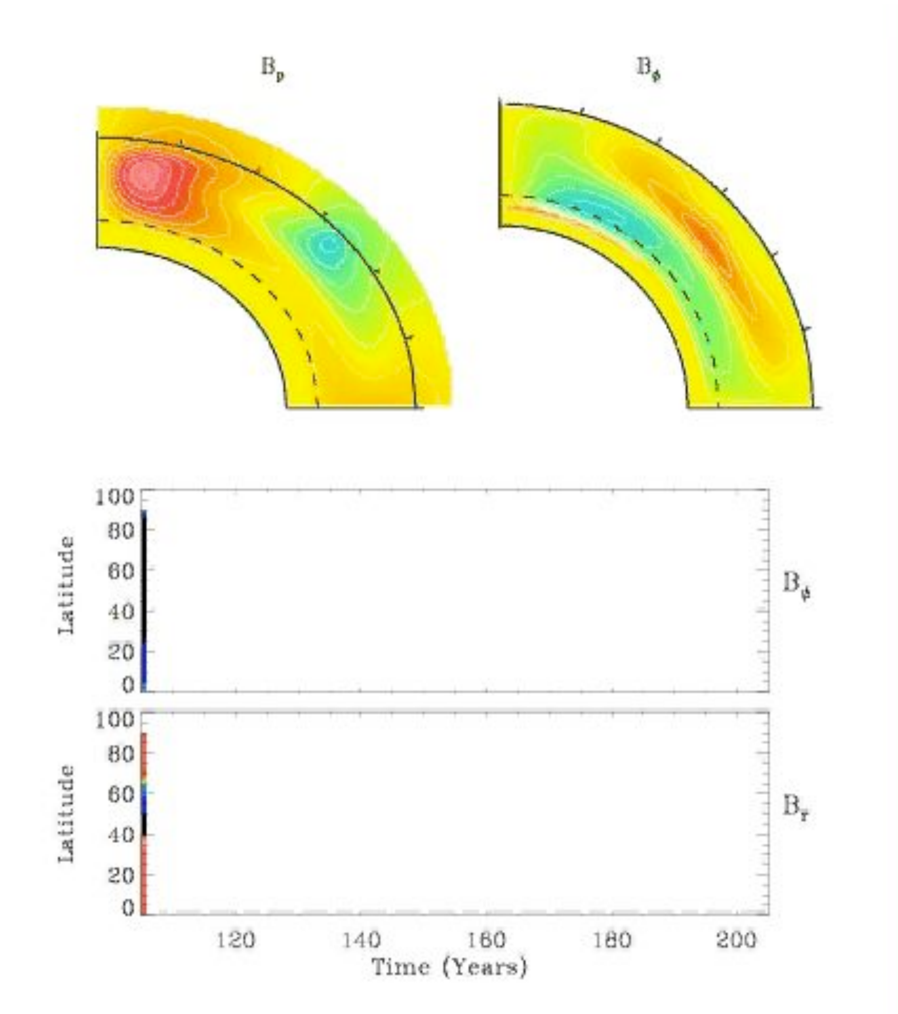

Slow down cycle period:
$T=\exp(22.84)v_0^{-0.35}\eta_t^{-0.68}s_0^{0.017}$

For parameter values Identical to 1 cell case, find T=45 yr instead of 22

Jouve & Brun 2007, A&A, 474, 239

Mean Field Dynamo

Influence on dynamo solution of changing various ingredient profiles (shear, meridional flow)

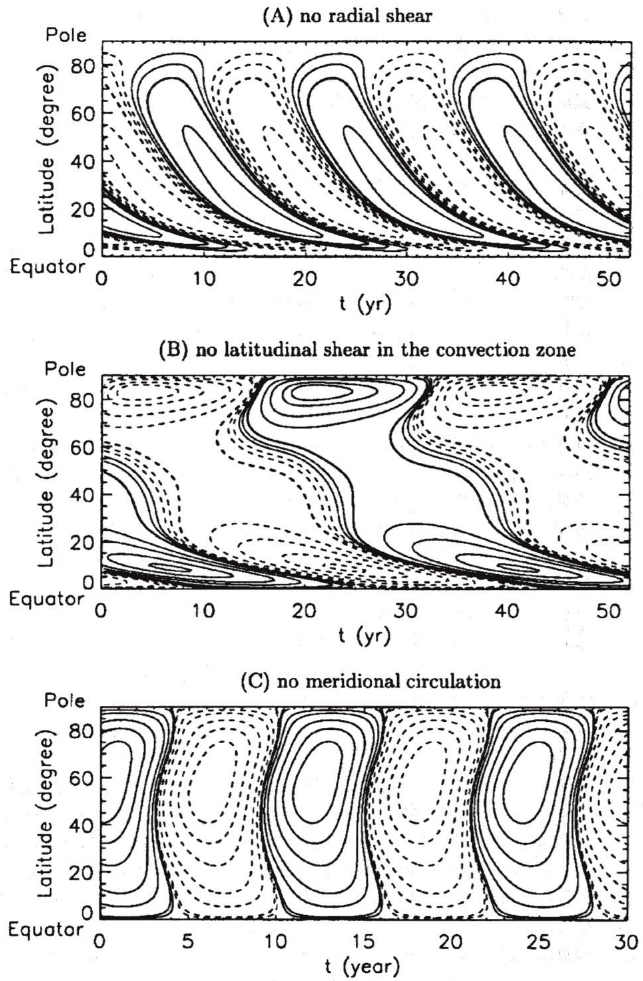

FIG. 4.—Three toroidal field butterfly diagrams resulting from various numerical "surgical" experiments. The format is the same as in Fig. 3*a*. (*a*) Solution where the radial shear was artificially shut off, with only the latitudinal shear left to contribute to the generation of toroidal fields. (*b*) Opposite experiment, i.e., the latitudinal shear has been artificially shut off. For these two solutions all parameter values are otherwise identical to the reference solution of Figs. 2 and 3. (*c*) Solution where the meridional circulation has been turned off. The resulting butterfly diagram bears a striking resemblance to that produced by mean field interface dynamos (see text).

Butterfly Diagram

Dynamo can be cyclic (solar or anti-solar) or stationnary

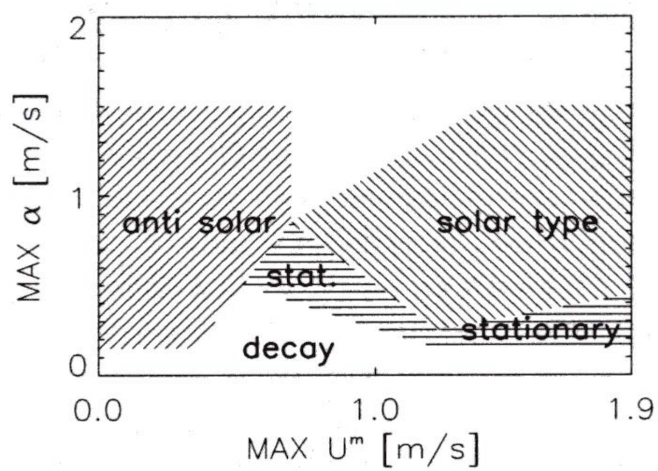

Fig. 11. The different types of solution found for varying strengths of the α-effect and the flow speed. The terms *solar type* and *anti solar* refer to equatorward and poleward drifting field belts, respectively, while *stationary* refers to a stationary field. The magnetic diffusivity always has a value of 10^{11} cm^2/s.

(Stix 1972, Choudhuri et al. 1995, Charbonneau et Dikpati 2001, Kuker et al. 2002, …..)

Earth's Magnetic Field Reversal

Matuyama -> Bruhnes -780,000 yr

Leonhardt
& Fabian 2007

Dominant multipole over dipole

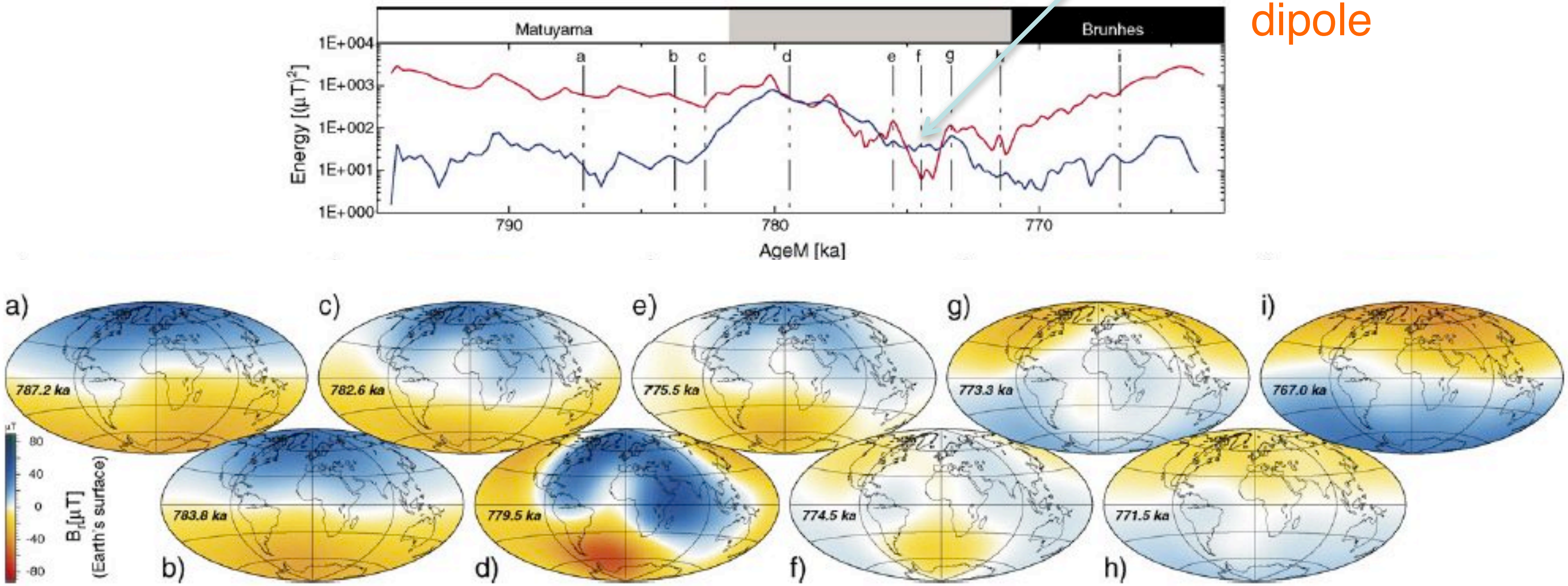

Reversal takes about 6 kyr, with a precursor of ~2.5 kyr, a reversal of ~1 kyr and rebound of ~2.5 kyr (Valet et al. 2008-2012)

Solar Reversals

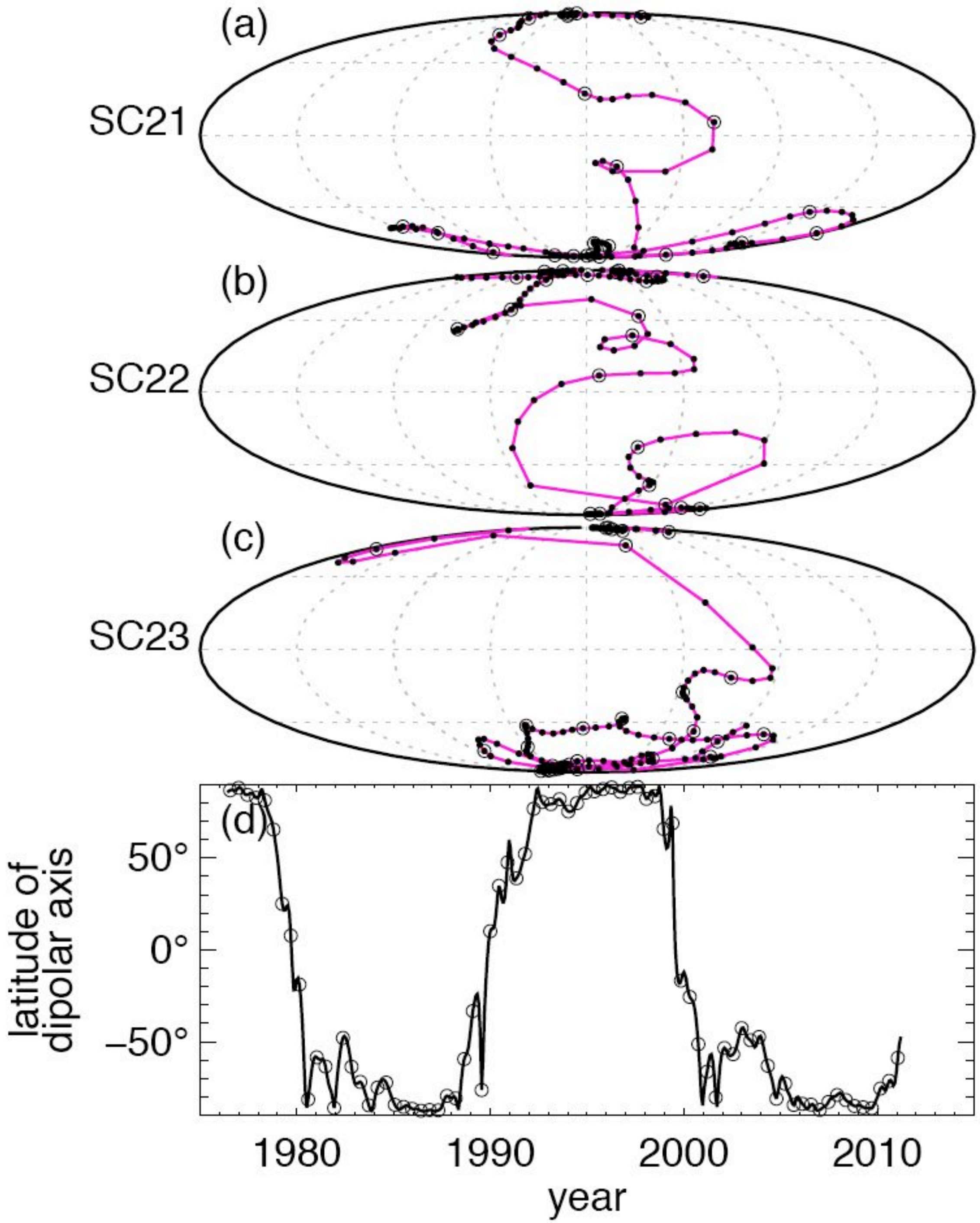

Derosa, Brun, Hoeksema 2012

Quadrupole vs Dipole Strenght

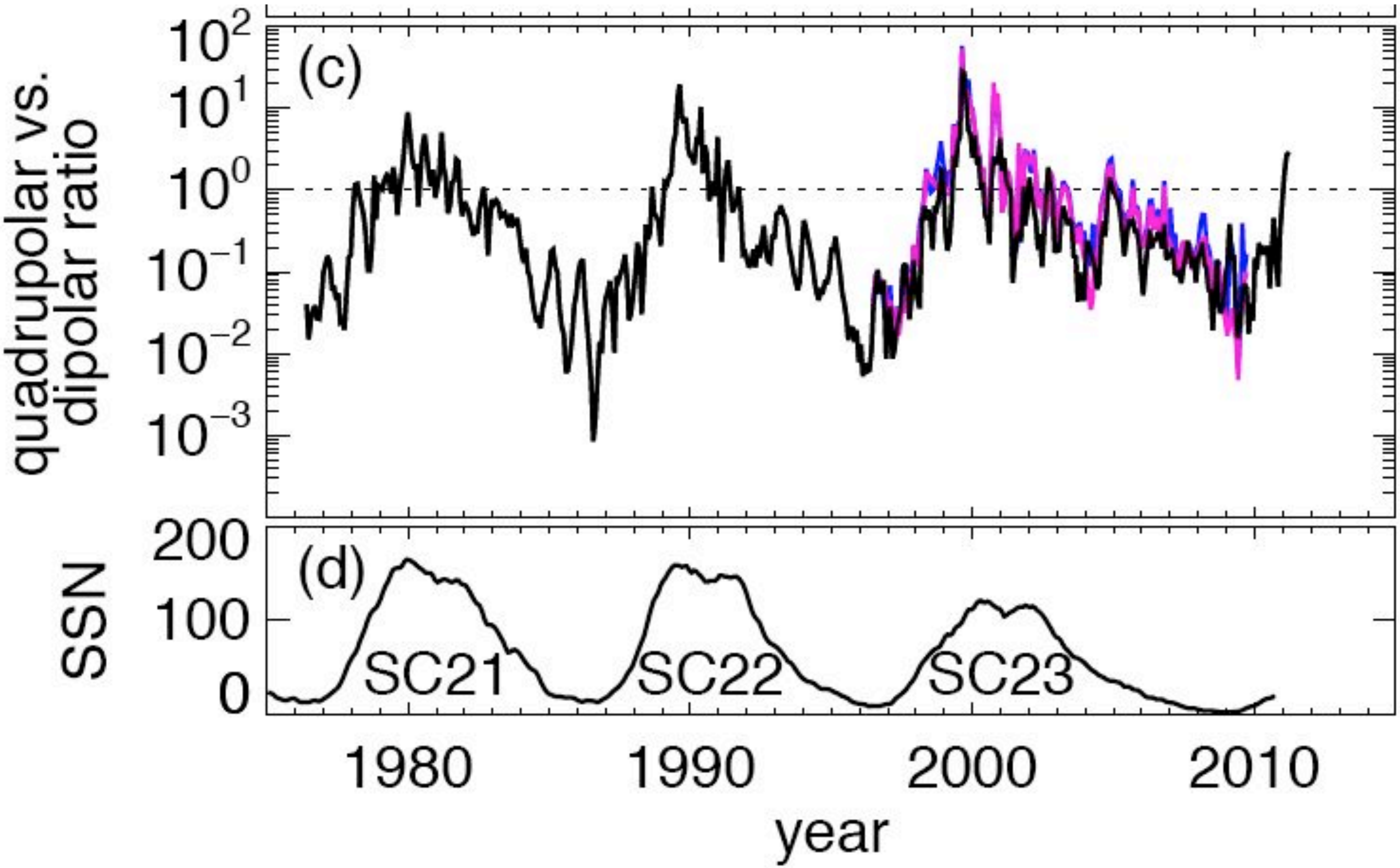

Derosa, Brun, Hoeksema 2012

Axisymmmetric Modes

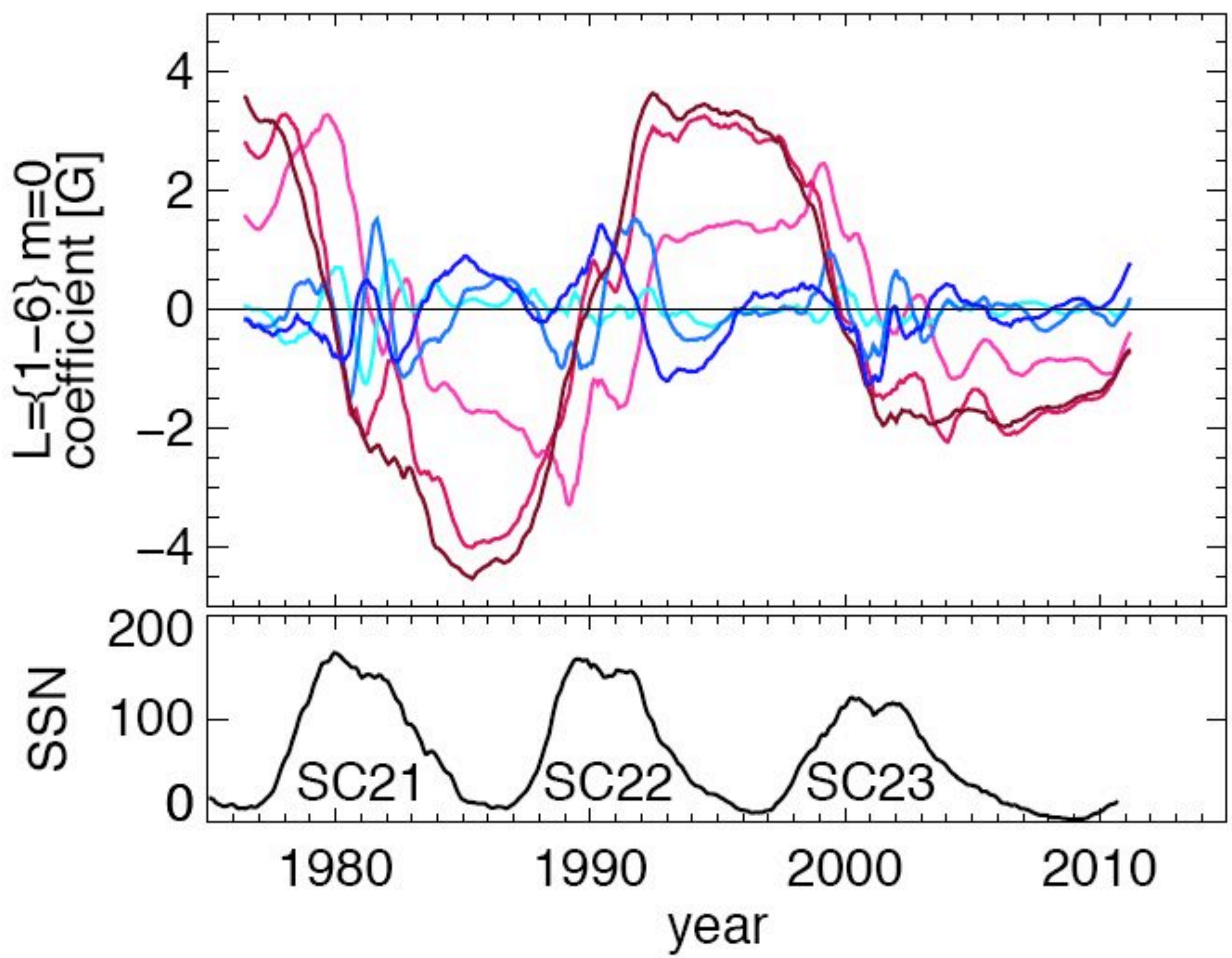

Quad ~ 25% Dip
Except at reversal where it dominates.

Fig. 10.— [XXX Energy in the first 3 odd ($\ell = \{1, 3, 5\}$ are {dark red, red, light red}) and even ($\ell = \{2, 4, 6\}$ are {dark blue, blue, light blue}) axisymmetric (m=0) degrees ℓ as a function of time for Wilcox.]

Derosa, Brun, Hoeksema 2012

Assessing Symmetries of Induction Equation

$$\frac{\partial \mathbf{B}}{\partial t} = \nabla \times (\mathbf{V} \times \mathbf{B}) + \eta \Delta \mathbf{B}$$

Knowing that vectorial product and curl change vector parity, but Laplacian retains it:

If V is symmetric: V^S x B^A -> C^S so $\nabla \times \mathbf{C}^S \rightarrow \mathbf{D}^A$

V^S x B^S -> C^A so $\nabla \times \mathbf{C}^A \rightarrow \mathbf{D}^{\bar{S}}$

=> Generates fields of same family => Uncoupled Dynamo solutions (families)

If V is anti-symmetric: V^A x B^A -> C^A so $\nabla \times \mathbf{C}^A \rightarrow \mathbf{D}^{\bar{S}}$

V^A x B^S -> C^S so $\nabla \times \mathbf{C}^S \rightarrow \mathbf{D}^A$

=> Generates field of the opposite family => Coupled Dynamo solutions

In current Babcock-Leigthon dynamo models ingredients yields uncoupled families

Gubbins & Zhang 1993, DeRosa, Brun & Hoeksema 2012, ApJ

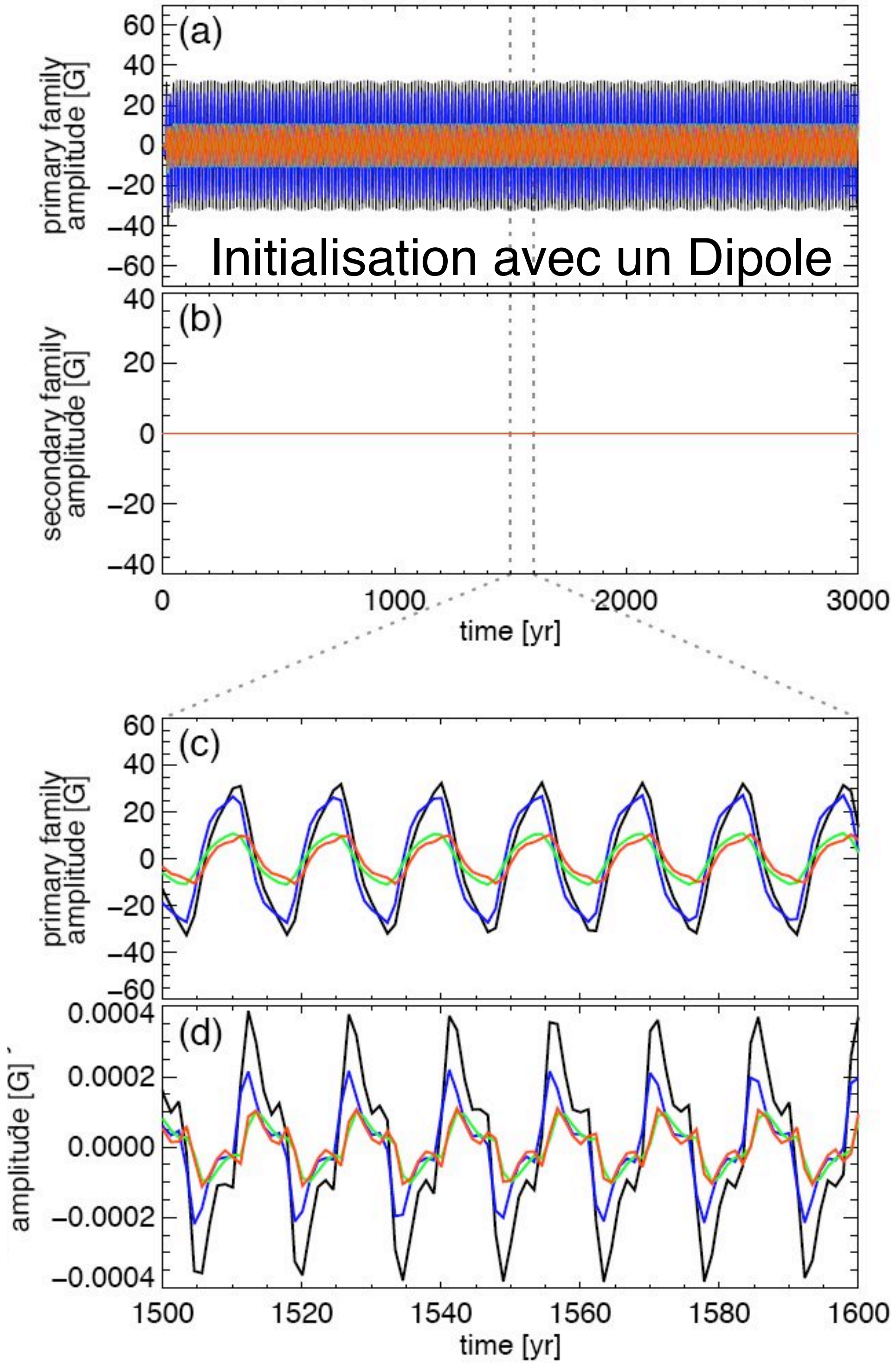
(a)
Initialisation avec un Dipole
primary family amplitude [G]
(b)
secondary family amplitude [G]
time [yr]
(c)
primary family amplitude [G]
(d)
amplitude [G]
time [yr]

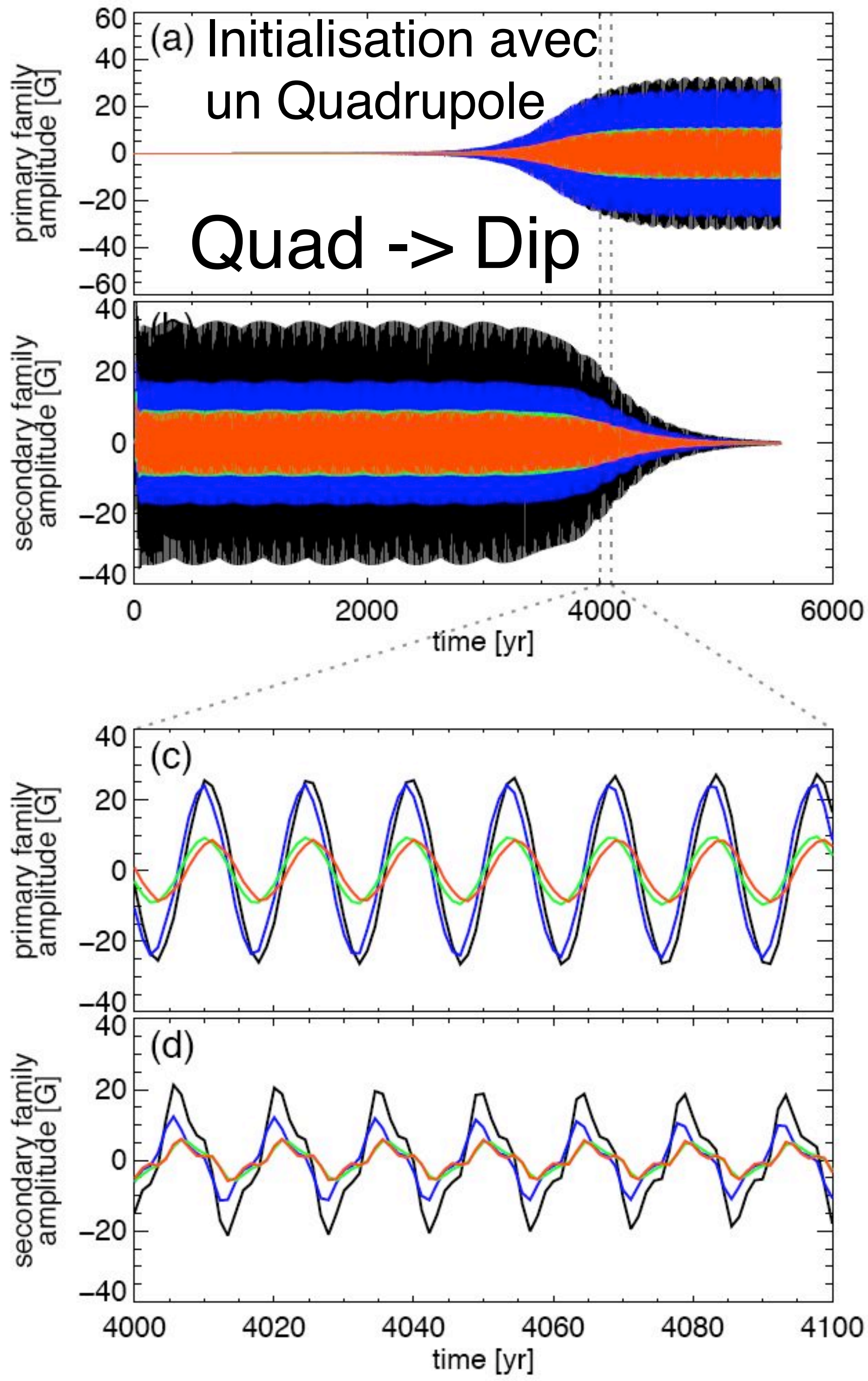
(a) Initialisation avec un Quadrupole
Quad -> Dip
primary family amplitude [G]
secondary family amplitude [G]
time [yr]
(c)
primary family amplitude [G]
(d)
secondary family amplitude [G]
time [yr]

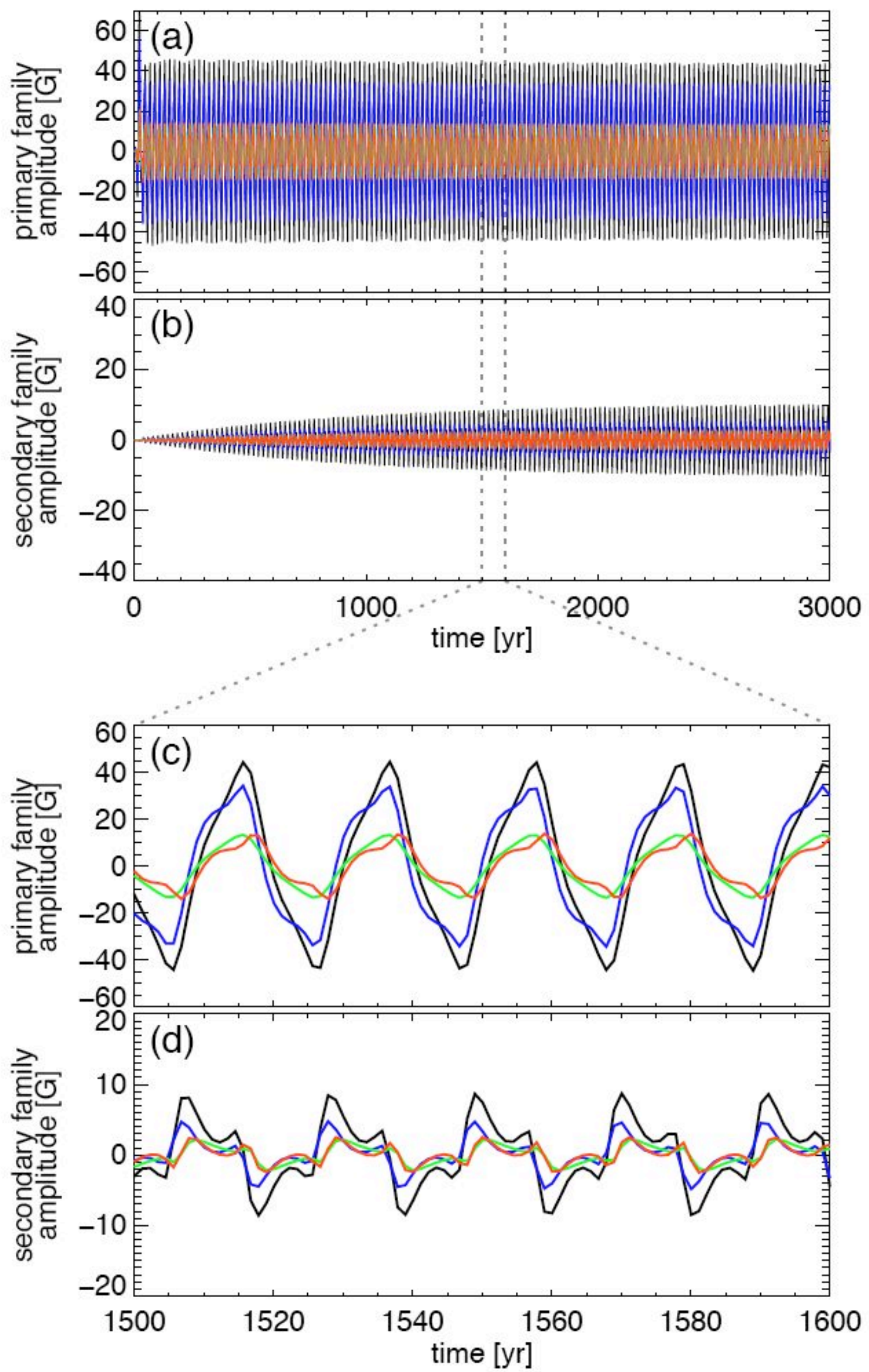

Asymmetry of Babcock-Leigthon term of 0.1%
Could be Meridional Flow.

Dip + Quad !

Derosa, Brun, Hoeksema 2012

Intermittent State: Malkus-Proctor B-L dynamo models

$$\begin{cases} \dfrac{\partial \mathbf{B}}{\partial t} = \nabla \times (\mathbf{V} \times \mathbf{B}) - \nabla \times (\eta_m \nabla \times \mathbf{B}) \\ \rho \dfrac{\partial v_\phi}{\partial t} = \left[\dfrac{1}{4\pi} (\mathbf{B}.\nabla)\mathbf{B} + \qquad \nabla . \sigma \qquad \right] .\hat{\mathbf{e}}_\phi \end{cases}$$

Trois paramètres :

$$D = \frac{\alpha_{\rm BL} \Omega_0 R_\odot^3}{\eta_t^2}$$

Nombre dynamo, taux de croissance du champ magnétique

$$V = V_0 + v_\phi$$

$$\Omega = \Omega_{\rm bg} + \omega$$

$$P_m = \frac{\nu}{\eta_t}$$

Nombre de Prandtl magnétique, rapport entre viscosité et diffusivité magnétique

$$R_e = \frac{v_0 R_\odot}{\eta_t}$$

Nombre de Reynolds, amplitude de la circulation méridienne

Intermittent Dynamo States in Mean field Dynamo

Dynamo alpha-omega

Bushby 2006
see also
Brun et al. 2018, sub.
Moss & Brooke 2000
Covas et al. 2005

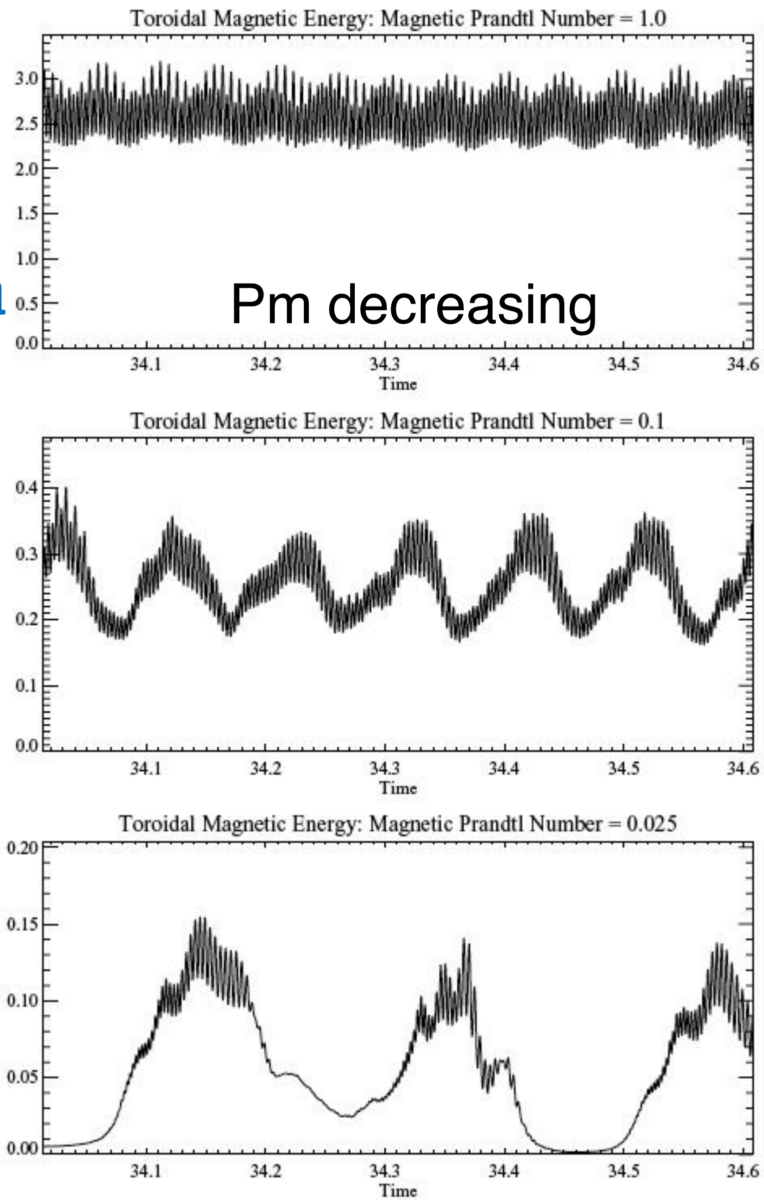

Figure 6. The time-dependence of the magnetic energy in the toroidal field for $\tau = 1.0$ (top panel), $\tau = 0.1$ (middle panel) and $\tau = 0.025$ (bottom panel). The dynamo number is fixed at $D = -2.5 \times 10^6$. The modulation becomes more pronounced and more chaotic for smaller values of the magnetic Prandtl number.

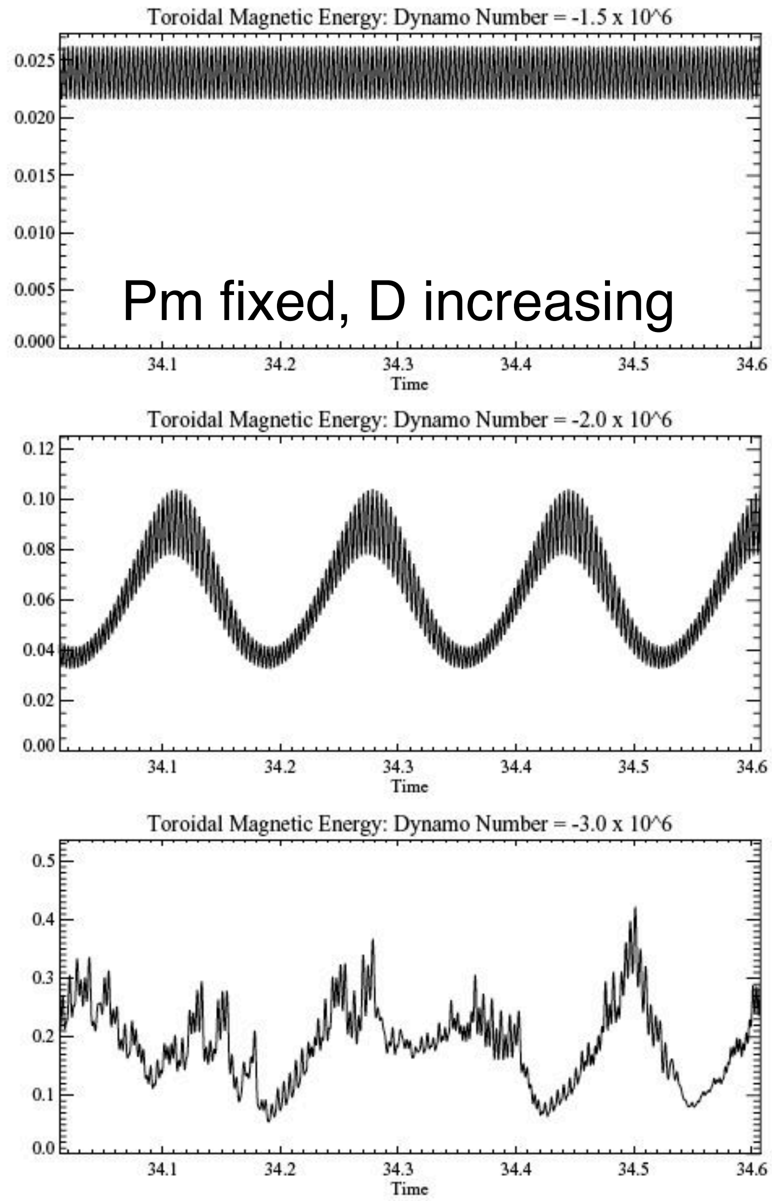

Figure 7. The time-dependence of the magnetic energy in the toroidal field for $D = -1.5 \times 10^6$ (top panel), $D = -2.0 \times 10^6$ (middle panel) and $D = -3.0 \times 10^6$ (bottom panel). The magnetic Prandtl number is fixed at $\tau = 0.05$.

Energy reservoirs in a Magnetized Convection Zone

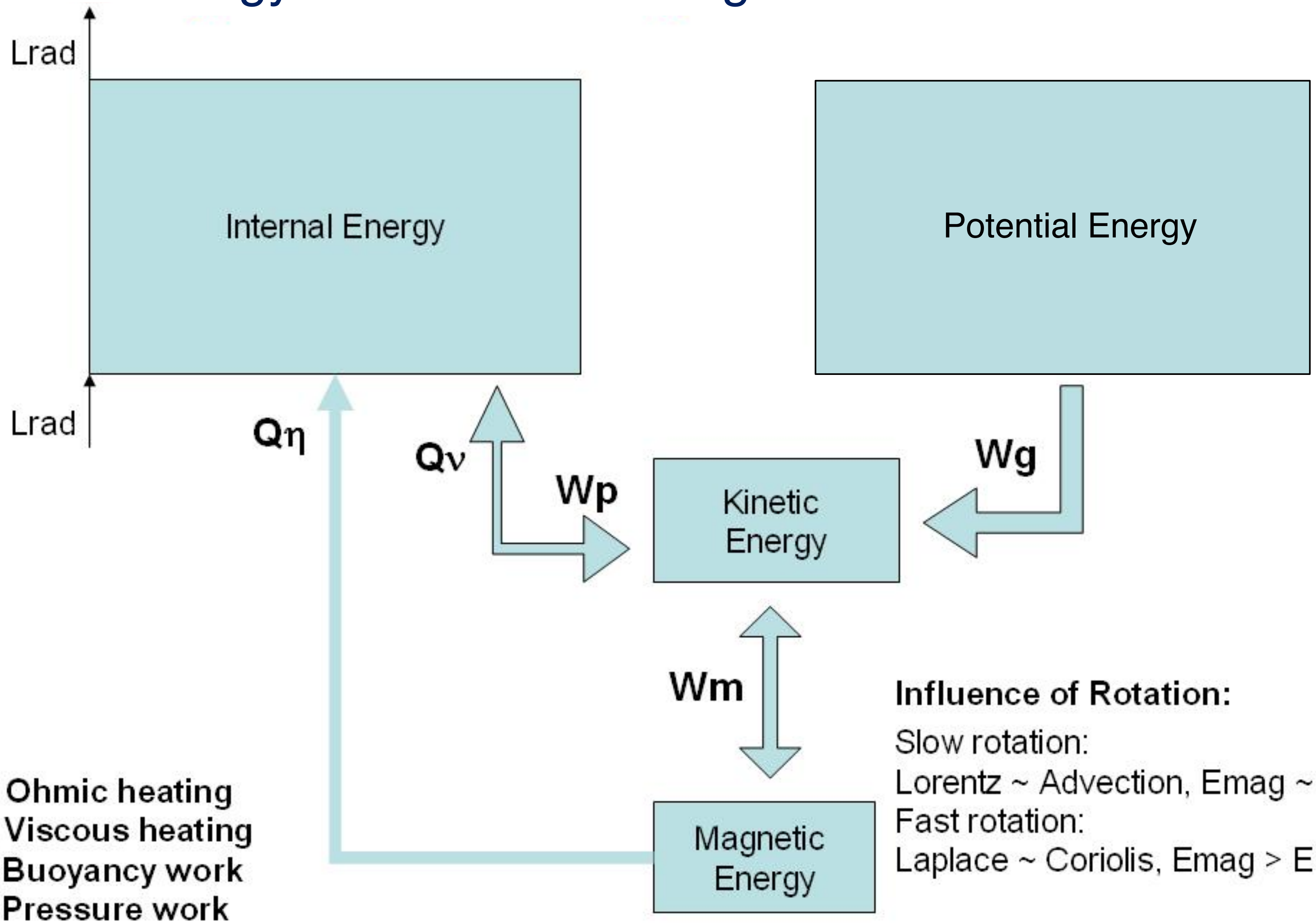

Qη: Ohmic heating
Qν: Viscous heating
Wg:Buoyancy work
Wp:Pressure work
Wm: Lorentz force work

Influence of Rotation:

Slow rotation:
Lorentz ~ Advection, Emag ~ Eke
Fast rotation:
Laplace ~ Coriolis, Emag > Eke

(Brandenburg et al. 1996, Brun et al. 2004)

Various Dynamo Regimes and Scalings

Equilibrium field : $B_{eq} \sim \mathrm{sqrt}(8\pi P_{gaz}) \sim \mathrm{sqrt}(\rho_*)$

If magnetic Reynolds number Rm ~1 , $v = \eta/L$, then

Laminar (weak) scaling: Lorentz ~ diffusion =>

$$B^2_{weak} \sim \rho\nu\eta/L^2$$

Turbulent (equipartition) scaling: Lorentz ~ advection =>

$$B^2_{turb} \sim \rho v^2 \sim \rho\eta^2/L^2 \Leftrightarrow |B_{weak}| \sim |B_{turb}|\, P_m^{1/2}$$

Magnetostrophic (strong) scaling: Lorentz ~ Coriolis =>

$$B^2_{strong} \sim \rho\Omega\eta$$

With ρ density, ν kinematic viscosity, η magnetic diffusivity, Ω rotation rate, v, L characteristic velocity & length scales, $P_m = \nu/\eta$ the magnetic Prandtl nb

Fauve et al. 2010, Christensen 2010, Brun et al. 2015

Kinematic vs dynamic (nonlinear) Dynamo

If Lorentz force can be neglected in Navier-Stokes equation, we call it a *kinematic dynamo*, l'instabilité est linéaire avec une croissance exponentielle

Dans le cas contraire (ce qui arrive pour des champs B d'amplitudes finies), on parle de *dynamo dynamique*, il y a rétroaction de la force de Laplace sur les mouvements, l'instabilité sature et le champ magnétique atteint une amplitude finie. L'énergie magnétique ME=$\mathrm{B}^2/8\pi$ est proche de l'équipartition avec l'énergie cinétique KE=$0.5\rho \mathrm{v}^2$ des mouvements fluides.

Remarque: la force de la Laplace peut se décomposer en 2 parties,

$$\mathbf{F} = \frac{1}{c}\mathbf{J} \times \mathbf{B} = \frac{1}{4\pi}(\nabla \times \mathbf{B}) \times \mathbf{B}$$
$$= \boxed{-\frac{1}{8\pi}\nabla \mathbf{B}^2}_a + \boxed{\frac{1}{4\pi}(\mathbf{B} \cdot \nabla)\mathbf{B}}_b$$

Une pression magnétique (terme a) perpendiculaire aux lignes de champ magnétique et une tension magnétique (terme b) le long de celles-ci.

Getting Cycle in similar Models

Ghizaru et al. 2010

Model has been run for several centuries

30 yr period

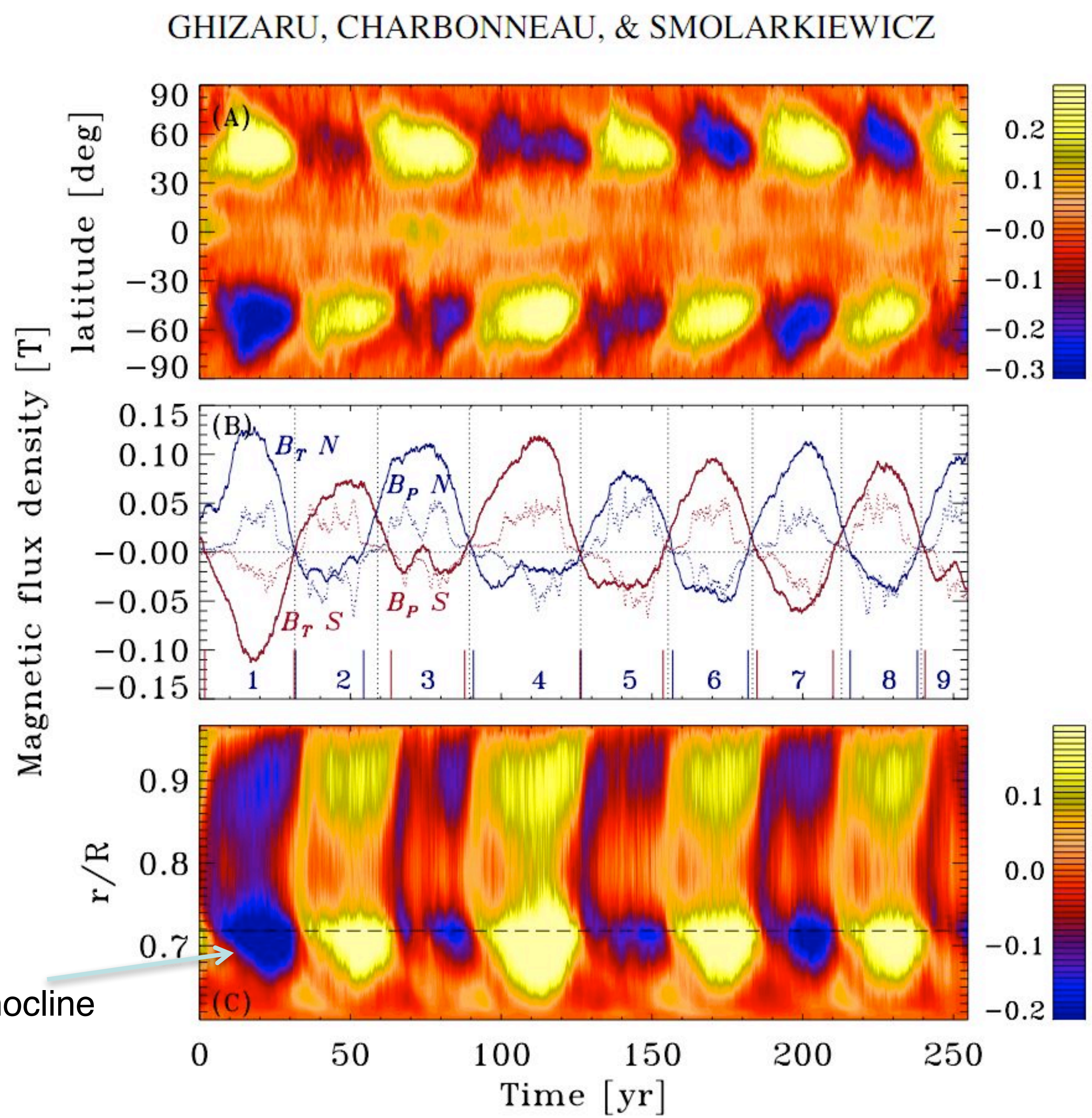

Turbulent pumping and shearing in imposed tachocline

Effect of Stratification on Dynamo Wave Propagation

Kapyla et al. 2014, 2016

Caveat:
Relative High Rotation (4 times solar)

$\Delta\rho = 5$

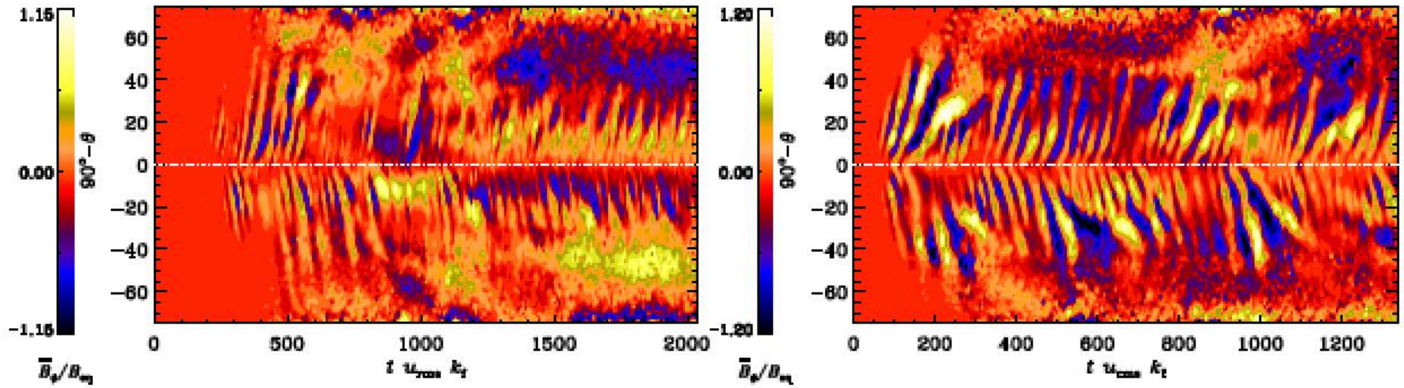

Fig. 4.— Same as Figure 3 but for Runs B1 (top) and B2 (bottom).

$\Delta\rho = 30$

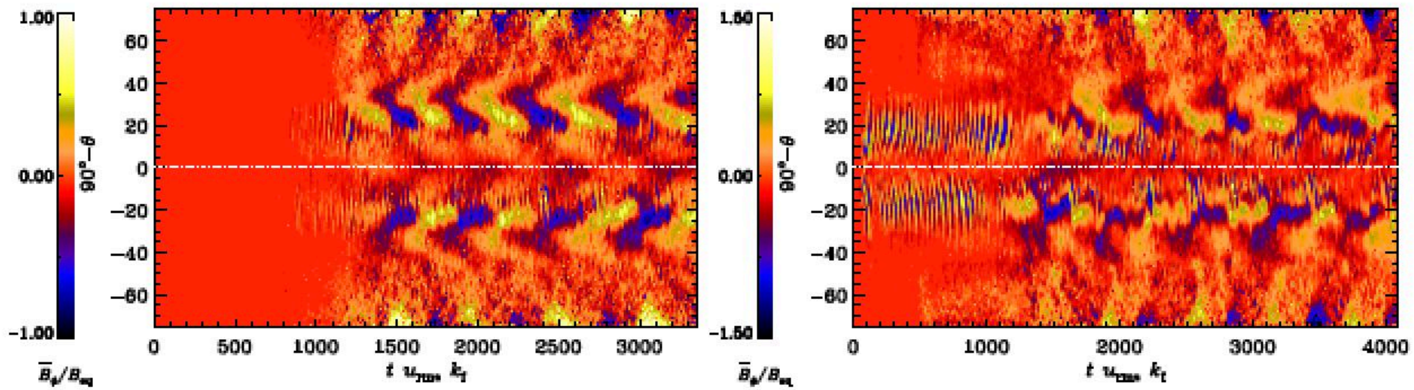

Fig. 5.— Same as Figure 3 but for Runs C1 (top panel) and C2 (bottom). Note the difference in cycle frequency between early times when the frequency is similar to that of Run B2 (Figure 4) and late times.

Higher stratification: Modify locations of Omega and alpha effects

Cyclic Nonlinear Stellar Dynamo

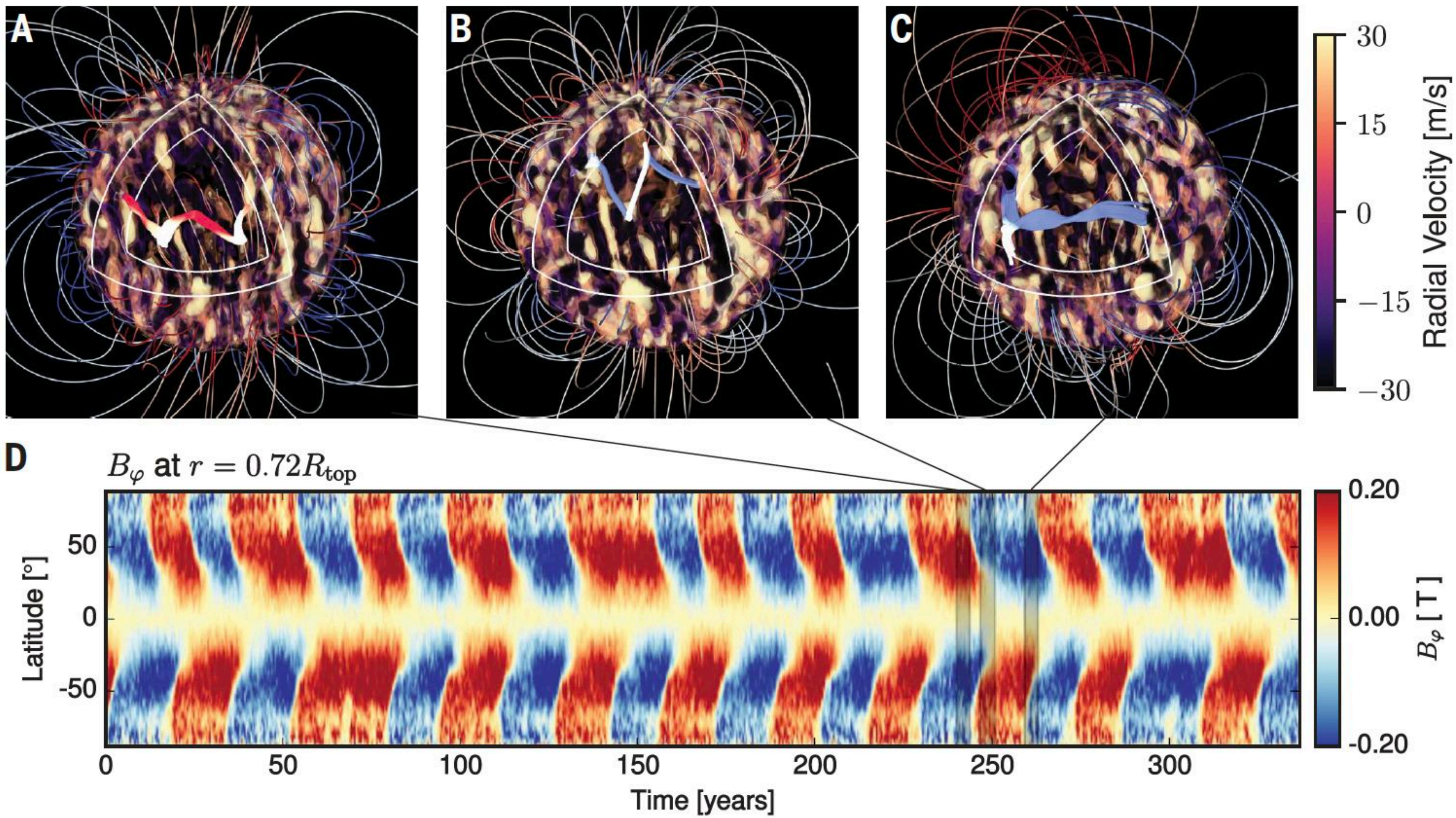

Strugarek et al. 2017, Science

3-D cyclic dynamo: new nonlinear solution

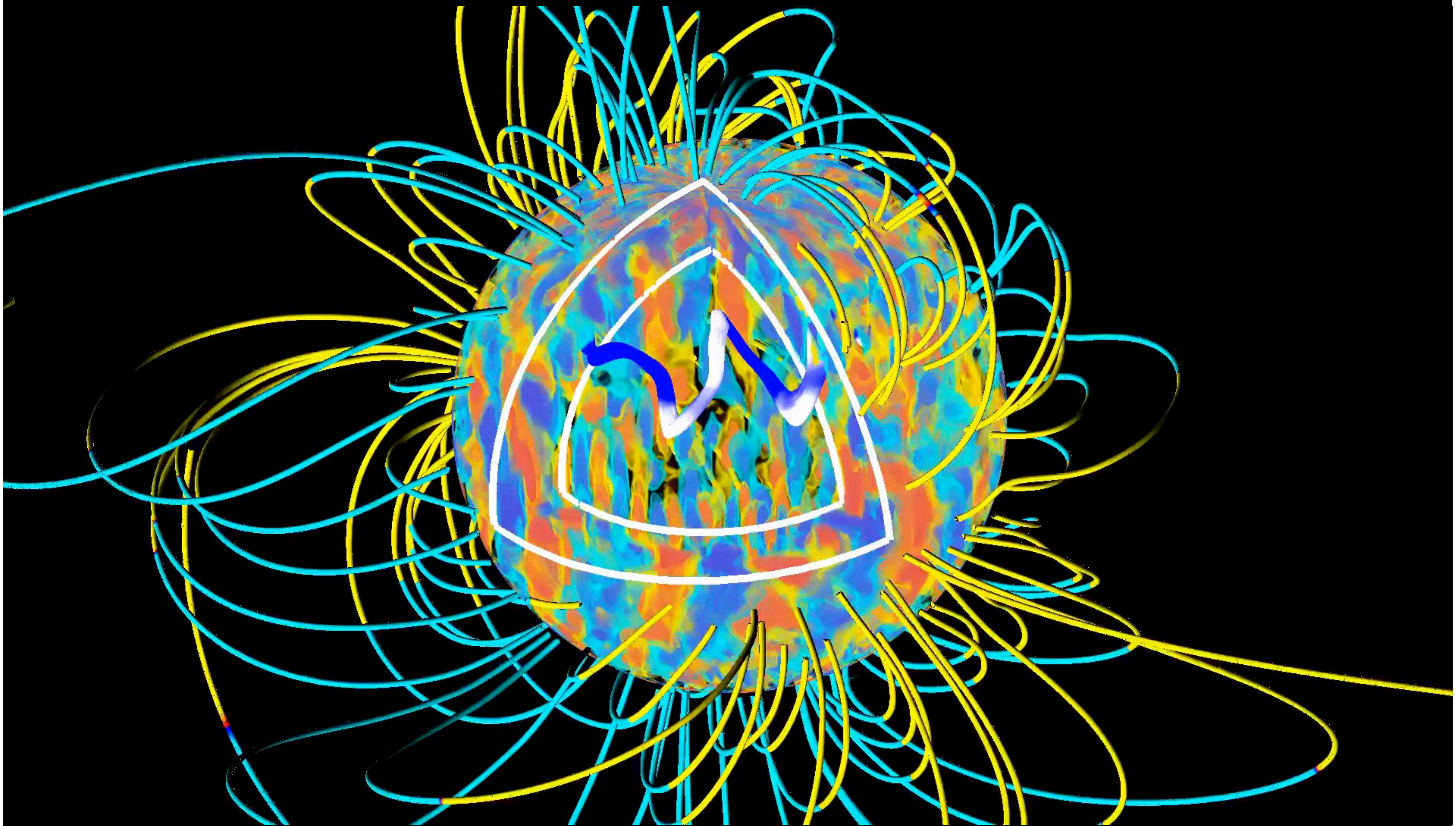

Strugarek et al. 2017, Science

Parker-Yoshimura Rule

In kinematic theory the propagation direction of such a wave is given by the Parker-Yoshimura rule (e.g., Parker 1955; Yoshimura 1975) as

$$\mathbf{S} = -\lambda\overline{\alpha}\hat{\varphi} \times \nabla \frac{\Omega}{\Omega_0}, \tag{19}$$

where $\lambda = r\sin\theta$ and $\overline{\alpha} = -\tau_o\langle \mathbf{v}' \cdot \boldsymbol{\omega}' \rangle/3$. Thus $\overline{\alpha}$ depends on the convective overturning time τ_o and the kinetic helicity.

uncorrect sign

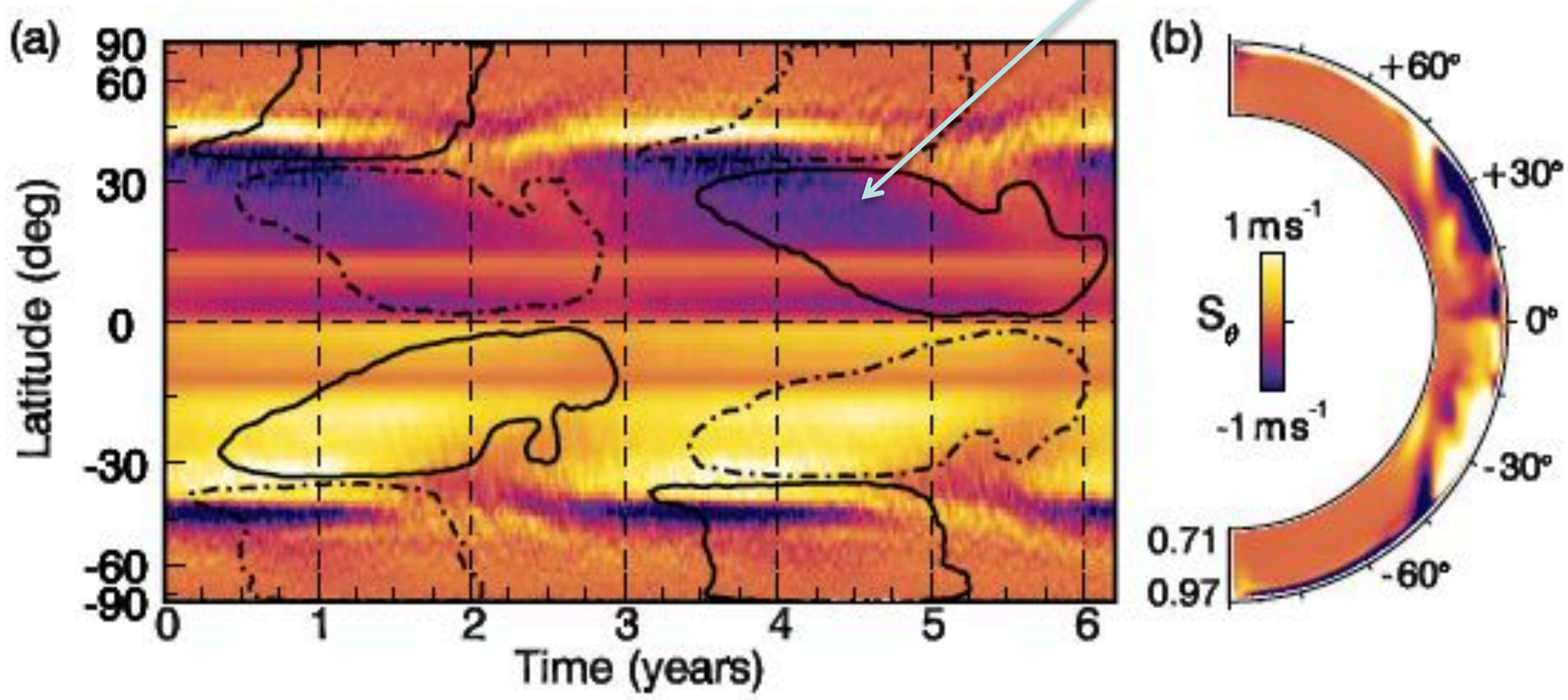

Non-linear dynamo wave I

Correct sign

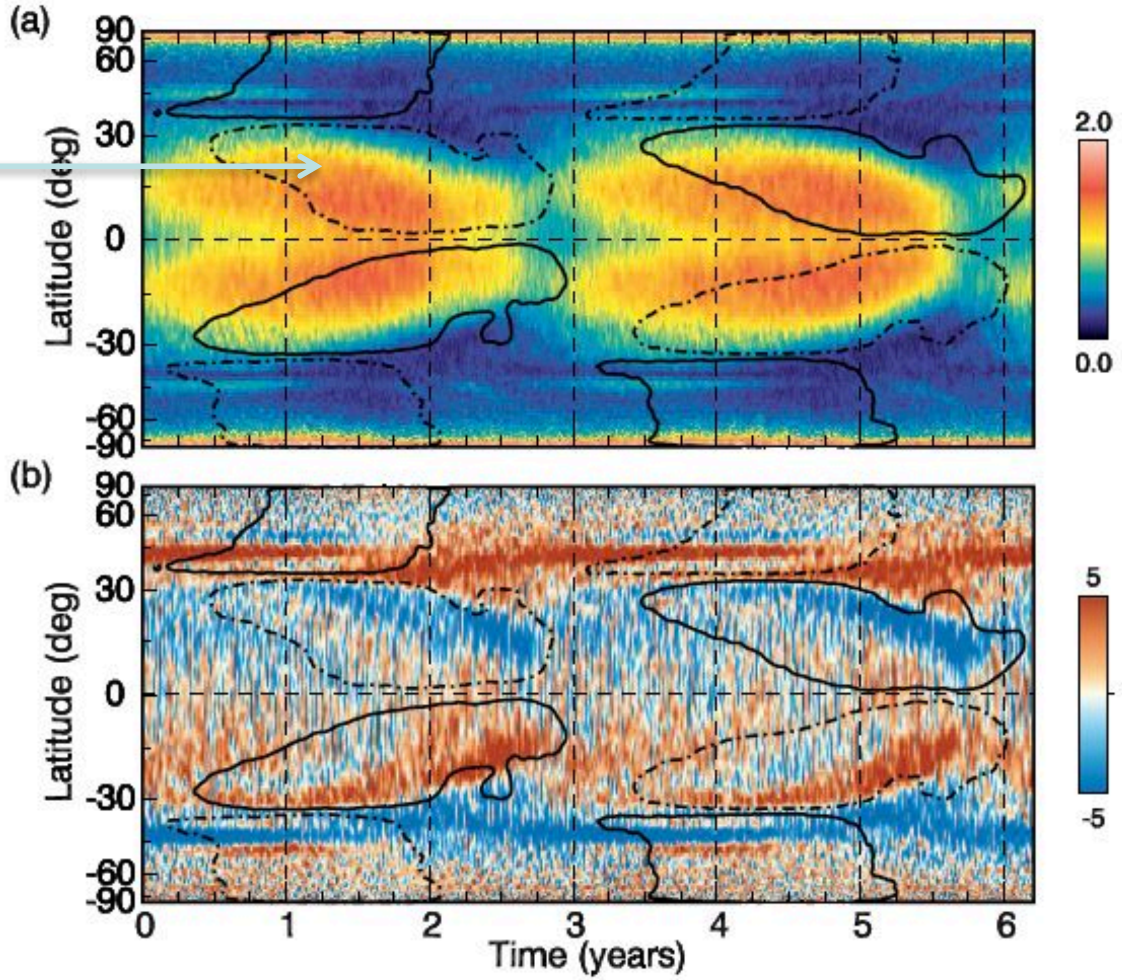

Figure 11. Coevolution of the mean toroidal magnetic field $\langle B_\varphi \rangle$ at $0.92 R_\odot$ over the average magnetic polarity cycle with (a) the magnitude of the mean angular velocity gradient $R_\odot |\nabla\Omega| / \Omega_0$ and (b) latitudinal velocity $\langle v_\theta \rangle$ of the evolving meridional circulation in units of $m\,s^{-1}$. Here $\langle B_\varphi \rangle$ is overlain with positive magnetic field as solid lines and negative field as dashed lines, with the contours corresponding to a 1 kG strength field.

Interaction between Shear and Bphi

Augustson et al. 2015

Non-linear dynamo wave II

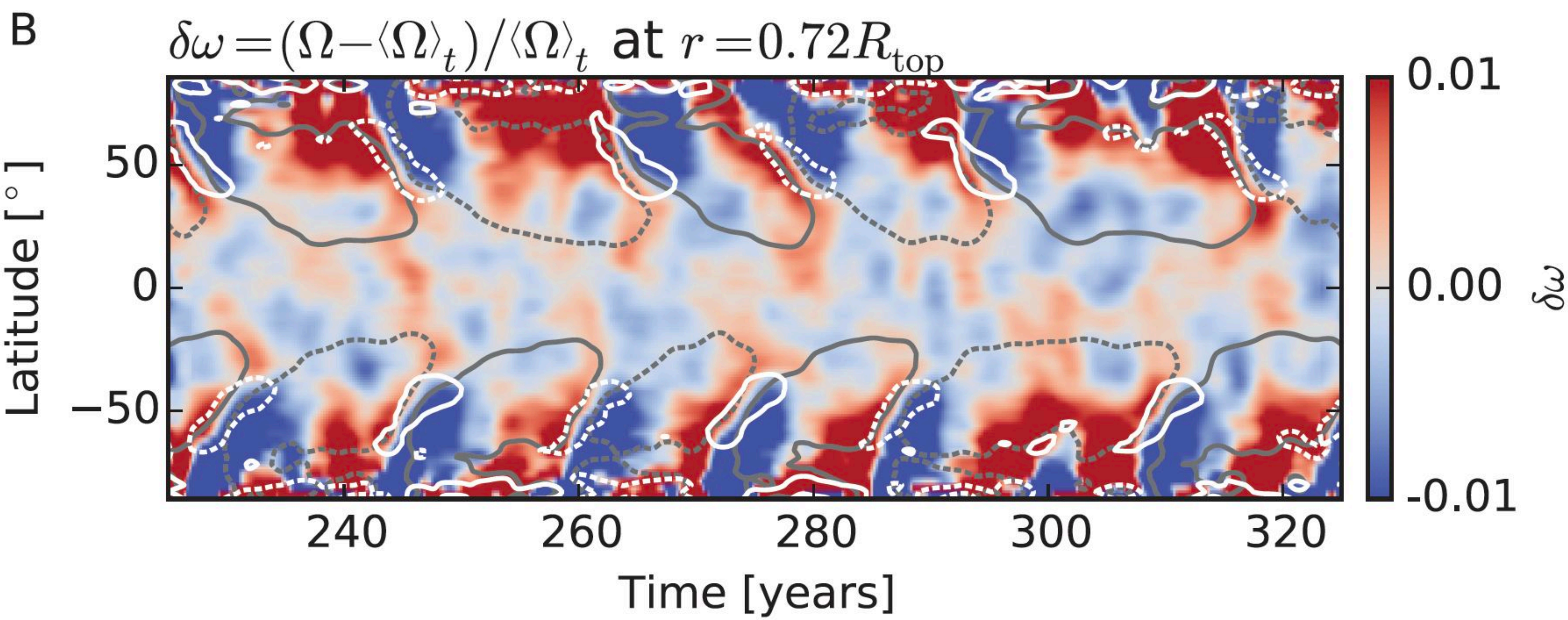

RESEARCH

STELLAR ACTIVITY

Reconciling solar and stellar magnetic cycles with nonlinear dynamo simulations

A. Strugarek,[1,2]* P. Beaudoin,[1] P. Charbonneau,[1] A. S. Brun,[2] J.-D. do Nascimento Jr.[3,4]

Strugarek et al. 2017, Science

Getting Maunder like minimun

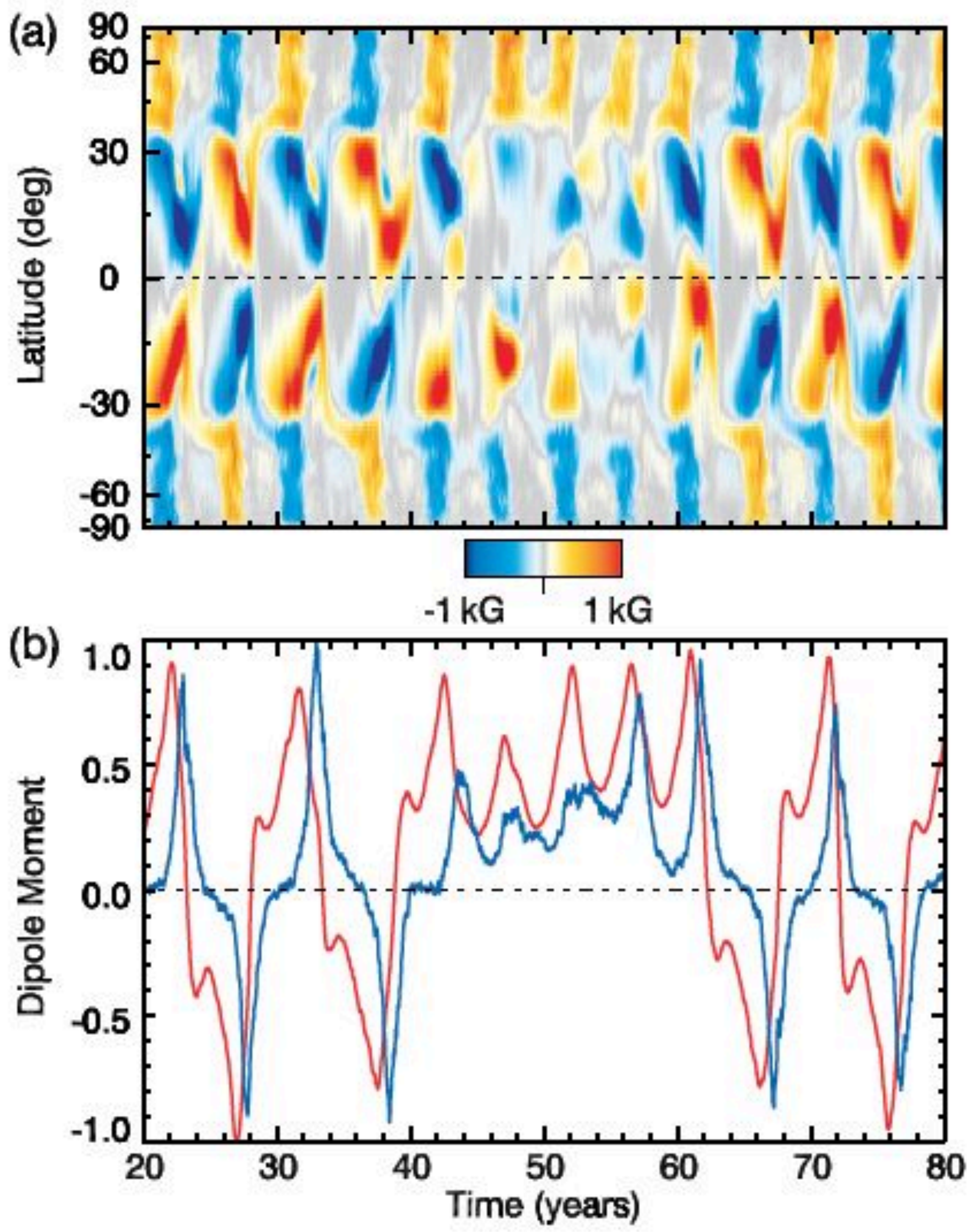

Quadrupole dominates over Dipole during reversal and Grand minimum phase

Augustson, Brun et al. 2015, ApJ

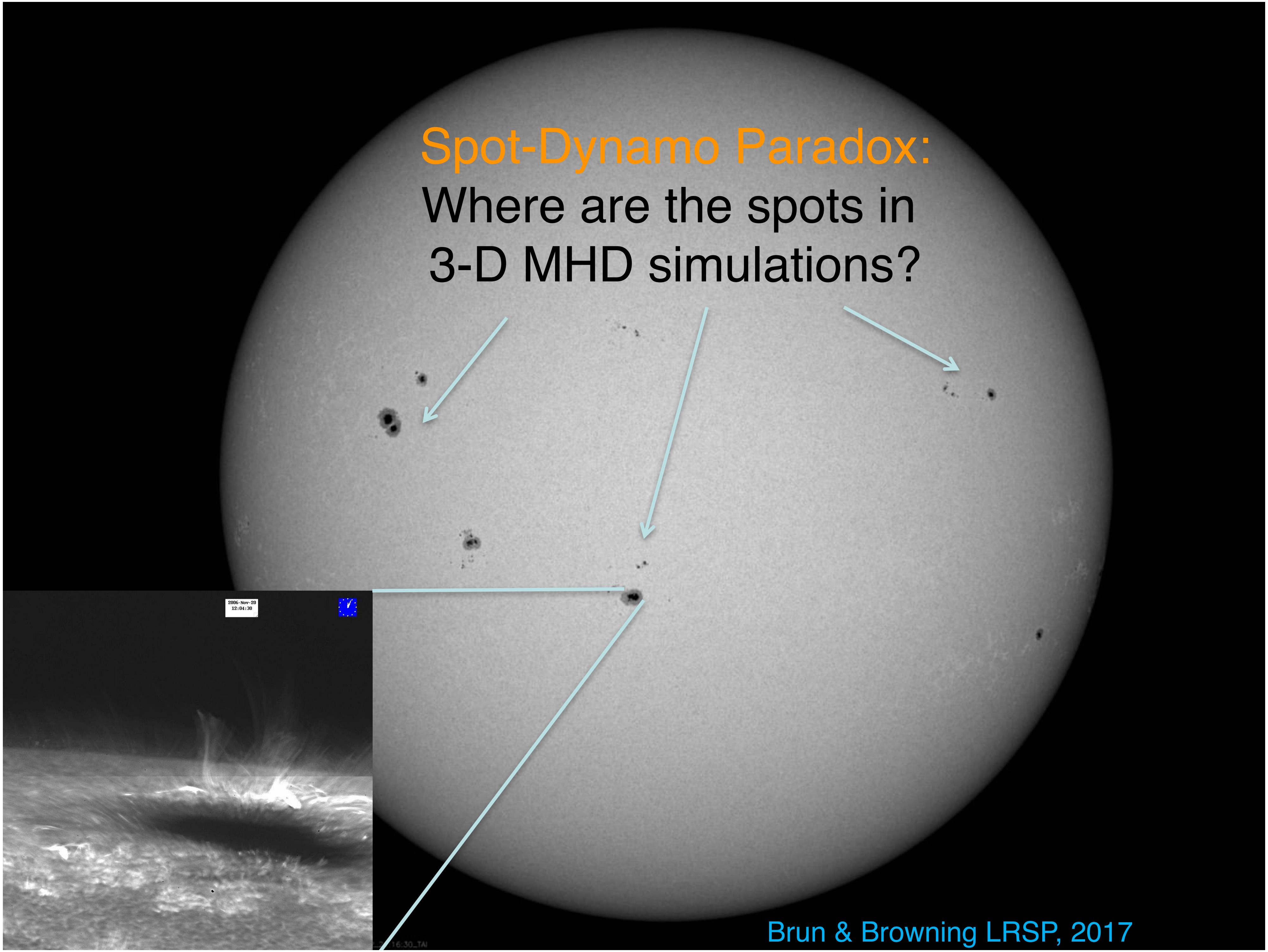
Spot-Dynamo Paradox:
Where are the spots in
3-D MHD simulations?
2006-Nov-20
12:04:30
Brun & Browning LRSP, 2017

Babcock-Leighton Mechanism and Polar Cap Reversal

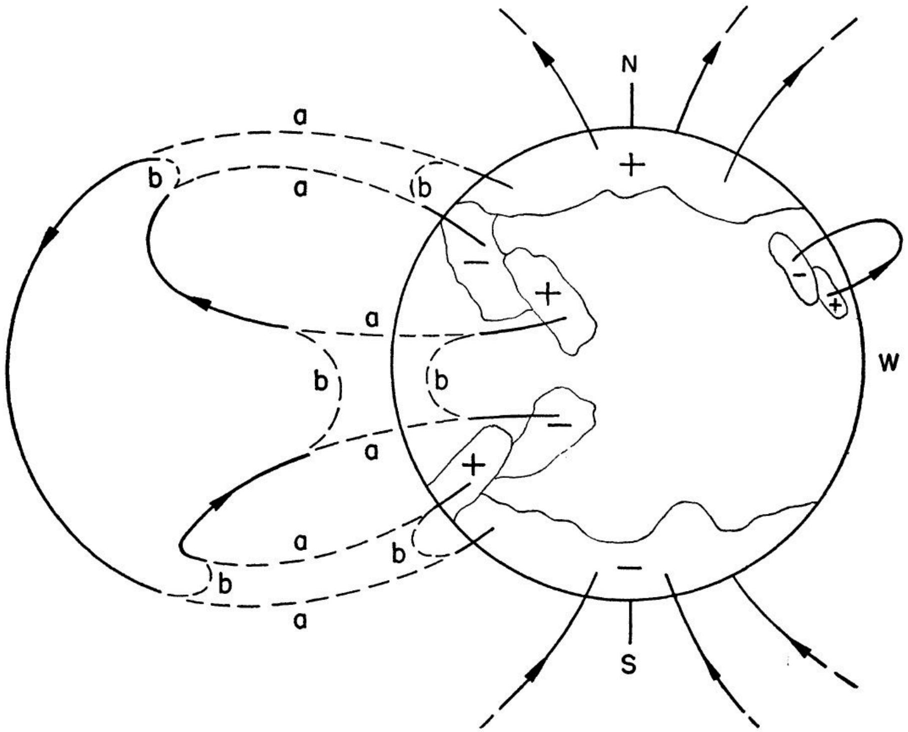

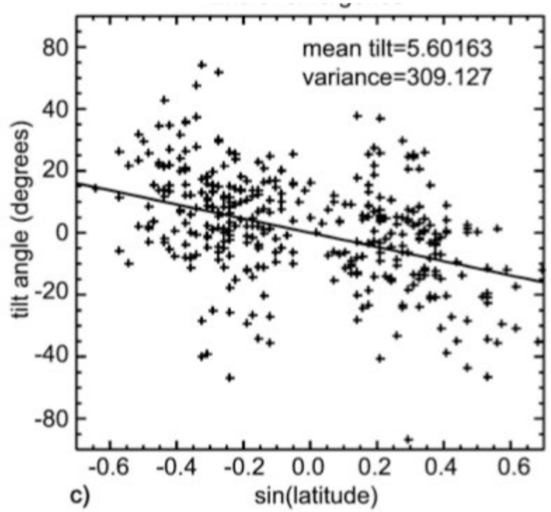

Joy's Law
Tilt of AR

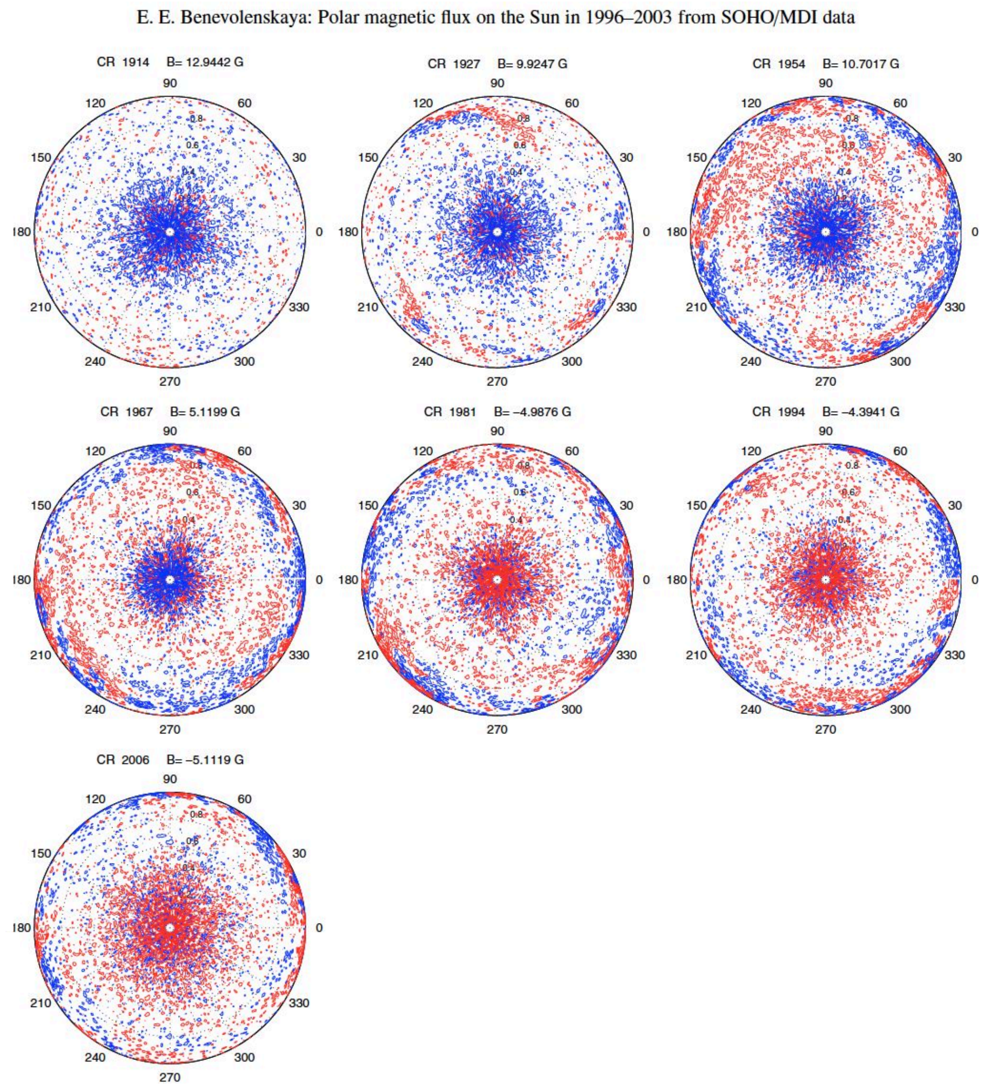

How important is it to get the 11yr dynamo?

Magnetic Wreaths vs Turbulence

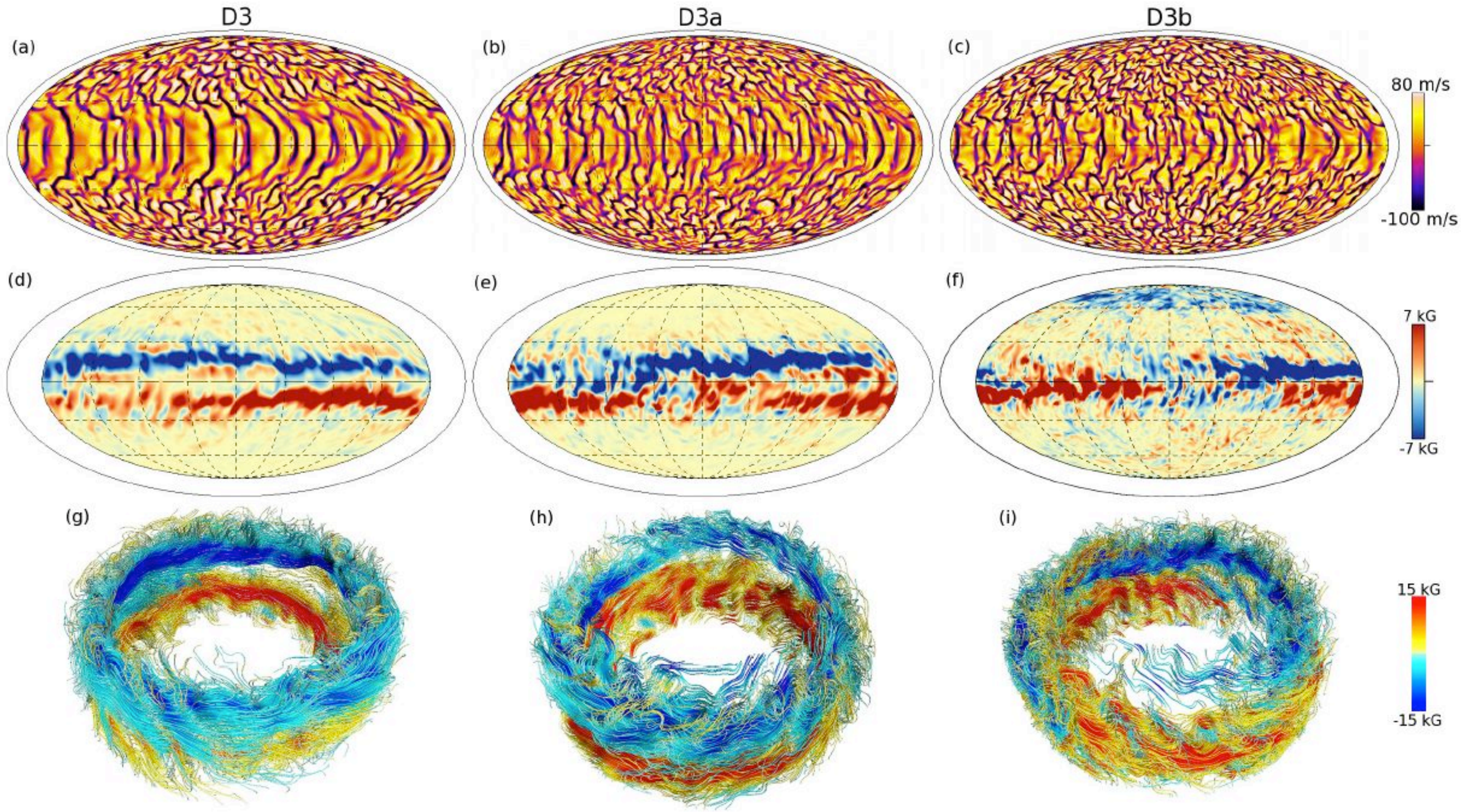

Nelson et al. 2013a, 2014

Magnetic Wreath and Intermittency yielding flux emergence

Magnetic « nuggets » source
of buoyant Omega-loop (see next slide)

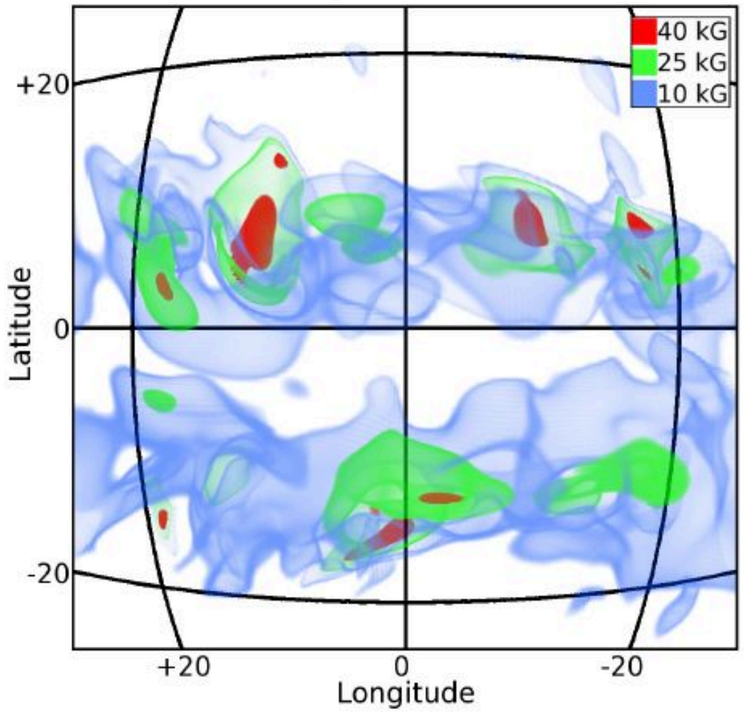

Figure 17. Three-dimensional volume renderings of isosurfaces of magnetic field amplitude in case S3. Blue surfaces have amplitudes of 10 kG, green surfaces represent 25 kG, and red surfaces indicate 40 kG fields. Grid lines indicate latitude and longitude at 0.72 $R_\odot$ as they would appear from the vantage point of the viewer. Small portions of the cores of these wreaths have been amplified to field strengths in excess of 40 kG while the majority of the wreaths exhibit fields of about 10 kG or roughly in equipartition with the mean kinetic energy density (see Figure 2).

Mean close between 4 models
But not extreme values!
Most turbulent case S3
is 35% more intense

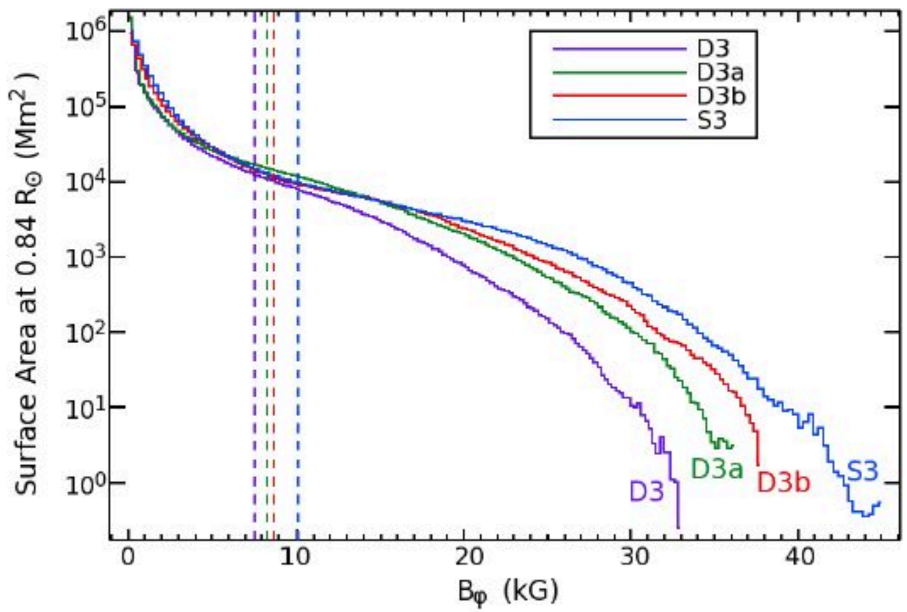

Figure 2. Probability distribution functions for unsigned B_ϕ at mid-convection zone for cases D3 (purple), D3a (green), D3b (red), and S3 (blue) showing the surface area covered by fields of a given magnitude. Distributions are averaged over about 300 days when fields are strong and as steady as possible. Dashed vertical lines show the field-strength at which equipartition is achieved with the maximum fluctuating kinetic energy (FKE) at mid-convection zone for each case. Case D3b shows a deficit of field in the 10 kG range, but an excess of surface area covered by extremely strong fields above 25 kG range, as well as higher peak field strengths. Case S3 shows significantly greater regions of fields in excess of 20 kG than all other cases.

Nelson et al. 2013, ApJ

Wreaths can generate Buoyant Loops

Evolution of Omega-loops

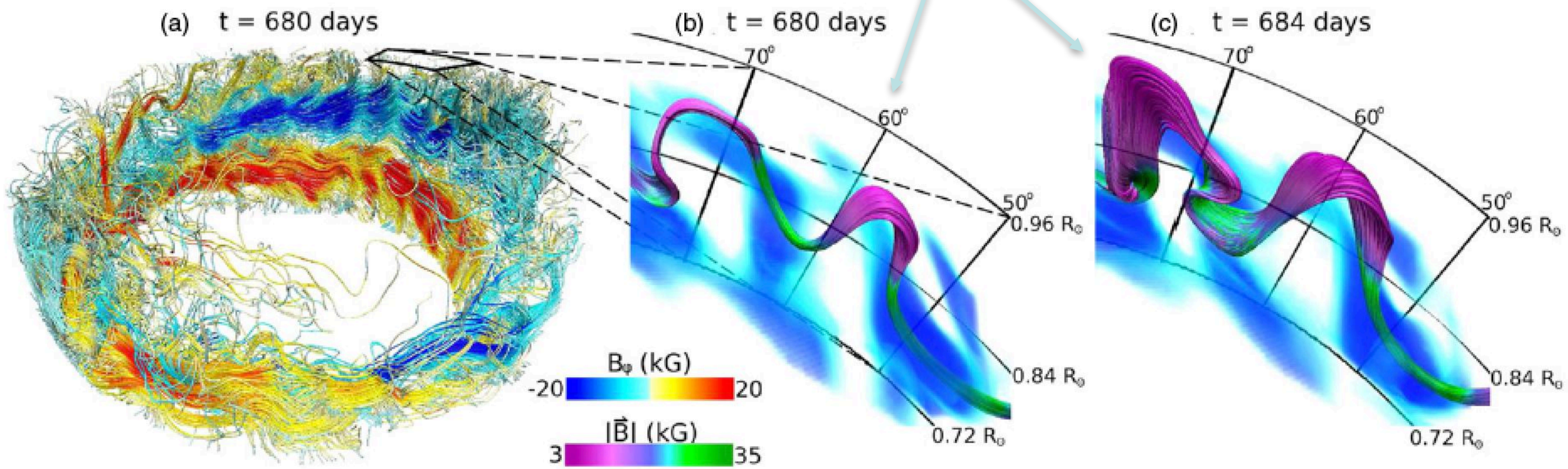

Nelson et al. 2011, 2013, 2014

Towards getting first “spot-dynamos”…